Towards Skyrmion Stars: Large Baryon Number Configurations in the Einstein-Skyrme Model

Probert, Gavin Idris

Towards Skyrmion Stars: Large Baryon Number Configurations in the Einstein-Skyrme Model

Gavin Idris Probert

A Thesis presented for the degree of

Doctor of Philosophy

Centre for Particle Theory

Department of Mathematical Sciences

University of Durham

England

September 2005

Dedicated to

All my friends, family and loved ones. Thank you for believing in me when I lost the way.

Towards Skyrmion Stars: Large Baryon Number Configurations in the Einstein-Skyrme Model

Gavin Idris Probert

Submitted for the degree of Doctor of Philosophy

September 2005

Abstract

The large baryon number sector of the Einstein-Skyrme model has been investigated, as a possible model for baryon stars. Self-gravitating hedgehog skyrmions have been studied previously and the existence of stable solitonic stars excluded due to energy considerations. However, in this thesis it is demonstrated that by generating self-gravitating skyrmions using harmonic maps, one can achieve multi-baryon bound states.

The question of the spatial symmetry of such configurations is discussed and it is argued that, although low baryon number solutions have various symmetries, approximate spherical symmetry is recoverered in the case of very large baryon numbers. Plausible structures are obtained, that possess baryon numbers typical to neutron stars and one concludes that indeed, the Einstein-Skyrme system can be used as a toy model for baryon stars.

Declaration

The work in this thesis is based on research carried out at the Centre for Particle Theory, the Department of Mathematical Sciences, the University of Durham, England. No part of this thesis has been submitted elsewhere for any other degree or qualification and is all my own work unless referenced to the contrary in the text.

Acknowledgements

This research has been supported by a PPARC studentship. For this support, the author is genuinely grateful.

There are many people who have impacted so positively on my life at Durham. Firstly, I would like to give my sincere thanks to my supervisor, Dr. Bernard Piette, for all the patience and support he has shown me. More than just his academic guidance, I would like to thank him for encouraging me and having faith in my work when others may have easily given up on me!

I would also like to note my appreciation to Prof. Ian Moss, for interesting discussions about the work.

To my office mates, Emily, Matt & Harald. Thanks for fruitful discussions (sometimes about maths!) and the general sense of camaraderie in our joint struggle.

A source of endless fun and mutual support, I would like to give heartfelt thanks to my housemates Anton & Debs. Through ritual whingeing, late night doughnut raids to Tescos and Playstation marathons, we certainly bonded well and I hope we stay close forever.

Unreserved gratitude is offered to numerous close friends, who stayed by me through difficult times and despite my awful treatment of them. Lisa, James, Dave,

little Phil, Fern, Jeff, Chris & Keri. You are amazing! I will never put you through that again.

Love and thanks go to my family. To Aunty Avril & Uncle Glyn for countless removal trips to university and their constant support. To Mum and Dad for their love and belief in me, for backing me through all my interests and for giving me the gift of curiosity as a child. I hope to one day make you as proud as you deserve.

Finally to you, Ange. From the moment I got to know you my life started getting better. As you know, I had lost my way for a while. You gave me confidence, self respect and happiness once again. I honestly believe that without you in my life, and your help with my faith, that I would have never completed this work. I love everything about you. Thank you cariad.

July 3, 2006

Contents

List of Figures

List of Tables

Chapter 1

Introduction

1.1 The Skyrme Model and associated field ansatze

The Skyrme model, in its initial form, was proposed and developed by T.H.R. Skyrme in a series of papers during 1954-1962, as a non-linear field theory of pions [1], [2]. Skyrme's initial idea was to think of baryons (in particular nucleons) as secondary structures arising from a more fundamental mesonic fluid. Thus only the pion fields were required in the model.

This differed from the contemporary view point of Yukawa, which required both fundamental fermionic fields for the nucleons and the fundamental bosonic fields of the pions. The latter were thought to bind the nucleons together.

The key property of the Skyrme model was that the nucleons arose as solitons in a topological manner and thus possessed a conserved topological charge. This charge, or winding number, allowed the possibility of constructing fermions from more fundamental bosonic fields [3]. The approach shares features with Kelvin's vortex model of the atom in that secondary structures, distinguished by their con-

served topological charateristics, are used to model varius nuclei or atoms [4].

In the Skyrme model the topological charge is interpreted as the baryon number. The lowest energy stable solutions to the model are termed *Skyrmions* and can be thought of as baryonic solitons. Formally, they are localised solutions to the classical field equations of the model. In practice, due to the high degree of non-linearity involved in the model, ansatze are taken for the Skyrme field. Thus the term Skyrmion is often used to mean the approximate localised solutions.

Interest in the Skyrme model flourished following work by 't Hooft and Witten, amongst others, on effective approaches to QCD. It is well known that the coupling of QCD increases at low energy scales (of the type relevant to the formation of nucleons from quarks). Consequently, standard perturbation techniques are inapplicable in such regimes.

't Hooft demonstrated an alternative approach, in which QCD can effectively be described, at low energy, in terms of the weak interactions of mesons, [5]. Moreover, Witten showed that baryons should arise as solitons in this description and that the Skyrme model possessed all the general features of a low energy effective field theory for QCD, [6].

The Skyrme model is described by the following Lagrangian density in the field variable $U(\mathbf{x}, t)$. U itself is an $SU(N)$ valued scalar field, where N is the number of flavours of interest. Much previous work has centred on the $SU(2)$ model.

$$\mathcal{L} = -\frac{f_\pi^2}{4} Tr\left(\partial_\mu U \partial^\mu U^\dagger\right) + \frac{1}{32e^2} Tr\left(\left[\left(\partial_\mu U\right) U^\dagger, \left(\partial_\nu U\right) U^\dagger\right]^2\right) \tag{1.1}$$

Here, f_π and e are constants relating to the model. These are usually fixed, such that the model gives the correct value for the nucleon energy.

One should note the presence of the second term, quartic in derivatives, which differs the Skyrme Lagrangian from the Yang-Mills Lagrangian. It is the second term which allows stability of solitonic solutions, as can be seen by an application of Derrick's theorem, [7].

For simplicity one will outline the production of a topological charge for the $SU(2)$ model. The following homotopy analysis can however be extended to the $SU(N)$ model, as outlined later.

Note that as U takes values in $SU(2)$, one can think that at a given time the field defines a map between coordinate space and the $\mathbb{S}^3$ group N-fold, $U(\mathbf{x}) : \mathbb{R}^3 \to \mathbb{S}^3$. Also, finite energy considerations impose that U should take a fixed value on the $\mathbb{S}^3$ group N-fold at spatial infinity, such that $U(\mathbf{x}) \to \mathbf{1}$ as $|\mathbf{x}| \to \infty$. This is effectively the one point compactification $\mathbb{R}^3 \cup \{\infty\} \simeq \mathbb{S}^3$.

The field can therefore be thought of as a map between the spatial infinity 3-sphere and the group N-fold, also a 3-sphere. As such, it falls into distinct homotopy classes characterised by their winding number, the homotopy group for this case being the integers. The integer winding numbers are conserved topological charges as no continuous deformations can change a given state to one in a different homotopy class. In the Skyrme model the winding number is interpreted as the baryon number of the Skyrmion and thus baryon number conservation is achieved.

The conserved topological charge can be calculated as $\int d^3x B_0$, where the topological current is defined as

$$B_\mu = \frac{1}{24\pi^2}\epsilon_{\mu\nu\rho\sigma} Tr\left[\left(U^\dagger \partial^\nu U\right)\left(U^\dagger \partial^\rho U\right)\left(U^\dagger \partial^\sigma U\right)\right] \tag{1.2}$$

For a detailed review of the Skrme model, the reader is referred to [8].

1.1.1 Hedgehog ansatz

Any field equations derived from the model, will be highly non-linear partial differential equations. To make progress one usually adopts an ansatze for the Skyrme field.

A particular ansatz for the field, taken by Skyrme in his initial papers, is the Hedgehog ansatz.

$$U(\mathbf{x}, t) = exp\left(i\vec{\sigma}\cdot\hat{n}h(r)\right) \tag{1.3}$$

In this ansatz the field, characterised by a profile function $h(r,t)$, is purely radial and thus the resulting Skyrmions are always spherically symmetric.

For the field to be well defined at the origin then $h(r=0) = B_1\pi$ and for finite energy $h(r=\infty) = B_2\pi$, where $B_1, B_2 \in \mathbb{Z}$. The baryon number of the Skyrmion is found to be $B_1 - B_2$, however, for the remainder of this thesis we shall take $B_2 = 0$, as is the common practice.

The fact that $\hat{n}$ is the unit radial vector and that the product of two Pauli matrices is given by $\sigma_i\sigma_j = i\epsilon_{ijk}\sigma_k + \delta_{ij}\mathbf{I}$, leads to the square of $(\vec{\sigma}\cdot\hat{n})$ being unity and the following convenient expression

$$U = \cos h \cdot \mathbf{I} + in\cdot\sigma \sin h \tag{1.4}$$

1.1.2 Rational map ansatz

An alternative ansatz proposed by Houghton et al., following a similar technique used by Donaldson et al. and Jarvis et al. in monopole theory, is the rational map ansatze, [9].

Points on $\mathbb{S}^2$ can be labelled by their stereographic coordinate $z = tan(\theta/2)e^{i\phi}$ and its conjugate, via projection onto the complex plane. A rational map of degree Q is a map between 2-spheres defined to be a ratio of polynomials in z, having maximum order Q, possessing no common factors and with one polynomial being exactly of order Q.

$$R(z) = \frac{p(z)}{q(z)} \tag{1.5}$$

It has been previously outlined that $SU(2)$ Skyrmions can be thought of as maps between $\mathbb{R}^3 \cup \{\infty\}$ and the field manifold $SU(2)$, which are essentially maps between 3-spheres. Houghton et al. proposed, therefore, that Skyrmions could be constructed from rational maps between concentric $\mathbb{S}^2$ in $\mathbb{R}^3$ and 2-spheres of latitude on $\mathbb{S}^3$. This leads to a modification of the ansatz to

$$U(r, z) = exp\,(i\vec{\sigma} \cdot \hat{n_R} h(r)) \tag{1.6}$$

where the unit vector associated with the rational map is given by

$$\hat{n_R} = \frac{1}{1 + |R|^2} \left(2\Re(R), 2\Im(R), 1 - |R|^2\right) \tag{1.7}$$

It can be shown that the baryon number for Skyrmions constructed in this way, is equal to the degree Q of the rational map, providing one takes the boundary conditions $h(r = 0) = \pi$ and $h(r = \infty) = 0$.

The approximate solutions of the field equations obtained using the rational map ansatze, are an improvement on those obtained for multi-baryons, using the hedgehog ansatze. By this, one means that the energies of the solutions obtained more closely resemble those found from dynamically evolving well separated single baryons. Further, the solutions possess the correct symmetries. For the $SU(2)$ model, all multi-baryon states are non-spherically symmetric. For example, a two baryon Skyrmion naturally forms a torus, whereas three baryons will bind into a tetrahedral structure [9].

1.1.3 $SU(N)$ Harmonic map ansatz

If one wishes to study the general $SU(N)$ Skyrme model, one can use the extension of the rational map ansatz due to Ioannidou et al., known as the projector or harmonic map ansatz [10]. These are completely euqivalent to the rational map ansatze, when studying the $SU(2)$ model.

One takes the following ansatz for the $SU(N)$ field

$$U(r, z, \bar{z}) = e^{2ih(r)(P-\frac{1}{N})} \tag{1.8}$$

where P is an $N \times N$ hermitian projection operator which depends only on the angular variables.

Expanding and using the fact that $P^2 = P$, one arrives at the following, more convenient form of the ansatz.

$$U = e^{-2ih/N}\left(\mathbf{I} + (e^{2ih} - 1)P\right) \tag{1.9}$$

Here the general scheme is to decompose the Skyrme field, which at a given

instant is effectively a map from $\mathbb{S}^3$ to the group manifold of $SU(N)$, into a product of a radial and angular functions. P is a hermitian projector between the two sphere and the manifold of $\mathbb{CP}^{N-1}$ and h(r) is a radial profile function living in the remaining quotient space $SU(N)/\mathbb{CP}^{N-1}$.

It can be shown that, for a suitable choice of the boundary conditions for h(r), i.e. $h(r=0)=\pi$ and $h(r=\infty)=0$, the degree of the total map is reduced to the degree of the map $\mathbb{S}^2 \rightarrow \mathbb{CP}^{N-1}$, which is again an integer.

The advantage of the rational or harmonic map ansatze, is that they allow one to study minimal energy Skyrmions with specific spatial symmetries, simply by using maps that possess these symmetries. This will become important when studying specific Skyrmion configurations coupled to gravity.

1.2 Summary of related work

The idea behind this research project, was to re-explore the Einstein-Skyrme model and ask 'Can structures resembling baryon stars arise as low energy Skyrmions coupled to gravity?'. This seems a plausible enquiry. After all, neutron stars are structures made of superdense neutron matter, for which the equation of state is not well understood, [11]. The interactions between the neutrons should be described by QCD and it has already been detailed that the Skyrme model is, in essence, an appropriate effective field theory for QCD.

The Skyrme field coupled to gravity has already been studied by, amongst others, Luckock and Moss, [12], [13], [14]. The research involved studying a Skyrme field

in the presence of an external gravitational field. Interesting non-trivial structures were found, for example, black holes surrounded by a pion cloud. These black holes, termed *hairy* or *coloured* are extremely interesting, in that they violate the usual no-hair theorems. In short, the associated horizons cannot be totally defined in terms of their mass, charge and angular momentum, because of the extra chiral fields involved. What is more, the coloured black hole solutions are stable.

Although the focus of this work was not directly the same as in this thesis, the papers formed extremely valuable conributions to the academic community. They were the first to study the Skyrme model in the presence of gravity and paved the way for much similar research. Since then, violations of the no-hair theorems have been found for various non-linear field theories coupled to gravity and much further study of the Skyrme black hole has been undertaken, [15], [16], [17], [18], [19], [20], [21], [22].

Resulting from such study, many other interesting solutions have been found. For many non-linear field theories, non-trivial stable gravitationally bound configurations of the field have been obtained. Perhaps the most well known of these are the particle-like gravitationally bound Yang-Mills fields, known as the Bartnick-McKinnon solutions [23], [24].

In contrast to the work of Luckcock & Moss, this thesis investigates Skyrmions not in an external gravitational field, but where the field is due to the baryon distribution in th Skyrmion itself. The baryons then settle in their own gravitational field.

Similar work was caried out by Bizon & Chmaj, [25], [26]. Self-gravitating Skyrmions were studied using the sphercal hedgehog ansatze for the Skyrme field.

It was hoped that the inclusion of gravity would lead to multi-baryon bound states and thus the possibility of using the Einstein-Skyrme system as a toy model for baryon stars. Unfortunately this was not the case and all multi-baryon solutions were found to be energetically unfavourable.

There is however an alternative approach, which will be used in this thesis. Instead of imposing spherical ansatze on the field, as would be reasonable for baryon stars, and then hoping that the energies are reduced by gravitational binding, why not use energetically favourable ansatze for the field which produce non-spherical Skyrmions. Then one hopes that somehow spherical symmetry can be recovered. This thesis takes the harmonic map ansatze for self-gravitating $SU(N)$ Skyrmions and hopes that energetically favourable states of multi-baryons are produced. The isssue of symmetry is then dealt with and the question of how one studies the extremely large baryon numbers required to model baryon stars is addressed.

The author notes at this point, that independently to this research some similar studies at low baryon number have been published in parallel [27], [28]. The author points out that although the solutions at low baryon number, detailed in this thesis, were obtained before these publications, they were not submitted for publication as one wished to wait until the issue of symmetry and large baryon numbers had been resolved. Neither of these concerns are addressed in [27], [28], because the focus of that reasearch was not towards baryon stars.

Chapter 2

Self-Gravitating Skyrmions

The action for the Skyrme model, including gravitational interactions, can be formed from the standard Skyrme action for the matter field and the Einstein-Hilbert action for the gravitational field (along with a suitable boundary term, denoted here by S_{GH}), [25]. Thus the starting point for the study of self-gravitating Skyrmions is the action

$$S = \int_{\mathcal{M}} \sqrt{-g} \left(\mathcal{L}_{Sk} - \frac{R}{16\pi G} \right) d^4x + S_{GH} \tag{2.1}$$

Here $\mathcal{L}_{Sk}$ is the standard Lagrangian density for the $SU(N)$ Skyrme model but now defined on the (generally curved) manifold $\mathcal{M}$.

$$\mathcal{L}_{Sk} = \frac{f_\pi^2}{4} Tr(\mathbf{K}_\mu \mathbf{K}^\mu) + \frac{1}{32e^2} Tr\left([\mathbf{K}_\mu, \mathbf{K}_\nu][\mathbf{K}^\mu, \mathbf{K}^\nu]\right). \tag{2.2}$$

In the above, the $\mathbf{K}_\mu$ are current valued objects, defined as $(\nabla_\mu U)U^{-1}$. Note that now the Skyrme field U can be thought of as a map from the curved space-time $\mathcal{M}$ into $SU(N)$.

In the gravitational part of the action, R is the Ricci scalar associated with the manifold $\mathcal{M}$. G, f_π and e are the fundamental constants of the model, being re-

spectively Newton's gravitational constant, the pion decay constant and the Skyrme coupling.

Finally, S_{GH} is the appropriate regularised *Gibbons-Hawking* action for the model and is the necessary boundary contribution to ensure that variation of the action leads to Einstein's equation, [29]. For a fuller discussion of the need for such a term, along with its explicit calculation, see App. A.

2.1 Metric Ansatze

For the metric on the manifold $\mathcal{M}$, it is reasonable to choose that associated with the following line element

$$ds^2 = -A^2(r)\left(1-\frac{2m(r)}{r}\right)dt^2 + \left(1-\frac{2m(r)}{r}\right)^{-1}dr^2 + r^2(d\theta^2+\sin^2\theta d\phi^2). \quad (2.3)$$

This is a sensible choice of metric that captures the nature of the curvature that would result in the situation of interest. First, the main area of interest in this work is in the static properties of gravitating skyrmions, thus one should choose a metric associated with a static gravitational field.

Second, rather than the mass m and coefficient A being constants they are promoted to radial fields. This encodes the fact that one is not studying the properties of Skyrmions in a fixed curved background (eg Skyrmions in the presence of a fixed mass) but rather the more interesting problem of bound states of baryons interacting with their own gravitational field.

Finally, for any reasonable astrophysical interpretation of gravitating Skyrmions, e.g. as neutron stars, then it is reasonable to assume that the gravitational field possesses spherical symmetry. This is captured in the form of the metric (2.3).

Actually, most of the configurations that will be presented will not possess exact spherical symmetry and thus the resulting gravitational field should not be assumed to be purely radial. However, the configurations will possess an approximately spherical distribution of baryons, with this symmetry becoming more enhanced as the baryon number increases. In effect then, although the configurations will only be approximations to true gravitating Skyrmions, the discrepancy due to this mismatch of symmetry will not be significant. This is particularly the case in the regime of astrophysical relevance (high baryon number) and when one considers that the gravitational back-reaction of the matter field is relatively small.

2.2 The Gravitational part of the Action

Using this ansatze for the metric on $\mathcal{M}$ it is possible to calculate both S_{GH} and R directly.

$$R = \frac{-2}{Ar^2}\left(-A''r^2 - 2A'r + 2A''rm + A'm + 3A'rm' + Arm'' + 2Am'\right) \tag{2.4}$$

where $'$ denotes a derivative with respect to the radial coordinate r.

Noting that from (2.3)

$$\sqrt{-g} = A(r)r^2 sin(\theta) \tag{2.5}$$

and that $S_{GH} = -\frac{1}{2G}\int dtm(\infty)$ (shown in App. A), then the gravitational part of the action simplifies as follows

$$
\begin{aligned}
S_{Grav} &= -\frac{1}{2G}\int dt\left[m(\infty)+\int\left(A''r^2+2A'r-2A''rm-A'm\right.\right.\\
&- \left.\left.3A'rm'-Arm''-2Am'\right)dr\right]\\
&= -\frac{1}{2G}\int dt\left[m(\infty)+\int\left(\frac{d}{dr}\left[A'r^2-2A'mr-Am'r\right]\right.\right.\\
&+ \left.\left.A'm-Am'\right)dr\right] \qquad (2.6)
\end{aligned}
$$

Now using the fact that asymptotic flatness of space-time imposes $A(r=\infty)=1$ and $m(r=\infty)=const.$, and that there is no mass at the origin, one obtains

$$
\begin{aligned}
S_{Grav} &= -\frac{1}{2G}\int dt\left[m(\infty)+\left(\left[A'r^2-2A'mr-Am'r+Am\right]_0^\infty-2\int Am'dr\right)\right]\\
&= -\frac{1}{G}\int dt\left(m(\infty)-\int Am'dr\right) \qquad (2.7)
\end{aligned}
$$

2.3 The Matter part of the Action

In deriving the form of the matter part of the action, it is convenient to change from spherical polar coordinates (r, θ, ϕ) to stereographic coordinates $(r, z, \bar{z})$, via projection onto the complex plane such that

$$z = tan\left(\frac{\theta}{2}\right) e^{i\phi} \tag{2.8}$$

The Jacobian for this transformation is easily calculated to be

$$|J| = \frac{i}{\sqrt{|z|^2}(1+|z|^2)} \tag{2.9}$$

and thus the area form becomes

$$dA = sin\theta d\theta d\phi = \frac{2i}{(1+|z|^2)^2} dz d\bar{z} \tag{2.10}$$

In stereographic coordinates, the currents become

$$\begin{aligned} \mathbf{K}_\theta &= (\partial_\theta U)U^{-1} \\ &= (\frac{\partial z}{\partial \theta}\partial_z U + \frac{\partial \bar{z}}{\partial \theta}\partial_{\bar{z}} U)U^{-1} \\ &= \frac{1}{2}\frac{(1+|z|^2)}{\sqrt{|z|^2}}(z\mathbf{K}_z + \bar{z}\mathbf{K}_{\bar{z}}) \end{aligned} \tag{2.11}$$

and

$$\begin{aligned} \mathbf{K}_\phi &= (\partial_\phi U)U^{-1} \\ &= (\frac{\partial z}{\partial \phi}\partial_z U + \frac{\partial \bar{z}}{\partial \phi}\partial_{\bar{z}} U)U^{-1} \\ &= i(z\mathbf{K}_z - \bar{z}\mathbf{K}_{\bar{z}}) \end{aligned} \tag{2.12}$$

For what follows, let $\mathcal{L}_{Sk_1}$ denote the first term in the Skyrme Lagrangian density, that which is quadratic in derivatives. $\mathcal{L}_{Sk_2}$ will label the Skyrme term, that which is

quartic in derivatives. Thus, noting that the metric is purely diagonal and referring to eqn. (2.2), it is clear that

$$\begin{aligned}\mathcal{L}_{Sk_1} &= \frac{f_\pi^2}{4}Tr(g^{\mu\mu}\mathbf{K}_\mu^2) \\ &= \frac{f_\pi^2}{4}Tr\left(S(r)\mathbf{K}_r^2 + \frac{1}{r^2}(\mathbf{K}_\theta^2 + \frac{1}{sin^2\theta}\mathbf{K}_\phi^2)\right) \\ &= \frac{f_\pi^2}{4}Tr\left(S(r)\mathbf{K}_r^2 + \frac{(1+|z|^2)^2}{r^2}|\mathbf{K}_z|^2\right) \end{aligned} \tag{2.13}$$

Here the third line has been obtained by direct substitution of the currents in stereographic coordinates from eqns. (2.11) and (2.12). Note that for convenience, the function $S(r)$ has been defined as follows:

$$S(r) = \left(1 - \frac{2m(r)}{r}\right) \tag{2.14}$$

In a similar manner, the Skyrme term can be rewritten as

$$\begin{aligned}\mathcal{L}_{Sk_2} &= \frac{1}{32e^2}Tr\left(g^{\mu\mu}g^{\nu\nu}[\mathbf{K}_\mu, \mathbf{K}_\nu]^2\right) \\ &= \frac{1}{16e^2}Tr\left(\frac{S(r)}{r^2}\left([\mathbf{K}_r, \mathbf{K}_\theta]^2 + \frac{1}{sin^2\theta}[\mathbf{K}_r, \mathbf{K}_\phi]^2\right) + \frac{1}{r^4 sin^2\theta}[\mathbf{K}_\theta, \mathbf{K}_\phi]^2\right) \\ &= \frac{1}{16e^2}Tr\left(\frac{S(r)(1+|z|^2)^2}{r^2}|[\mathbf{K}_r, \mathbf{K}_z]|^2 - \frac{(1+|z|^2)^4}{4r^4}[\mathbf{K}_z, \mathbf{K}_{\bar{z}}]^2\right) \end{aligned} \tag{2.15}$$

where the factor of two has arisen due to the symmetry under the interchange $\mu \leftrightarrow \nu$.

Now using the Harmonic Map Ansatze, $U = e^{-2ih(r)/N}(\mathbf{I} + (e^{2ih(r)} - 1)P)$, as discussed in section 1.1.3, one can calculate the relevant currents and their commutators. Note that in what follows the argument of both $h(r)$ and $S(r)$ shall be dropped and a dash will denote differentiation with respect to the radial coordinate

r.

$$\begin{aligned}
\mathbf{K}_r &= \left(\partial_r e^{-2ih/N}(\mathbf{I} + (e^{2ih} - 1)P)\right) U^{-1} \\
&= \frac{-2ih'}{N} UU^{-1} + 2ih' e^{-2ih/N} e^{2ih} PU^{-1} \\
&= \frac{-2ih'}{N}\mathbf{I} + 2ih' e^{2ih} P(\mathbf{I} + (e^{-2ih} - 1)P) \\
&= 2ih'(P - \frac{1}{N}\mathbf{I}) \qquad (2.16)
\end{aligned}$$

Note that in order to arrive at the above result, the fact that P is a projection matrix and thus $P^2 = P$, was used. One should also remember that $\mathbf{I}$ is, in this context, always the $N \times N$ identity matrix, where N denotes the number of flavours included in the model.

Next one finds

$$\begin{aligned}
\mathbf{K}_z &= e^{-2ih/N}(e^{2ih} - 1)\partial_z PU^{-1} \\
&= (e^{2ih} - 1)\partial_z P(\mathbf{I} + (e^{-2ih} - 1)P) \\
&= (e^{2ih} - 1)(\partial_z P + (e^{-2ih} - 1)(\partial_z P)P) \\
&= (1 - e^{-2ih})\partial_z P \qquad (2.17)
\end{aligned}$$

and

$$\begin{aligned}
\mathbf{K}_{\bar{z}} &= e^{-2ih/N}(e^{2ih} - 1)\partial_{\bar{z}} PU^{-1} \\
&= (e^{2ih} - 1)\partial_{\bar{z}} P(\mathbf{I} + (e^{-2ih} - 1)P) \\
&= (e^{2ih} - 1)(\partial_{\bar{z}} P + (e^{-2ih} - 1)(\partial_{\bar{z}} P)P) \\
&= (e^{2ih} - 1)\partial_{\bar{z}} P \qquad (2.18)
\end{aligned}$$

In the above calculations it was necessary to use the useful identities discussed

in [10]. Namely

$$\begin{aligned}(\partial_z P)P &= \partial_z P \\ P(\partial_z P) &= 0 \\ P(\partial_{\bar{z}} P) &= \partial_{\bar{z}} P \\ (\partial_{\bar{z}} P)P &= 0 \end{aligned} \tag{2.19}$$

Now it is straightforward to calculate the commutators needed in eqn. (2.15), as follows. Again the identities in (2.19) will be used.

$$\begin{aligned}[\mathbf{K}_r, \mathbf{K}_z] &= 2ih'(1-e^{-2ih})\left[\left(P-\frac{1}{N}\mathbf{I}\right), \partial_z P\right] \\ &= 2ih'(1-e^{-2ih})\left(P(\partial_z P) - \frac{1}{N}\partial_z P - (\partial_z P)P + \frac{1}{N}\partial_z P\right) \\ &= -2ih'(1-e^{-2ih})\partial_z P \end{aligned} \tag{2.20}$$

$$\begin{aligned}[\mathbf{K}_r, \mathbf{K}_{\bar{z}}] &= 2ih'(e^{2ih}-1)\left[\left(P-\frac{1}{N}\mathbf{I}\right), \partial_{\bar{z}} P\right] \\ &= 2ih'(e^{2ih}-1)\left(P(\partial_{\bar{z}} P) - \frac{1}{N}\partial_{\bar{z}} P - (\partial_{\bar{z}} P)P + \frac{1}{N}\partial_{\bar{z}} P\right) \\ &= 2ih'(e^{2ih}-1)\partial_{\bar{z}} P \end{aligned} \tag{2.21}$$

and finally

$$\begin{aligned}[\mathbf{K}_z, \mathbf{K}_{\bar{z}}] &= (1-e^{-2ih})(e^{2ih}-1)[\partial_z P, \partial_{\bar{z}} P] \\ &= 2(cos2h-1)[\partial_z P, \partial_{\bar{z}} P] \\ &= -4sin^2 h[\partial_z P, \partial_{\bar{z}} P] \end{aligned} \tag{2.22}$$

Having calculated the explicit form of the currents for the Harmonic Map Ansatze and their commutation relations, it is straightforward to obtain the Lagrangian

density for the matter fields.

$$\begin{aligned}
\mathcal{L}_{Sk_1} &= \frac{f_\pi^2}{4} Tr\left(S\mathbf{K}_r^2 + \frac{(1+|z|^2)^2}{r^2}|\mathbf{K}_z|^2\right) \\
&= \frac{f_\pi^2}{4} Tr\left(-4Sh'^2\left(P - \frac{\mathbf{I}}{N}\right)^2 + \frac{(1+|z|^2)^2}{r^2}(1-e^{-2ih})(e^{2ih}-1)|\partial_z P|^2\right) \\
&= -f_\pi^2 Tr\left(\frac{Sh'^2}{N}\left((N-2)P + \frac{\mathbf{I}}{N}\right) + sin^2 h\frac{(1+|z|^2)^2}{r^2}|\partial_z P|^2\right) \\
&= -f_\pi^2\left(Q_N Sh'^2 + sin^2 h\frac{(1+|z|^2)^2}{r^2} Tr|\partial_z P|^2\right) \qquad (2.23)
\end{aligned}$$

Here, the fact that $\mathbf{I}$ was the $N \times N$ identity matrix and thus its trace is simply N, was used, along with the fact that $TrP = 1$, [10]. The *flavour factor* Q_N has been defined as $\frac{(N-1)}{N}$.

Using the commutation relations of eqns. (2.20) - (2.22), the Skyrme term becomes

$$\begin{aligned}
\mathcal{L}_{Sk_2} &= \frac{1}{16e^2} Tr\left(\frac{S(r)(1+|z|^2)^2}{r^2}|[\mathbf{K}_r, \mathbf{K}_z]|^2 - \frac{(1+|z|^2)^4}{4r^4}[\mathbf{K}_z, \mathbf{K}_{\bar{z}}]^2\right) \\
&= -\frac{1}{e^2}\frac{(1+|z|^2)^2}{r^2} \times \\
&\quad Tr\left(Sh'^2 sin^2 h|\partial_z P|^2 + \frac{(1+|z|^2)^2}{4r^2} sin^4 h[\partial_z P, \partial_{\bar{z}} P]^2\right) \qquad (2.24)
\end{aligned}$$

It is now finally possible to combine eqns. (2.7), (2.23) and (2.24) to obtain the full action for the gravitating $SU(N)$ Skyrmions.

$$\begin{aligned}
S &= S_{Grav} + \int dt \int \sqrt{-g}\,(\mathcal{L}_{Sk_1} + \mathcal{L}_{Sk_2})\, dr dz d\bar{z} \\
&= \int\left(4\pi \int dr A\left[\frac{m'}{4\pi G} - f_\pi^2\left(Q_N Sh'^2 r^2 + \mathcal{C} sin^2 h\right)\right.\right. \\
&\quad \left.\left. - \frac{1}{e^2}\left(\mathcal{C} Sh'^2 sin^2 h + \frac{\mathcal{I} sin^4 h}{2r^2}\right)\right] - \frac{m(\infty)}{G}\right) dt \qquad (2.25)
\end{aligned}$$

In the above, the following angular integrals have been defined.

$$\mathcal{C} = \frac{i}{2\pi}\int Tr\left(|\partial_z P|^2\right) dz d\bar{z} \qquad (2.26)$$

$$\mathcal{I} = \frac{i}{4\pi}\int (1+|z|^2)^2 Tr\left([\partial_z P, \partial_{\bar{z}} P]^2\right) dz d\bar{z} \tag{2.27}$$

2.4 Scaling

It is convenient at this point to combine the three parameters of the model (G, f_π and e), into one dimensionless coupling constant. This can be done by an appropriate scaling of the radial lengths and masses to dimensionless variables, such as

$$r \rightarrow x = e f_\pi r \tag{2.28}$$

and, similarly

$$m(r) \rightarrow \mu(x) = e f_\pi m(r) \tag{2.29}$$

As a result of these scalings we can rewrite the metric function simply as $S(x) = \left(1 - \frac{2\mu(x)}{x}\right)$.

Thus one obtains the simplified Lagrangian for the model

$$L = \frac{4\pi f_\pi}{e}\left[\int dx A\left(\frac{\mu'}{\alpha} - Q_N S h'^2 x^2 - \mathcal{C} sin^2 h(1+Sh'^2) - \frac{\mathcal{I} sin^4 h}{2x^2}\right) - \frac{\mu(\infty)}{\alpha}\right] \tag{2.30}$$

One should note that for the static solutions, which are those presented in this work, the Hamiltonian of the system is just given by $H = -L$.

2.5 The Euler-Lagrange Equations

In order to find solutions, or, more precisely, approximations to solutions of the Einstein-Skyrme model, one searches for stationary points of the action. Thus form-

ing the Euler-Lagrange equations

$$\frac{\partial L}{\partial \psi(x)} = \partial_x \frac{\partial L}{\partial \psi'(x)} \tag{2.31}$$

for the three fields $\psi(x) = A(x), \mu(x)$ and $h(x)$, one obtains

$$A' = 2\alpha A h'^2 \left(Q_N x + \frac{\mathcal{C} sin^2 h}{x} \right) \tag{2.32}$$

$$\mu' = \alpha \left(Q_N S h'^2 x^2 + \mathcal{C} sin^2 h (1 + S h'^2) + \frac{\mathcal{I} sin^4 h}{2x^2} \right) \tag{2.33}$$

and

$$A sin2h \left(\mathcal{C}(1 + S h'^2) + \frac{\mathcal{I} sin^2 h}{x^2} \right) = \left[2AS h' \left(Q_N x^2 + \mathcal{C} sin^2 h \right) \right]' \tag{2.34}$$

One should at this point note that although solutions must obey all three of these equations simultaneously, eqn. (2.34) is actually linear in the field $A(x)$ and thus the final two equations are really independent of this field. To elucidate this one performs the derivative on the right hand side of eqn. (2.34), substitutes for $A'(x)$ from eqn. (2.32) and cancels out the linear dependence on $A(x)$. Thus, defining $V(x) = (Q_N x^2 + \mathcal{C} sin^2 h)$, one obtains

$$h'' = \frac{1}{SV} \left[\frac{sin2h}{2} \left(\mathcal{C}(1 + S h'^2) + \frac{\mathcal{I} sin^2 h}{x^2} \right) - \frac{2\alpha h'^3 S V^2}{x} - S' h' V - S h' V' \right] \tag{2.35}$$

The next chapter will discuss approximate solutions to eqns. (2.32) - (2.35) at low baryon number, for the $SU(2)$ model. Note that the procedure is as follows. One first minimises the harmonic map quantities $\mathcal{C}$ and $\mathcal{I}$, over all possible harmonic maps of the required degree. This has been done for many cases and one will take these values from, [9] & [30]. These minimal values are then substituted into the field equations so that the extremal forms of the fields can be found.

Chapter 3

Low Baryon Number Configurations

3.1 Numerical Methods

The system of equations (2.32) to (2.35) comprise two first order and one second order coupled differential equations, which cannot be solved analytically. Thus numerical integration must be used. To simplify matters, the metric field $A(x)$ decouples from the differential equations for $\mu(x)$ and $h(x)$. As such the solution to these equations is independent of the solution for $A(x)$. Thus one really has to solve a second order equation for $h(x)$, coupled to a first order equation for $\mu(x)$. Once the solutions for $h(x)$ and $\mu(x)$ are known, they can then be used in the numerical integration of (2.32), to find the form of $A(x)$.

Taking the two coupled equations (2.33) & (2.35), (one second order and one first order), one requires three pieces of independent boundary information to define the solutions completely.

One has the following:

$$\begin{aligned} h(x=0) &= \pi \\ h(x=\infty) &= 0 \\ \mu(x=0) &= 0 \end{aligned} \tag{3.1}$$

One therefore possesses information about $h(x)$ at two points but no information about its derivative. This is known as a boundary value problem. A useful technique for the numerical integration of such problems is known as the *Shooting Method.*

Effectively one applies a vector of initial data at one boundary. In this case it will be ($h(0)$, $h'(0)$ and $\mu(0)$), where $h'(0)$ is a plausible estimate for the derivative of $h(x)$ at $x = 0$. One then evolves the fields radially, according to the coupled differential equations (2.33) and (2.35) until the second boundary is reached. In general, the value of the fields obtained will not correspond to the second boundary conditions. That is $h(\infty) \neq 0$. An error vector is then calculated describing the discrepancy from the required boundary condition and a suitable algorithm is used to calculate a better estimate for the initial derivative, $h'(0)$. This is then used to start the evolution from the initial boundary once again.

The process is repeated iteratively, with better and better estimates for the initial derivative calculated at each step using a suitable root finding algorithm e.g. the *dichotomic* method. Eventually a solution will be found such that the discrepancy from the final boundary condition is less than some specified tolerance. This solution for $h(x)$ and $\mu(x)$ is then accepted and can be used with the boundary condition $A(\infty) = 1$ to integrate (2.32).

3.2 Asymptotic Expansions

Unfortunately there is a caveat to the above description. Although one has the boundary information given in (3.1), a close inspection of the system of differential equations (2.32) to (2.35) reveals that the boundary values cannot be directly applied. This is because the differential equations themselves are not well defined at the point $x = 0$. (This can be true even if the solutions to the equations are well defined). Thus one has to use (3.1) to determine starting values at a small distance from the origin, $x = \delta$.

One proceeds by making a series expansion of the fields $h(x)$ and $\mu(x)$ about the origin. Thus

$$h(x) = \pi + x^p(a_1 + a_2x + ...) \tag{3.2}$$

and

$$\mu(x) = x^r(b_1 + b_2x + ...) \tag{3.3}$$

Here, one will assume nothing other than the following. That p and r are positive and, in general, non-integer powers of x and that p and r are both non-zero. This second requirement comes from the fact that the original boundary data, (3.1), must be recovered at $x = 0$.

Substituting the general expansions into the differential equations for $h(x)$ and $\mu(x)$, one can determine information about p, r, a_i and b_i by comparing terms order by order.

Starting with (2.33), the left hand side is given by μ' and thus the term of lowest order in x is

$$rb_1x^{r-1} \tag{3.4}$$

substituting the field expansions into the right hand side (and being careful to expand $sin^2 h(x)$ and $sin^4 h(x)$ about $h(x) = \pi$), one obtains a lowest order term of

$$\alpha a_1^2 (Q_N p^2 + \mathcal{C}) x^{2p} \tag{3.5}$$

Now, one notes that p and r are non-zero and there is thus no reason for the coefficient of these lowest order terms to be zero. Thus equating exponents and coefficients we have

$$r = 2p + 1 \tag{3.6}$$

$$b_1 = \frac{\alpha a_1^2}{2p+1} (Q_N p^2 + \mathcal{C}) \tag{3.7}$$

One has to be slightly careful here though. If, in some circumstance, $p = 1$ then there is another contribution to (3.5), coming from terms with order $4p - 2$ (=$2p$). In this case, the lowest order terms on the right hand side of the differential equation are

$$\alpha a_1^2 \left(Q_N p^2 + \mathcal{C} + a_1^2 \left(\frac{\mathcal{I}}{2} + \mathcal{C} p^2 \right) \right) x^{2p} \tag{3.8}$$

and thus one has

$$r = 2p + 1 \tag{3.9}$$

$$b_1 = \frac{\alpha a_1^2}{2p+1} \left(Q_N p^2 + \mathcal{C} + a_1^2 \left(\frac{\mathcal{I}}{2} + \mathcal{C} p^2 \right) \right) \tag{3.10}$$

To determine p itself, one has to turn to the second order equation for $h(x)$, (2.35). Multiplying this equation through by $S(x)V(x)$ and then substituting the the field expansions in, together with the shown fact that $r = 2p + 1$, the lowest order term on the left hand side is

$$Q_N a_1 p(p-1) x^p \tag{3.11}$$

Similarly, the lowest order term on the right hand side of (2.35) is given by

$$a_1(\mathcal{C} - 2Q_N p)x^p \tag{3.12}$$

Equating coefficients and rearranging for p (noting that p is non-negative), one obtains

$$p = \frac{-Q_N + \sqrt{Q_N^2 + 4Q_N\mathcal{C}}}{2Q_N} \tag{3.13}$$

As a result, the form of $h(x)$ and $\mu(x)$ will depend both on the number of included flavours N and the degree of the harmonic map used, as one might expect.

One proceeds as follows. Taking the specific parameters of the problem one wishes to solve, i.e. Q_N, $\mathcal{C}$, $\mathcal{I}$ and α, one can calculate the values of p, r and b_1 to obtain the explicit field expansions about the origin. Truncating after the first power of x, one uses the expansions to calculate boundary data near the origin, at $x = \delta$. One applies this data and numerically integrates the coupled differential equations according to the previously described prescription. The estimated parameter, which is found via the *Shooting Method* is, in this case, a_1.

Once solutions have been found for $\mu(x)$ and $h(x)$, the solution for $A(x)$ can be found subject to the condition $A(\infty) = 1$.

3.3 $SU(2)$ Solutions

3.3.1 Solutions with Baryon number 1

Solutions to the field equations have been found numerically for a variety of baryon numbers. For a single baryon, in the $SU(2)$ model, the harmonic map quantities are minimised at $\mathcal{C} = \mathcal{I} = 1$. Consequently,it can be shown that the ansatze are completely equivalent to the Hedgehog Ansatze, [9]. One would therefore expect the solutions obtained to be identical to those previously found by Bizon & Chmaj, [25].

Table 3.3.1 lists information about the solutions obtained at a variety of coupling values, α. Listed are the values of the shooting parameter, $h'(0)$ $(=a_1)$, the minimum value of the metric function $S(x) = \left(1 - \frac{2\mu(x)}{x}\right)$ (used to check for the presence of horizons) and the value of the ADM mass per baryon. This was calculated using $\frac{M_{ADM}}{B} = \frac{4\pi\mu(\infty)}{\alpha}$ as in [25].

The data identically reproduces that obtained by Bizon & Chmaj, as expected. The main features to note are the affects of the coupling value α. Firstly, increasing α effectively increases the strength of gravity in the model. This is mirrored by a reduction in S_{min} caused by a greater warping of space by the self-gravitating Skyrmion. Further, the ADM mass reduces as α increases, showing the gravitational binding energy of the Skyrmion.

Perhaps the most striking phenomenon is that for each value of α, there exist two solutions. The two branches of solutions identify at a specific value of the coupling and above this value, no other solution can be obtained. This value of the coupling is known as the critical coupling α_{crit}.

Remembering that increasing α is the same as increasing the strength of gravity, one might conclude that the critical coupling is the point at which gravity becomes so strong that a singularity forms. However two questions are not answered by this explanation. 'Why are there two branches of solutions below α_{crit}?' and 'Why is S_{min} far from zero at the critical coupling, if a horizon is formed?'. One concludes that there must be another explanation for this phenomenon.

The answer is that the two branches represent two different local extrema of the action. The upper being an unstable branch and the lower being globally regular solitons that are the stable minima. The difference in energy between these two types of solution reduces as the coupling is increased. Eventually, at the critical coupling, the two branches coincide. The different solutions annihilate and no further solutions can be found. The phenomena is detailed in [25].

α	$h'(0)$	S_{min}	M_{ADM}/B
1×10^{-6}	-2.0075	1.0000	72.9238
0.0001	-2.0081	0.9994	72.9004
0.01	-2.0798	0.9328	70.5300
0.02	-2.1783	0.8587	68.0462
0.04	-2.7820	0.6156	62.4090
0.0403	-2.8602	0.5975	62.3008
0.040375	-2.9158	0.5856	62.2727
0.040378	-2.9269	0.5833	62.2715
0.040378	-2.9337	0.5819	62.2715
0.040375	-2.9450	0.5797	62.2727
0.0403	-3.0055	0.5680	62.3025
0.04	-3.1033	0.5506	62.4271
0.02	-5.8360	0.3591	80.6829
0.01	-8.8605	0.3850	109.4264

Table 3.1: *Numerically obtained solutions for a B=1 self-gravitating Skyrmion. One should note that the physical mass per baryon can be calculated as* $\frac{M_{ADM} f_\pi}{B\epsilon}$

The actual form of the solutions for the fields $h(x)$, $\mu(x)$ and $A(x)$ are shown in figures 3.2 and 3.3. These were obtained at couplings of $\alpha = 1 \times 10^{-6}$ and $\alpha_{crit} = 0.040378$, respectively.

One can see that fields change over a smaller region, at the higher coupling value. This represents a shrinking in the size of the Skyrmion, due to gravitational

compression. The readers attention is drawn to the plots of $A(x)$. One notes that the actual boundary condition $A(\infty) = 1$ appears not to have been satisfied. This is however, simply an artefact of the integration procedure. The solutions for $h(x)$ and $\mu(x)$ are, as previously stated, independent of the solution for $A(x)$. Thus these solutions were obtained first and satisfy the correct boundary conditions.

When the solution for $A(x)$ was obtained, a boundary condition of $A(0) = 1$ was used for computational ease. This does not affect the form of any solutions and the precise solution for $A(x)$ can be obtained by the scaling $\frac{A(x)}{A(\infty)}$.

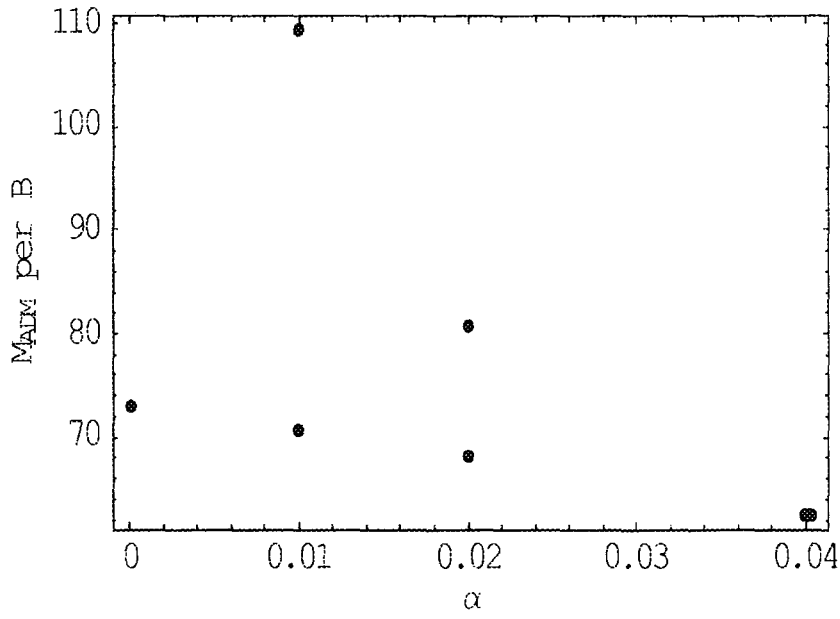

Figure 3.1: *The two branches of solutions obtained for B=1.*

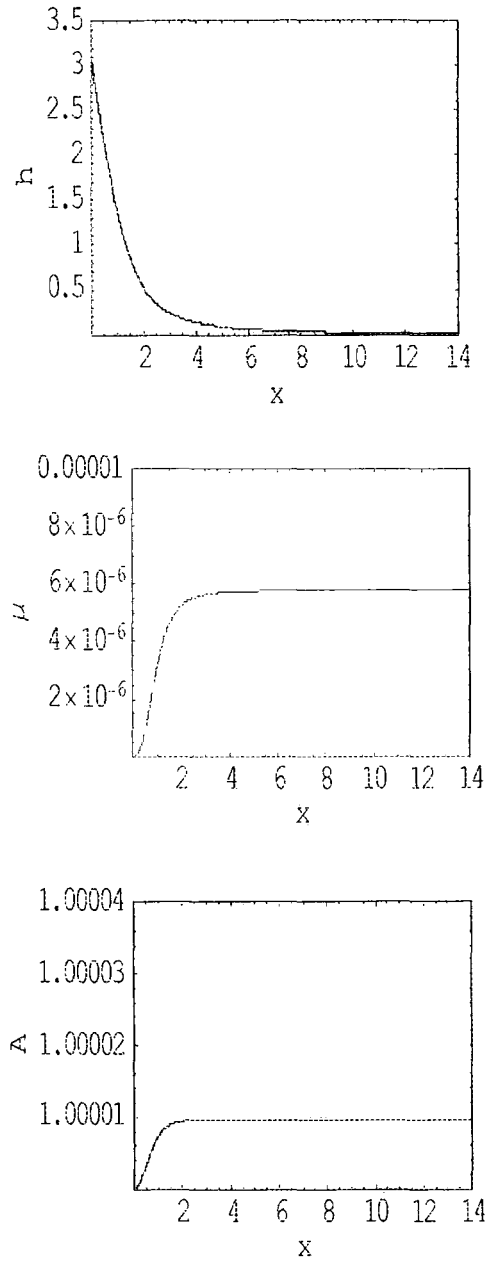

Figure 3.2: *Lower branch numerical solutions for the fields $h(x)$, $\mu(x)$ and $A(x)$ for B=1 at a coupling of $\alpha = 1 \times 10^{-6}$.*

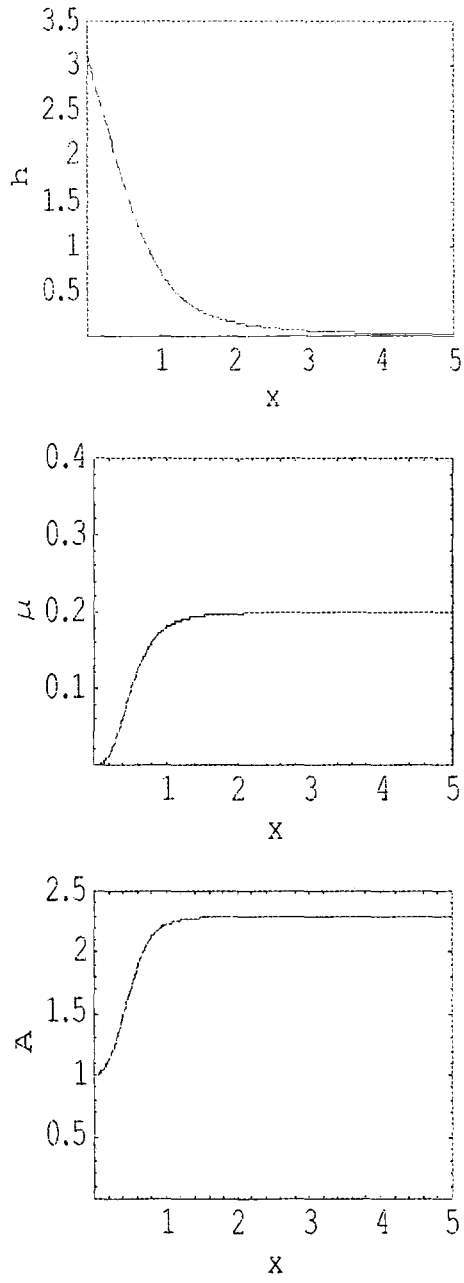

Figure 3.3: *Lower branch numerical solutions for the fields* $h(x)$, $\mu(x)$ *and* $A(x)$ *for* B=1 *at the critical coupling of* $\alpha_{crit} = 0.040378$.

3.3.2 B=2

For an $SU(2)$ Skyrmion containing two baryons, the quantities $\mathcal{C}$ and $\mathcal{I}$ are minimised at 2 and 5.81, respectively [9]. The flat space solution is toroidal in form and has an axial symmetry. Using these values, solutions for harmonic map generated self-gravitating Skyrmions with B=2, were obtained. The relevant data is summarised in table 3.3.2.

There is a crucial difference here, between the solutions obtained using the harmonic map ansatze, and those obtained previously by Bizon & Chmaj for the hedgehog ansatze. They found that for all solutions with B$\geq$ 2, the ADM mass per baryon was higher, than that for $B = 1$. Thus no self-gravitating bounds states could form as they would be unstable against decay into individual solitons.

This is not the case for the data in table 3.3.2. Clearly, comparing the solutions obtained at identical values of the coupling, $M_{ADM}(B = 2) < 2M_{ADM}(B = 1)$. This opens up the possibility once again, that solutions resembling baryon stars, could exist within the Einstein-Skyrme model.

α	$F'(0)$	S_{min}	M_{ADM}	M_{ADM}/B
1×10^{-6}	-1.4636	1.0000	143.0924	71.5462
0.0001	-1.4644	0.9990	143.0338	71.5169
0.001	-1.4721	0.9903	142.4998	71.2499
0.01	-1.5642	0.8995	137.0590	68.5295
0.02	-1.7241	0.7865	130.6999	65.3499
0.032	-2.3219	0.5765	122.0191	61.0096
0.0326	-2.5099	0.5408	121.4867	60.7434
0.03266	-2.5747	0.5302	121.4303	60.7151
0.032668	-2.6059	0.5253	121.4226	60.7113
0.032668	-2.6148	0.5240	121.4226	60.7113
0.03266	-2.6471	0.5192	121.4304	60.7152
0.0326	-2.7199	0.5090	121.4906	60.7453
0.032	-2.9903	0.4769	122.1390	61.0695
0.02	-6.0789	0.3403	145.3254	72.6627
0.01	-11.7721	0.2881	196.9852	98.4926
0.001	-71.4731	0.2497	600.7141	300.3570

Table 3.2: *Numerically obtained solutions for a B=2 self-gravitating Skyrmion. One should note that the physical mass per baryon can be calculated as* $\frac{M_{ADM} f_\pi}{Be}$

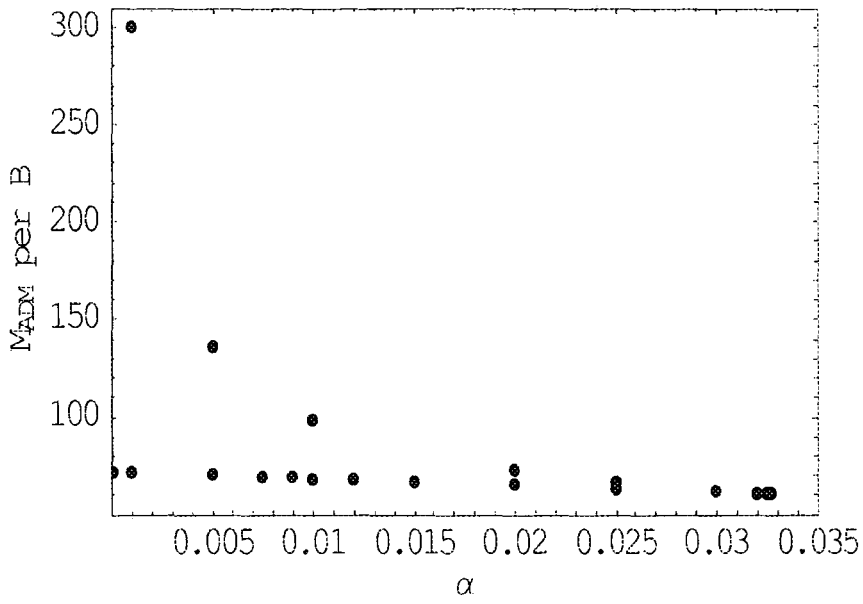

Figure 3.4: *The two branches of solutions obtained for B=2.*

Other features to note are as follows. Again there exists two branches of solutions. However, as the baryon number has increased, the critical coupling has decreased from 0.040378 to 0.032668.

The form of the individual fields are given in figures 3.5 and 3.6. One notes that the solutions represent slightly larger Skyrmions than for the B=1 case. This would be as expected in order to accommodate the extra baryon and is akin to the flat space solutions [9].

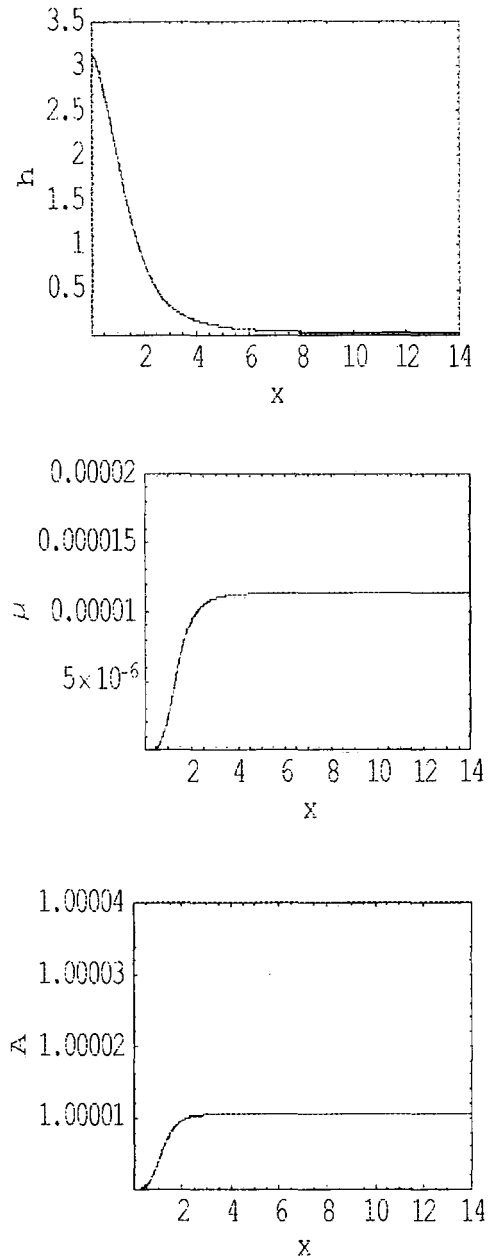

Figure 3.5: *Lower branch numerical solutions for the fields $h(x)$, $\mu(x)$ and $A(x)$ for B=2 at a coupling of $\alpha = 1 \times 10^{-6}$.*

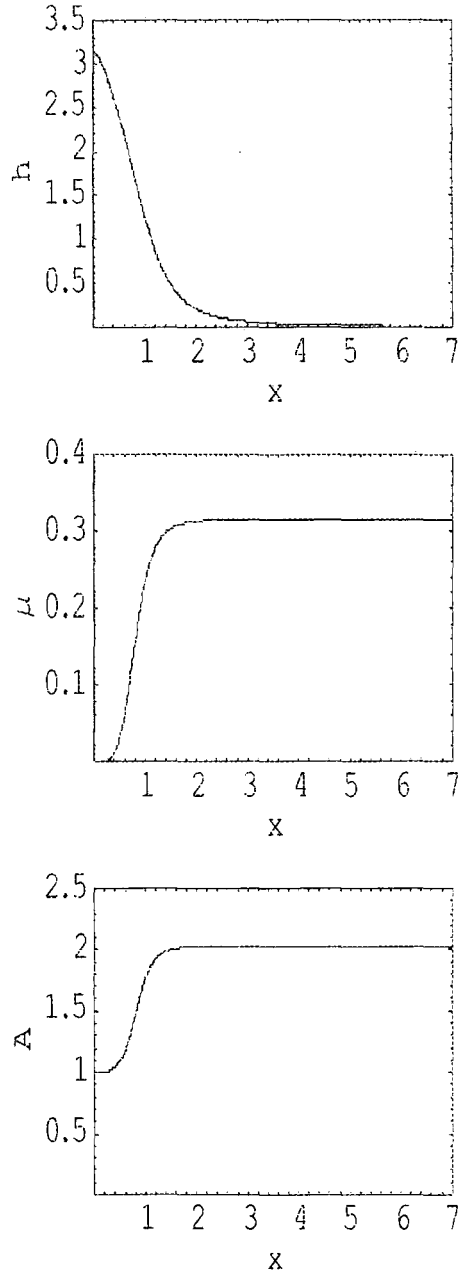

Figure 3.6: *Lower branch numerical solutions for the fields $h(x)$, $\mu(x)$ and $A(x)$ for B=2 at the critical coupling of $\alpha_{crit} = 0.032668$.*

3.3.3 B=3

At B=3, the situation is similar. The minimal map quantities $\mathcal{C}$ and $\mathcal{I}$ are 3 and 13.58 [30]. Again two branches of solutions exist but this time the critical coupling has been reduced to 0.027413.

Importantly, the solutions are even more energetically favourable than both the B=1 and B=2 cases. For example, at a coupling of $\alpha = 1 \times 10^{-6}$, the ADM mass per baryon is 70.1379. There is seen to be almost a 2 per cent binding (reduction in $\frac{M_{ADM}}{B}$) over the value of 71.5462 for B=2. Moreover there is an almost 4 per cent binding compared to the value of 72.9238, for the single baryon solution.

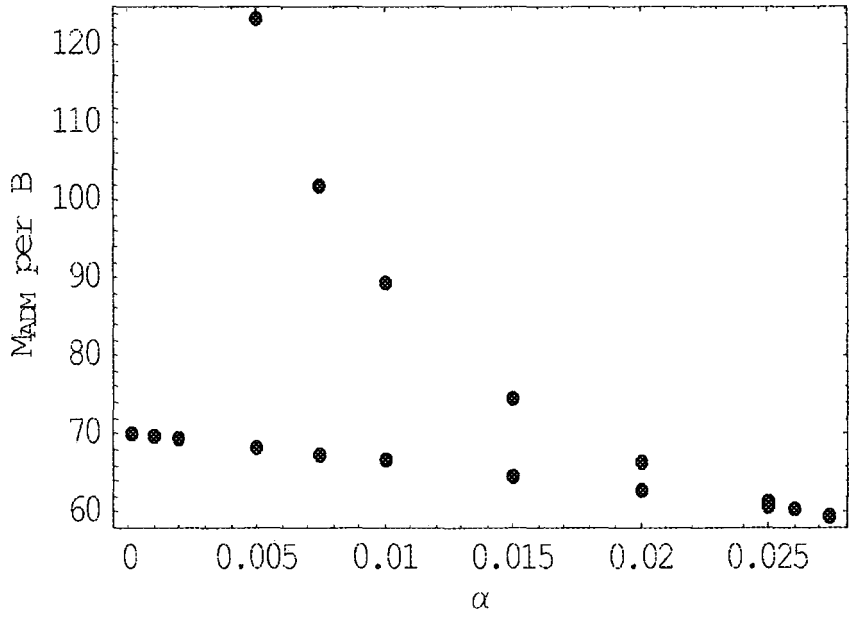

Figure 3.7: *The two branches of solutions obtained for B=3.*

α	$F'(0)$	S_{min}	M_{ADM}	M_{ADM}/B
1×10^{-6}	-0.9864	1.0000	210.4136	70.1379
0.0001	-0.9872	0.9988	210.3109	70.1036
0.001	-0.9954	0.9876	209.3750	69.7917
0.01	-1.0996	0.8712	199.7877	66.5959
0.02	-1.3173	0.7208	188.3560	62.7853
0.0274	-2.0827	0.5109	178.4857	59.4952
0.02741	-2.1090	0.5071	178.4688	59.4896
0.027413	-2.1254	0.5047	178.4637	59.4879
0.027413	-2.1508	0.5012	178.4638	59.4879
0.02741	-2.1679	0.4989	178.4689	59.4896
0.0274	-2.1962	0.4952	178.4863	59.4954
0.02	-5.1473	0.3470	199.2991	66.4330
0.01	-14.1405	0.2807	267.9163	89.3054

Table 3.3: *Numerically obtained solutions for a B=3 self-gravitating Skyrmion. One should note that the physical mass per baryon can be calculated as* $\frac{M_{ADM} f_\pi}{Be}$

3.3.4 B=4

The minimal values of $\mathcal{C}$ and $\mathcal{I}$ are 4 and 20.65, for the $B = 4$ Skyrmion [30]. Using these values, two branches of solutions, annihilating at a critical coupling of $\alpha_{crit} = 0.023673$, were obtained. Again the solutions obtained, which are approximations to true self-gravitating Skyrmions, are bound states. That is, the ADM mass per baryon is less, at each α, than for B=1,2 or 3.

Interestingly, the value of S_{min}, at the critical coupling, is still far from zero, at 0.4976. Thus total gravitational collapse still doesn't occur and the system is horizon free.

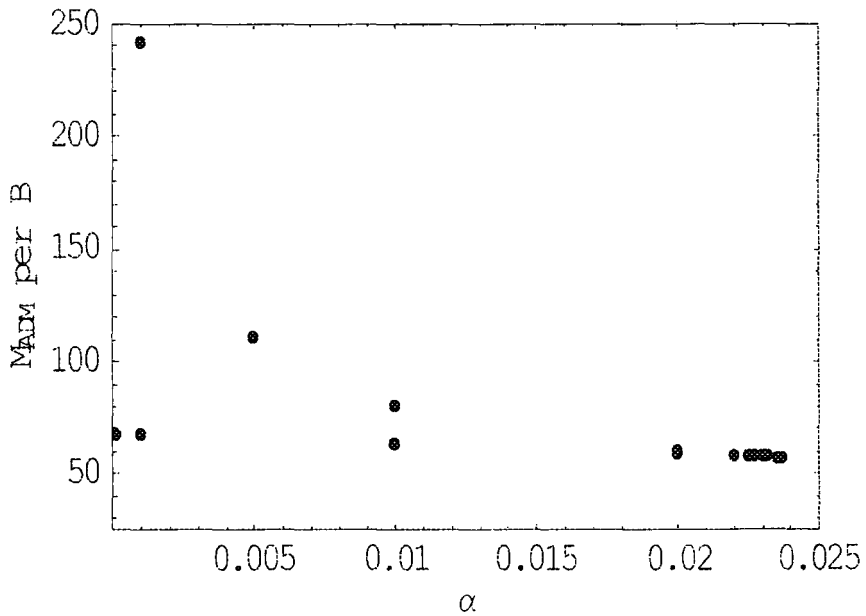

Figure 3.8: *The two branches of solutions obtained for B=4.*

α	$F'(0)$	S_{min}	M_{ADM}	M_{ADM}/B
1×10^{-6}	-0.8058	1.0000	269.2061	67.3153
0.0001	-0.8069	0.9985	269.0550	67.2638
0.001	-0.8169	0.9853	267.6787	66.9197
0.01	-0.9538	0.8460	253.4973	63.3743
0.02	-1.3277	0.6546	236.1382	59.0346
0.0235	-1.9302	0.5268	228.9570	57.2393
0.02367	-2.1479	0.5002	228.5489	57.1372
0.023673	-2.1726	0.4976	228.5414	57.1354
0.023673	-2.2037	0.4943	228.5414	57.1354
0.0235	-2.5104	0.4668	229.0054	57.2514
0.02	-4.7424	0.3743	241.5351	60.3838
0.01	-19.6255	0.2844	321.1271	80.2818
0.001	-472.9266	0.2370	967.8879	241.9720

Table 3.4: *Numerically obtained solutions for a B=4 self-gravitating Skyrmion. One should note that the physical mass per baryon can be calculated as* $\frac{M_{ADM} f_\pi}{Be}$

3.3.5 B=17

The B=17 Skyrmion was studied because it presents an interesting solution in flat space possessing icosahedral symmetry and an unusually low energy [31]. The harmonic map quantities $\mathcal{C}$ and $\mathcal{I}$ are minimised for this case, with values of 17 and 363.4.

One again finds two branches of solutions. This time α_{crit} is 0.011417. All solutions are again energetically favourable, when their ADM mass per baryon is compared to that of the lower baryon number solutions already presented. One is left to conclude that, in contrast to the hedgehog self-gravitating Skyrmions, those obtained using the harmonic map ansatze become more and more bound as more baryons are added. Therefore none are unstable to break-up.

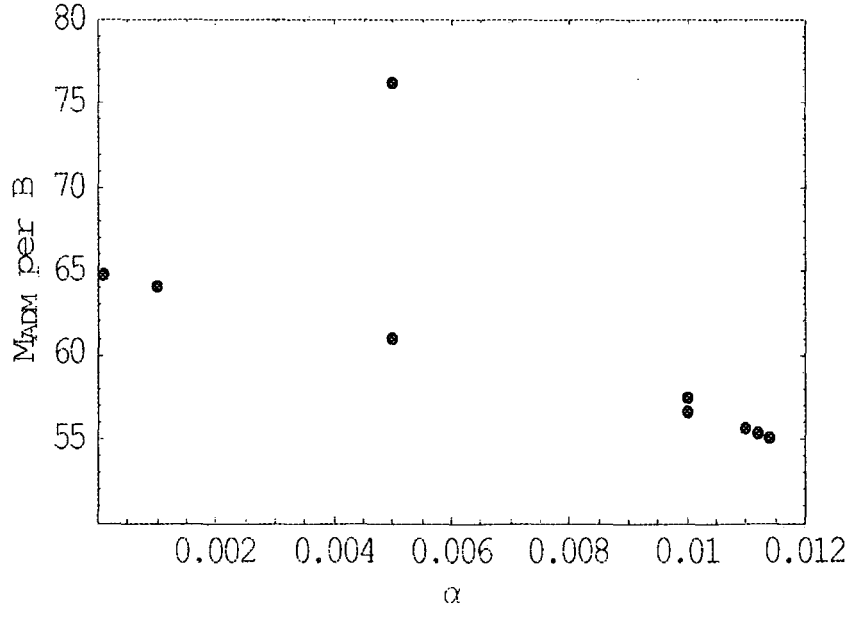

Figure 3.9: *The two branches of solutions obtained for B=17.*

α	$F'(0)$	S_{min}	M_{ADM}	M_{ADM}/B
0.0001	-0.0036	0.9964	1099.8185	64.6952
0.001	-0.0039	0.9642	1088.2619	64.0154
0.005	-0.0054	0.8149	1035.0773	60.8869
0.01	-0.0121	0.5874	960.9968	56.5292
0.0112	-0.0212	0.4923	939.9595	55.2917
0.0114	-0.0285	0.4540	936.0071	55.0592
0.011417	-0.0314	0.4431	935.6499	55.0382
0.011417	-0.0336	0.4358	935.6502	55.0382
0.0114	-0.0371	0.4252	936.0272	55.0604
0.0112	-0.0530	0.3922	940.8128	55.3419
0.011	-0.0653	0.3755	946.0005	55.6471
0.01	-0.1353	0.3291	976.5562	57.4445

Table 3.5: *Numerically obtained solutions for a B=17 self-gravitating Skyrmion. One should note that the physical mass per baryon can be calculated as* $\frac{M_{ADM} f_\pi}{Be}$

3.3.6 General Observations

There are several general comments that can be made regarding the approximations to self-gravitating Skyrmions thus far presented. The first thing to note is the relationship between the critical coupling and the baryon number. Bizon & Chmaj observed that the critical coupling decreased as $\alpha_{crit} \approx 0.040378B^{-2}$ [25]. However, for the harmonic map generated solutions, one observes $\alpha_{crit} \approx 0.040378B^{-\frac{1}{2}}$. This is shown in figure 3.10.

This is a significant improvement over the hedgehog Skyrmions. Quantitatively, it means that for a given value of the critical coupling, if a hedgehog Skyrmion can accommodate B baryons, it's harmonic map generated counterpart can hold B^4 baryons.

A crucial difference between the solutions presented here and those of Bizon & Chmaj, is that of energy. Baryon stars were ruled out as structures that could be studied in the Einstein-Skyrme model, as it was simply not energetically favourable to have multi-baryon states. However, by taking more suitable ansatze for the Skyrme field, one sees that the converse is true. For all baryon numbers greater than 1, the ADM mass per baryon is less than that of the $B = 1$ Skyrmion, as shown in figure 3.11. Bound multi-baryon self-gravitating states are admitted and the possibility of using the model to study baryon stars, is once again opened.

There are some concerns here. Firstly, the Euler-Lagrange equations become increasingly difficult to solve numerically, as the baryon number increases. That is why solutions only up to B=17, have been presented so far. In fact these solutions were of considerable difficulty to obtain. Clearly a better method is to be found if

one wishes to study Skyrmions of high enough baryon number to be astrophysically relevant.

The second concern is one of symmetry. The metric ansatze that has been used possesses spherical symmetry. Naturally one would expect this of a baryon star. The hedgehog ansatze give spherically symmetric solutions automatically, though they are energetically unfavourable.

Using the harmonic map ansatze allows bound states but does not directly lead to spherical symmetry. For example, the B=2 Skyrmion is known to be toroidal in flat space. Similarly, B=3 is tetrahedral, whilst B=4 is a cube [9]. This mismatching of symmetry must be overcome if one is to credibly study baryon stars. Both challenges will be addressed in this next chapter.

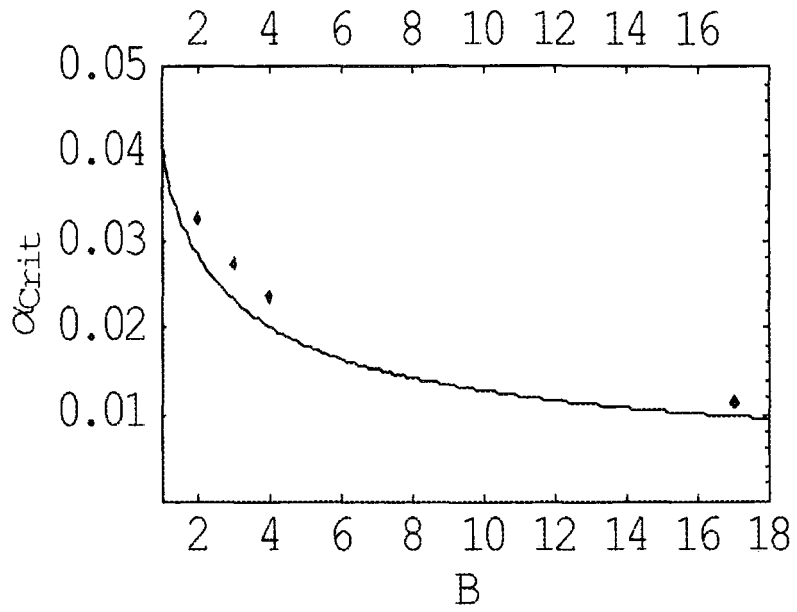

Figure 3.10: *The behaviour of α_{crit} as a function of the baryon number. Shown by dots are the obtained values for $B = 1, 2, 3, 4$ & 17, whilst the curve represents the function $\alpha_{crit} = 0.040378 B^{-\frac{1}{2}}$.*

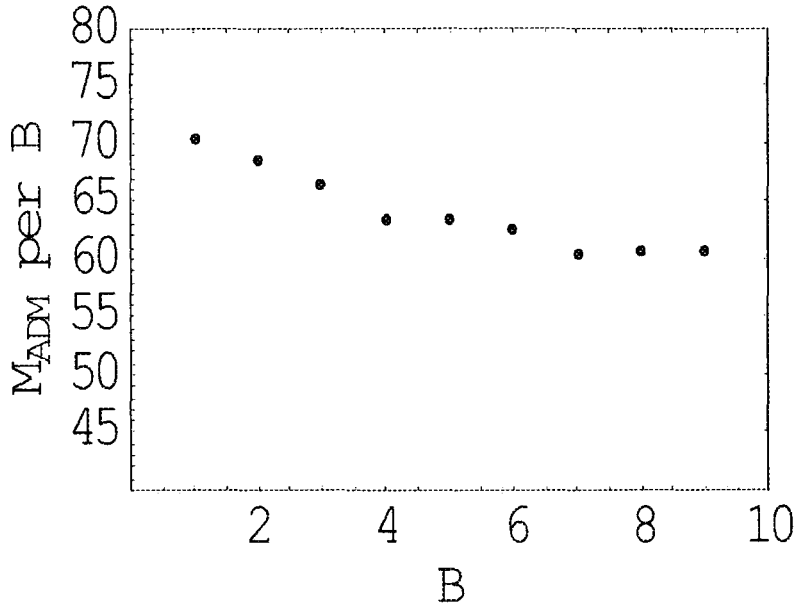

Figure 3.11: *The behaviour of M_{ADM} as a function of the baryon number at fixed $\alpha = 0.01$. One observes that, in general, multi-baryon states become more bound as more baryons are added. The trend is distorted by the low energies of the $B = 4$ and $B = 7$ Skyrmion. However this is to be expected as their flat-space counterparts are also known to be especially bound [9].*

Chapter 4

High Baryon Number Configurations

In the previous chapter it was demonstrated that the approximations obtained to true gravitating Skyrmions, generated from rational maps, did indeed become more bound with increasing baryon number. This qualitative behaviour is remarkably different to that obtained in [25] & [26] for Hedgehog Skyrmions and re-opens the possibility for using the Skyrme model to describe baryon stars.

Of course there are still difficulties to overcome. Firstly, the approximate solutions presented in the previous chapter are not truly spherically symmetric as one would wish for a baryon star. Also there are technical challenges involved with solving the Euler-Lagrange equations at high baryon number. This chapter will explore these issues and discuss possible ways of overcoming such challenges.

4.1 The shape and form of high baryon number configurations

The first area for improvement of the approximations to self-gravitating multi-baryon Skyrmions presented thus far is related to their spatial symmetry. In constructing the model, ansatze were taken for both the Skyrme field and the metric. The Harmonic Map Ansatze were taken for the Skyrme field because they give a better approximation to true multi-baryon Skyrmions in flat space than the Hedgehog Ansatze [10]. This leads directly to the possibility of bound multi-baryon configurations in the case with gravity.

The metric ansatze were that it should be staticity and spherical symmetry. These would be appropriate properties when trying to describe something like a baryon star.

However, the informed reader might here spot an area for careful consideration. If one studies Skyrmions constructed from Harmonic Maps in flat space, they will find non-spherical baryon distributions [9], [30] [31]. These symmetries are identical to those of true Skyrmions. Thus the question arises: Is it really appropriate to use a spherical metric?

There are three justifications to support the choice of metric. Firstly, one is not claiming that the configurations presented in Chapter 3 are anything other than approximations to true self-gravitating Skyrmions. As such they will have an energy higher than the true solutions to the model. However, the complexity of the Skyrme model means that any practical progress can only be made using ansatze for the Skyrme field such as the Hedgehog or Harmonic Map Ansatze. As such, one is

normally only finding approximations to Skyrmions, with or without gravity.

Secondly, one must consider that in the situation of interest, i.e. the construction of a realistic baryon star, a very small value of the coupling α should be taken. One is reminded that for realistic values of the Skyrme and Newton constants, a plausible value for α is $\alpha = 7.3 \times 10^{-40}$. At such low couplings the effect of gravity is really a small perturbation to the Skyrme model. As such, the small mismatch in the symmetry of the fields is not significant.

One of course could argue that even taking a small coupling constant, the effects of gravity should be far from small at very high baryon numbers. This will be seen to be correct. However, this leads directly to the final and most important justification for the choice of metric.

Throughout this research the goal has been to demonstrate the possibility of and then to construct baryon stars in the Einstein-Skyrme model. As such one is really interested in configurations containing extremely high numbers of baryons. For example, a typical neutron star might contain in the region of 10^{50} neutrons [32].

Now Battye and Sutcliffe, whilst investigating Skyrmions generated by the *Rational Map Ansatze* (which are equivalent to the Harmonic Map Ansatze for the $SU(2)$ model), discovered interesting spatial symmetries. Minimal energy solutions with B greater than six baryons (with the exception of two cases) possessed a shell-like structure, with the baryon density distributed solely over the surface of the shell. Interestingly, the baryon density on the shell is distributed along the edges of 12 pentagons and $2B - 14$ hexagons [30]. These configurations very much resemble the *fullerene cages* that exist in Carbon chemistry.

As the topological charge increases, the baryon density is effectively concentrated on an increasingly tight lattice distributed over the shell [31], [33], [34]. Thus for the case of interest in this thesis, very large baryon number configurations should possess the underlying spherical symmetry of the shell. Approximate spherical symmetry is restored and the choice of metric that has been used is appropriate.

There is a further technical challenge here. The numerical solution of the Euler-Lagrange equations (2.32) to (2.35) becomes increasingly difficult as more and more baryons are included. This is because the radius of the shell structure of the solution becomes very large, whilst the width of the shell is comparatively very small. In practice this means that the fields $h(x)$, $\mu(x)$ and $A(x)$ change over a very small region of the full integration interval. This makes the shooting algorithm used very sensitive to good initial information and the practical utility of the method is poor.

The problem is highlighted in Figs. 4.1 to 4.3. This solution set was obtained using the shooting algorithm for the case $B = 2 \times 10^6$ and $\alpha = 1 \times 10^{-6}$ and typify the form of the fields as the baryon number becomes large. The fields stay constant until a large value of the scaled radial coordinate x, in this case until $x \approx 1219$. The fields then change rapidly and assume another constant value which is continued for an infinite radius.

It is important, for what will come later, to note two things. Firstly, all three fields begin and end their transformation together. Secondly, the centre of the transformation, for the case shown, is at a radial position of $x \approx 1223$, whereas the width of the transformation region is ≈ 3. This means that the ratio of the width to the radius is $< 2.5 \times 10^{-3}$. Even at this relatively modest baryon number

of 2×10^6, one can clearly see the difficulties because of the difference in scale. Therefore numerical integration of the Euler-Lagrange equations for the order of baryon number one is really interested in, is practically impossible.

There is another way to find approximate solutions, motivated by the work of Kopeliovich [33], [34]. Using the known shell structure of solutions, Kopeliovich demonstrated a way of finding bounds on the energy of the solutions analytically. The Hamiltonian of the Skyrme model can not be integrated directly. However, by constructing ansatze for the fields of interest it may be possible to obtain the energy explicitly.

Kopeliovich studied the Skyrme model without gravity, thus having only one field to deal with, the profile $h(x)$. Ansatze were made for $h(x)$ which resembled a shell-like or domain wall solution and which depended on free parameters relating to the dimensions of the shell. This allowed the Hamiltonian to be integrated. Bounds on the energy of solutions could then be found by minimising the energy with respect to the free parameters of the ansatze.

Clearly Figs. 4.1 to 4.3 show that the shell-like structure of solutions is also inherent in the Einstein-Skyrme model. Thus, although ansatze will be used that are different to Kopeliovich's, one will proceed in a similar manner.

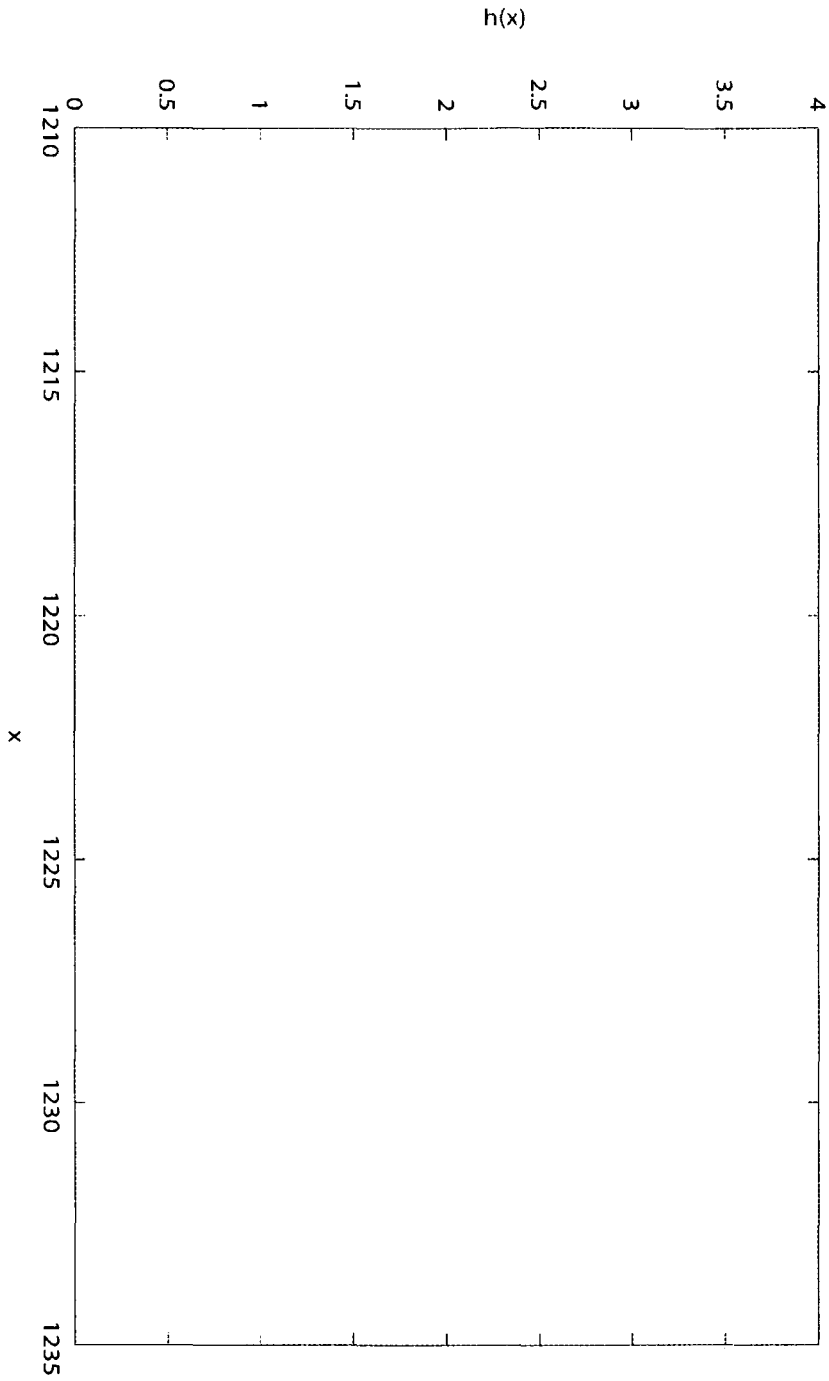

Figure 4.1: *Numerical solutions for* $h(x)$ *in the case of* $\mathcal{B} = 2 \times 10^6$ *and* $\alpha = 1 \times 10^{-6}$. *Clearly exhibited is the large radius and small width over which the fields change, showing the shell-like structure of the Skyrmion*

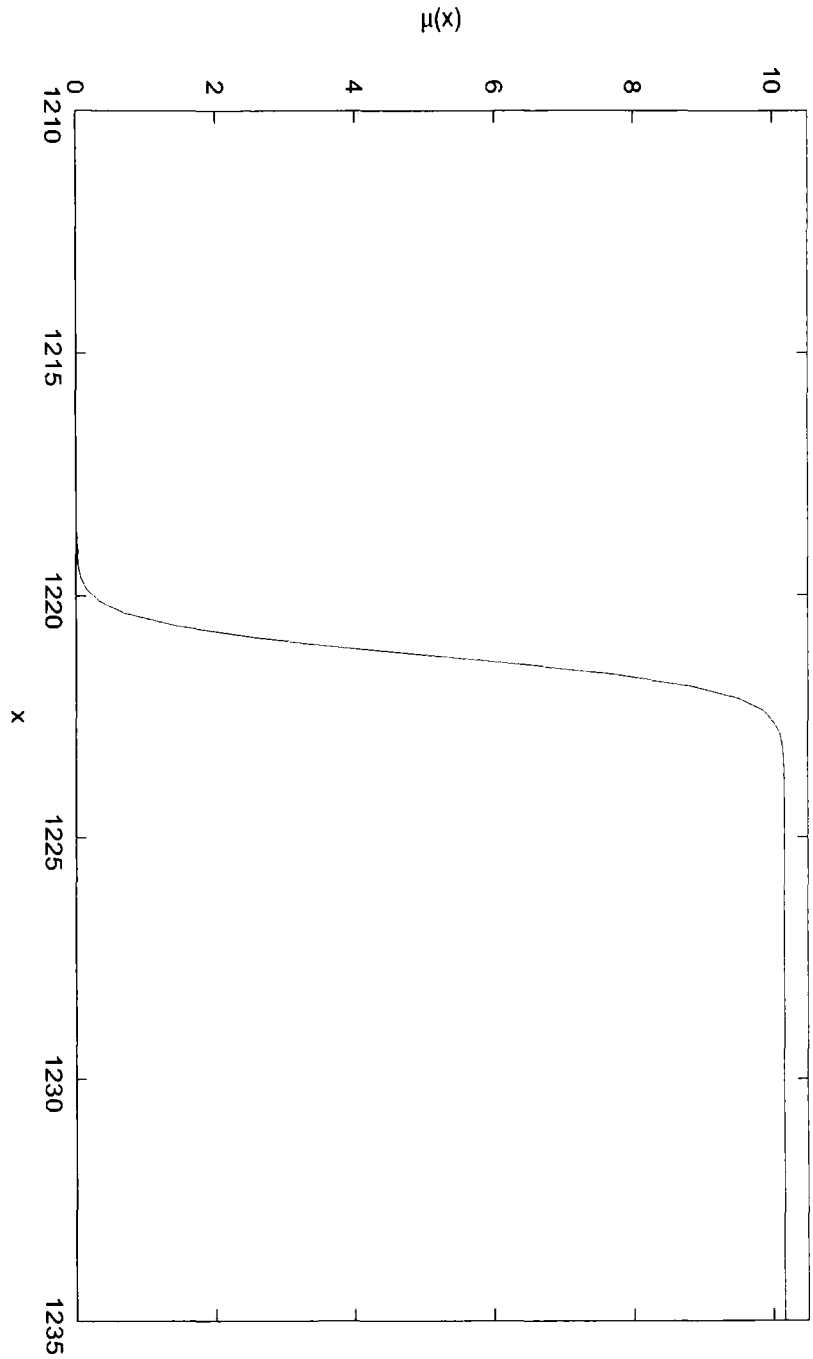

Figure 4.2: *Numerical solutions for $\mu(x)$ in the case of $\mathcal{B} = 2 \times 10^6$ and $\alpha = 1 \times 10^{-6}$. Clearly exhibited is the large radius and small width over which the fields change, showing the shell-like structure of the Skyrmion*

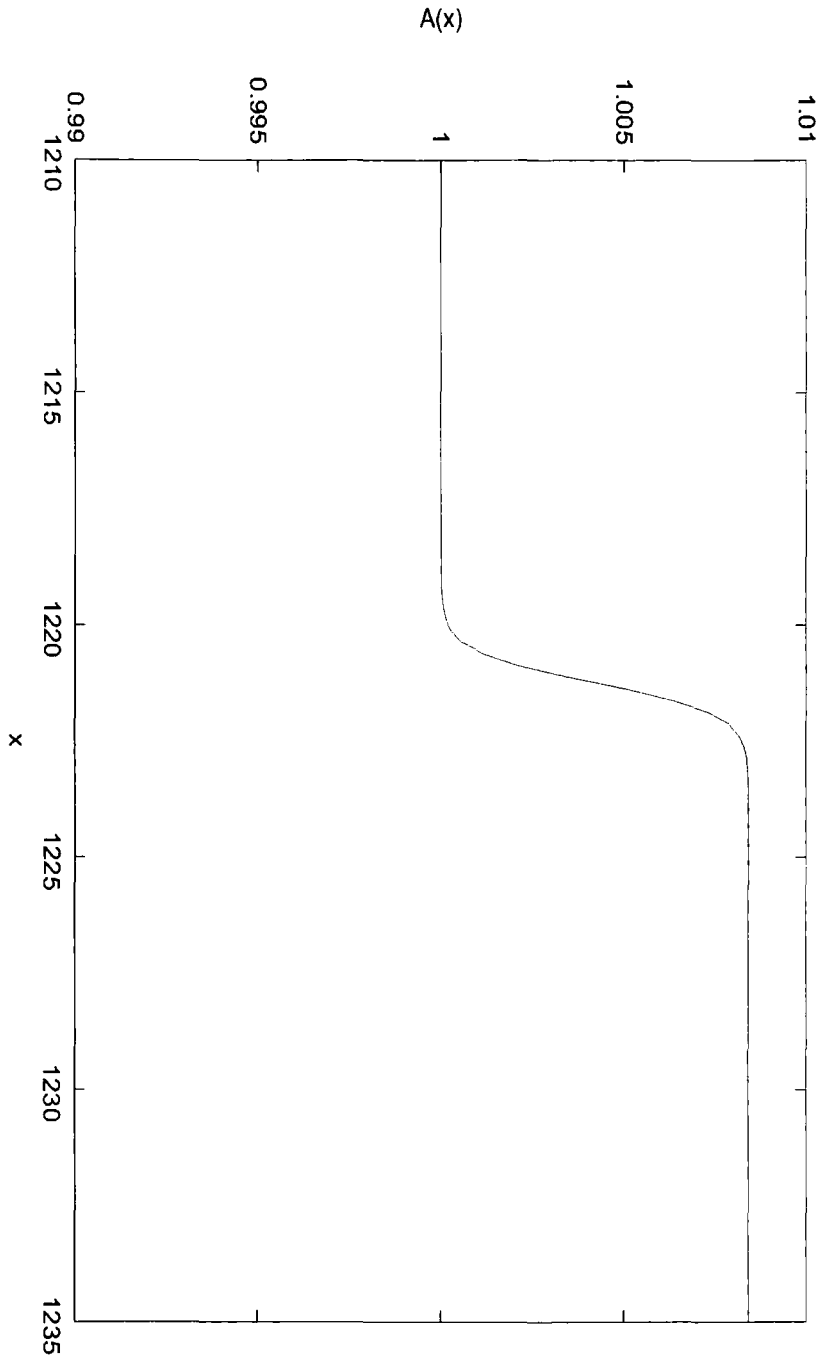

Figure 4.3: *Numerical solutions for* $A(x)$ *in the case of* $\mathcal{B} = 2\times10^6$ *and* $\alpha = 1\times10^{-6}$. *Clearly exhibited is the large radius and small width over which the fields change, showing the shell-like structure of the Skyrmion*

4.2 The Ramp Ansatze

So in order to find approximate solutions in the high baryon number regime, where the direct numerical solution of the Euler-Lagrange equations becomes difficult, it is convenient to use ansatze for the fields of interest. Obviously, any such ansatze should possess the general features discussed above.

Thus the following *Ramp Ansatze* were used for the fields $h(x)$, $\mu(x)$ and $A(x)$.

$$h(x) = \begin{cases} \pi & 0 \leq x < x_0 - \frac{W}{2} \\ \frac{\pi}{2} - (x - x_0)\frac{\pi}{W} & x_0 - \frac{W}{2} \leq x < x_0 + \frac{W}{2} \\ 0 & x \geq x_0 + \frac{W}{2} \end{cases}$$

$$\mu(x) = \begin{cases} 0 & 0 \leq x < x_0 - \frac{W}{2} \\ \frac{M}{2} + (x - x_0)\frac{M}{W} & x_0 - \frac{W}{2} \leq x < x_0 + \frac{W}{2} \\ M & x \geq x_0 + \frac{W}{2} \end{cases}$$

$$A(x) = \begin{cases} A_0 & 0 \leq x < x_0 - \frac{W}{2} \\ \frac{1+A_0}{2} + (x - x_0)\frac{1-A_0}{W} & x_0 - \frac{W}{2} \leq x < x_0 + \frac{W}{2} \\ 1 & x \geq x_0 + \frac{W}{2} \end{cases}$$

In the above there are four free parameters which define the exact form of the fields. These are W, the width of the shell over which the fields change, x_0, the radial position of the centre of this shell, M, the value of $\mu(x)$ at infinity and A_0 the value that $A(x)$ must take at the origin in order to ensure that $A(\infty) = 1$.

One should note here that, according to the ansatze, all fields change over the same region. This was as motivated by the previous numerical results. Further, one has explicitly taken the situation that there is no additional central mass around

which the Skyrmion gravitates. This is different from the case discussed by Luckock & Moss [12]. To change to this setup the Ramp ansatze have to be modified by adding a constant mass to the field $\mu(x)$.

The procedure for finding approximate solutions using the above ansatze is as follows. Instead of numerically integrating the field equations (2.32)-(2.35) one substitutes the Ramp ansatze into the reduced Hamiltonian for the model ((2.30) up to a change of sign) and attempts to integrate to find a closed expression for the energy. If such an expression can be found then one proceeds to find its stationary points. The resulting values of the parameters should characterise the approximate solutions for given values of the baryon number and coupling α etc.

One should not view this as an attempt to find minimal energy solutions (as this would be inappropriate for a gravitational system). However, the procedure is largely equivalent to finding solutions to the Euler-Lagrange equations. This is because in that approach one finds solutions which extremise the action, but as one is interested only in static field configurations, this amounts to finding stationary points of the energy functional.

The point of departure for the method outlined is the reduced Hamiltonian of the system of self-gravitating Skyrmions. From the expression for the Lagrangian (2.30), one obtains the following Hamiltonian (in which the arguments of all fields are explicitly stated).

$$H = -\frac{4\pi f_\pi}{e}\left[\int dx A(x)\left(\frac{\mu(x)'}{\alpha} - Q_N S(x)h(x)'^2x^2 - \mathcal{C}sin^2h(x)[1+S(x)h(x)'^2] - \frac{\mathcal{I}sin^4h(x)}{2x^2}\right) - \frac{\mu(\infty)}{\alpha}\right] \tag{4.1}$$

Ignoring the multiplicative factor $-\frac{4\pi f_\pi}{e}$, the expression comprises a radial integral of four distinct terms along with the boundary contribution $-\frac{\mu(\infty)}{\alpha}$. For simplicity, these terms will be dealt with separately and labelled as

$$H_1 = \int_0^\infty A(x)\frac{\mu(x)'}{\alpha}dx \tag{4.2}$$

$$H_2 = -\int_0^\infty A(x)Q_N S(x)h(x)'^2x^2dx \tag{4.3}$$

$$H_3 = -\int_0^\infty A(x)\mathcal{C}sin^2h(x)[1+S(x)h(x)'^2]dx \tag{4.4}$$

$$H_4 = -\int_0^\infty \frac{A(x)\mathcal{I}sin^4h(x)}{2x^2}dx \tag{4.5}$$

$$H_5 = -\frac{\mu(\infty)}{\alpha} \tag{4.6}$$

The first term contains the first derivative of the mass field. Noting the form of $\mu(x)$ from (4.2), it is clear that because the mass field only changes over the width of the shell, the integrand in H_1 vanishes everywhere except over the shell. The first contribution to the energy is thus

$$H_1 = \int_{x_0-\frac{W}{2}}^{x_0+\frac{W}{2}} A(x)\frac{\mu(x)'}{\alpha}dx \tag{4.7}$$

Noting from (4.2) that $\mu(x)' = \frac{M}{W}$ across the shell and substituting the ansatze for the metric field from (4.2), the integral becomes

$$H_1 = \frac{M}{\alpha W}\int_{x_0-\frac{W}{2}}^{x_0+\frac{W}{2}}\left(\frac{1+A_0}{2}+(x-x_0)\frac{1-A_0}{W}\right)dx \tag{4.8}$$

This can be further simplified as one realises that $(x-x_0)$ is an odd function about $x=x_0$ and the interval of integration is symmetrical about this point. This part of H_1 should therefore be identically zero. Mechanically ploughing through the

calculation shows this to be true. One is left with

$$H_1 = \frac{M}{\alpha W}\left[\frac{1+A_0}{2}x\right]_{x_0-\frac{W}{2}}^{x_0+\frac{W}{2}} \tag{4.9}$$

$$= \frac{M}{\alpha}\left(\frac{1+A_0}{2}\right) \tag{4.10}$$

Similar to the case for H_1, H_2 need only be integrated over the shell region. This is because it contains a derivative of the profile function $h(x)$ and, according to the ansatze, $h(x)$ is constant everywhere apart from within the shell. Thus, upon substitution of the ansatze, one obtains

$$\begin{aligned} H_2 &= -\int_{x_0-\frac{W}{2}}^{x_0+\frac{W}{2}} A(x)Q_N S(x)h(x)'^2 x^2 dx \\ &= -\int_{x_0-\frac{W}{2}}^{x_0+\frac{W}{2}} \left[\frac{1+A_0}{2}+(x-x_0)\frac{1-A_0}{W}\right] \\ &\quad \times Q_N\left(1-\frac{2\mu(x)}{x}\right)\frac{\pi^2}{W^2}x^2 dx \\ &= -\frac{Q_N\pi^2}{W^2}\int_{x_0-\frac{W}{2}}^{x_0+\frac{W}{2}} \left[\frac{1+A_0}{2}+(x-x_0)\frac{1-A_0}{W}\right] \\ &\quad \times\left[x^2-2x\left(\frac{M}{2}+(x-x_0)\frac{M}{W}\right)\right]dx \end{aligned} \tag{4.11}$$

Expanding and integrating term by term, one obtains

$$\begin{aligned} H_2 = &-\frac{Q_N\pi^2}{W^2}\left[\left(M\left(\frac{1+A_0}{2}\right)\left(\frac{2x_0}{W}-1\right)+Mx_0\left(\frac{1-A_0}{W}\right)\left(1-\frac{2x_0}{W}\right)\right)\left[\frac{x^2}{2}\right]_{x_0-\frac{W}{2}}^{x_0+\frac{W}{2}}\right. \\ &+\left(\left(\frac{1+A_0}{2}\right)\left(1-\frac{2M}{W}\right)+\left(\frac{1-A_0}{W}\right)\left(\frac{4x_0M}{W}-M-x_0\right)\right)\left[\frac{x^3}{3}\right]_{x_0-\frac{W}{2}}^{x_0+\frac{W}{2}} \\ &\left.+\left(\frac{1-A_0}{W}\right)\left(1-\frac{2M}{W}\right)\left[\frac{x^4}{4}\right]_{x_0-\frac{W}{2}}^{x_0+\frac{W}{2}}\right] \end{aligned} \tag{4.12}$$

Simply by evaluating and substituting the following

$$\left[\frac{x^2}{2}\right]_{x_0-\frac{W}{2}}^{x_0+\frac{W}{2}} = Wx_0 \tag{4.13}$$

$$\left[\frac{x^3}{3}\right]_{x_0-\frac{W}{2}}^{x_0+\frac{W}{2}} = Wx_0^2 + \frac{W^3}{12} \tag{4.14}$$

$$\left[\frac{x^4}{4}\right]_{x_0-\frac{W}{2}}^{x_0+\frac{W}{2}} = Wx_0^3 + \frac{W^3x_0}{4} \tag{4.15}$$

the explicit form of H_2, after simplification, is given by

$$\begin{aligned} H_2 = & -\frac{Q_N\pi^2}{W}\left[\left(\frac{1+A_0}{2}\right)\left(x_0^2 - Mx_0 + \frac{W^2}{12} - \frac{MW}{6}\right)\right. \\ & \left. + \left(\frac{1-A_0}{W}\right)\left(\frac{W^2x_0}{6} - \frac{MW^2}{12} - \frac{MWx_0}{6}\right)\right] \end{aligned} \tag{4.16}$$

Again H_3 need only be integrated across the width of the shell. The factor of $sin^2h(x)$ in the integrand is zero elsewhere because of the boundary conditions on $h(x)$. (These being $h(x) = \pi$ and $h(x) = 0$ before and after the shell respectively).

$$H_3 = -\int_{x_0-\frac{W}{2}}^{x_0+\frac{W}{2}} A(x)\mathcal{C}sin^2h(x)[1 + S(x)h(x)'^2]dx \tag{4.17}$$

$$\begin{aligned} = & -\mathcal{C}\int_{x_0-\frac{W}{2}}^{x_0+\frac{W}{2}} \left[\frac{1+A_0}{2} + (x-x_0)\frac{1-A_0}{W}\right] sin^2h(x) \\ & \times \left[1 + \frac{\pi^2}{W^2}\left(1 - \frac{2}{x}\left(\frac{M}{2} + (x-x_0)\frac{M}{W}\right)\right)\right] dx \end{aligned} \tag{4.18}$$

Expanding, the integral can be split as follows

$$H_3 = H_{31} + H_{32} + H_{33} + H_{34} + H_{35} \tag{4.19}$$

where

$$H_{31} = -\mathcal{C}\left(\frac{1+A_0}{2}\right)\left(1 + \frac{\pi^2}{W^2}\right)\int_{x_0-\frac{W}{2}}^{x_0+\frac{W}{2}} sin^2h(x)dx \tag{4.20}$$

$$H_{32} = -\mathcal{C}\left(\frac{1-A_0}{W}\right)\left(1 + \frac{\pi^2}{W^2}\right)\int_{x_0-\frac{W}{2}}^{x_0+\frac{W}{2}} (x-x_0)\,sin^2h(x)dx \tag{4.21}$$

$$H_{33} = \mathcal{C}\left(\frac{1+A_0}{2}\right)\frac{M\pi^2}{W^2}\int_{x_0-\frac{W}{2}}^{x_0+\frac{W}{2}}\frac{sin^2h(x)}{x}dx \tag{4.22}$$

$$H_{34} = \mathcal{C}\frac{M\pi^2}{W^2}\left[\left(\frac{1-A_0}{W}\right)+\frac{2}{W}\left(\frac{1+A_0}{2}\right)\right]\int_{x_0-\frac{W}{2}}^{x_0+\frac{W}{2}}(x-x_0)\frac{sin^2h(x)}{x}dx \tag{4.23}$$

and

$$H_{35} = \mathcal{C}\left(\frac{1-A_0}{W}\right)\frac{2M\pi^2}{W^3}\int_{x_0-\frac{W}{2}}^{x_0+\frac{W}{2}}(x-x_0)^2\frac{sin^2h(x)}{x}dx \tag{4.24}$$

Taking H_{31}, the integral can be performed by a simple change of variable from x to h. Noting that from (4.2) $\frac{dh}{dx} = -\frac{\pi}{W}$, one has

$$\begin{aligned}
H_{31} &= -\mathcal{C}\left(\frac{1+A_0}{2}\right)\left(1+\frac{\pi^2}{W^2}\right)\int_{\pi}^{0}sin^2h\left(\frac{-W}{\pi}\right)dh \\
&= \mathcal{C}\left(\frac{1+A_0}{2}\right)\left(\frac{W}{\pi}\right)\left(1+\frac{\pi^2}{W^2}\right)\int_{\pi}^{0}sin^2hdh \\
&= -\mathcal{C}\left(\frac{1+A_0}{2}\right)\left(\frac{W}{\pi}\right)\left(1+\frac{\pi^2}{W^2}\right)\int_{0}^{\pi}sin^2hdh \\
&= -\mathcal{C}\left(\frac{1+A_0}{2}\right)\left(\frac{W}{\pi}\right)\left(1+\frac{\pi^2}{W^2}\right)\left[\frac{1}{2}h-\frac{1}{4}sin2h\right]_0^{\pi} \\
&= -\mathcal{C}\left(\frac{1+A_0}{2}\right)\left(\frac{W}{2}\right)\left(1+\frac{\pi^2}{W^2}\right)
\end{aligned} \tag{4.25}$$

In the high baryon number regime, H_{32} has a negligible contribution to the total energy. This can be reasoned as follows. As described in section 5.1, when the baryon number increases, the effect on the fields is that they resemble more and more truly the proposed Ramp Ansatze. Further, the fields remain constant for longer and change over a comparatively small radial region. Concretely, one can say that for high baryon numbers, the fields follow the Ramp Ansatze with $x_0 >> W$.

Therefore, because one only integrates over the width of the shell in H_{32}, the actual radial position x is never far away from the centre of the shell x_0 and the

term $(x-x_0)$ is always very small. As the other factor in H_{32} is $sin^2h(x)$, thus never being larger than 1, one makes the approximation that $H_{32}=0$.

One similarly approximates H_{34} and H_{35} to zero. The approximations here are further qualified by the factor of x in the denominator, which will, over the region of integration, be large in comparison to $(x-x_0)$.

One is left to calculate H_{33}. This integral is difficult to handle explicitly because of the factor of $\frac{1}{x}$, however a good approximation can be made. Following the arguments outlined above, the radial position x does not vary significantly from the central position of the shell x_0, over the interval of integration. Thus one simply replaces the factor of $\frac{1}{x}$ in the integrand with the constant factor $\frac{1}{x_0}$. Integration can then proceed via a change of variables from x to h.

$$\begin{aligned} H_{33} &= \mathcal{C}\left(\frac{1+A_0}{2}\right)\frac{M\pi^2}{W^2}\int_{\pi}^{0}\frac{sin^2h}{x_0}\left(\frac{-W}{\pi}\right)dh \\ &= \mathcal{C}\left(\frac{1+A_0}{2}\right)\frac{M\pi}{Wx_0}\int_0^{\pi}sin^2hdh \\ &= \mathcal{C}\left(\frac{1+A_0}{2}\right)\frac{M\pi}{Wx_0}\left[\frac{1}{2}h-\frac{1}{4}sin2h\right]_0^{\pi} \\ &= \mathcal{C}\left(\frac{1+A_0}{2}\right)\frac{M\pi^2}{2Wx_0} \end{aligned} \tag{4.26}$$

Thus combining H_{31} and H_{33} one obtains

$$H_3=\mathcal{C}\left(\frac{1+A_0}{2}\right)\left(\frac{M\pi^2}{2Wx_0}-\frac{W}{2}-\frac{\pi^2}{2W}\right) \tag{4.27}$$

Moving on to the calculation of H_4 one sees that because there is a factor of $sin^4h(x)$, the boundary conditions on $h(x)$ mean that again integration needs only be performed over the width of the shell.

$$\begin{aligned} H_4 &= -\int_{x_0-\frac{W}{2}}^{x_0+\frac{W}{2}}\frac{A(x)\mathcal{I}sin^4h(x)}{2x^2}dx \\ &= -\mathcal{I}\int_{x_0-\frac{W}{2}}^{x_0+\frac{W}{2}}\left[\frac{1+A_0}{2}+(x-x_0)\frac{1-A_0}{W}\right]\frac{sin^4h(x)}{2x^2}dx \end{aligned} \tag{4.28}$$

At this point one can make an immediate simplification by using the type of approximation used in the calculation of H_3. Namely, contributions from the term containing the factor $\frac{(x-x_0)}{x^2}$ are negligible and will be ignored. One is left with

$$H_4 = -\frac{\mathcal{I}}{2}\left(\frac{1+A_0}{2}\right)\int_{x_0-\frac{W}{2}}^{x_0+\frac{W}{2}} \frac{sin^4h(x)}{x^2}dx \tag{4.29}$$

Next, the factor of $\frac{1}{x^2}$ is replaced with the constant factor $\frac{1}{x_0^2}$, an approximation already reasoned to be valid in the high baryon number regime. Thus

$$H_4 = -\frac{\mathcal{I}}{2x_0^2}\left(\frac{1+A_0}{2}\right)\int_{x_0-\frac{W}{2}}^{x_0+\frac{W}{2}} sin^4h(x)dx \tag{4.30}$$

The integration variable can now be changed to h and the remaining calculation is straightforward.

$$\begin{aligned} H_4 &= -\frac{\mathcal{I}}{2x_0^2}\left(\frac{1+A_0}{2}\right)\int_{\pi}^{0} sin^4h\left(\frac{-W}{\pi}\right)dh \\ &= -\frac{\mathcal{I}W}{2\pi x_0^2}\left(\frac{1+A_0}{2}\right)\int_0^{\pi} sin^4hdh \\ &= -\frac{\mathcal{I}W}{2\pi x_0^2}\left(\frac{1+A_0}{2}\right)\left[\frac{3}{8}h - \frac{1}{4}sin2h + \frac{1}{32}sin4h\right]_0^{\pi} \\ &= -\frac{3\mathcal{I}W}{16x_0^2}\left(\frac{1+A_0}{2}\right) \end{aligned} \tag{4.31}$$

The final contribution to the Hamiltonian (4.1), comes from the boundary contribution, H_5. This can be calculated straight from the ansatze for $\mu(x)$, (4.2).

$$\begin{aligned} H_5 &= -\frac{\mu(\infty)}{\alpha} \\ &= -\frac{M}{\alpha} \end{aligned} \tag{4.32}$$

Finally, the explicit form of the Hamiltonian is obtained by combining H_1 to H_5. One is reminded that, because of the approximations made, the following expression is valid in the regime where the baryon number is high. However, this is exactly the

regime one is interested in when considering Skyrmions of astrophysical relevance.

$$\begin{aligned} H = & -\frac{4\pi f_\pi}{e}\left[\frac{M}{\alpha}\left(\frac{1+A_0}{2}\right) - \frac{Q_N\pi^2}{W}\left[\left(\frac{1+A_0}{2}\right)\left(x_0^2 - Mx_0 + \frac{W^2}{12} - \frac{MW}{6}\right)\right.\right. \\ & + \left.\left(\frac{1-A_0}{W}\right)\left(\frac{W^2x_0}{6} - \frac{MW^2}{12} - \frac{MWx_0}{6}\right)\right] \\ & + \left.\mathcal{C}\left(\frac{1+A_0}{2}\right)\left(\frac{M\pi^2}{2Wx_0} - \frac{W}{2} - \frac{\pi^2}{2W}\right) - \frac{3\mathcal{I}W}{16x_0^2}\left(\frac{1+A_0}{2}\right) - \frac{M}{\alpha}\right] \end{aligned} \tag{4.33}$$

Indeed, one sees that the approximate total energy of the Einstein-Skyrme system depends upon the four free parameters of the Ramp ansatze. One proceeds to find stationary points of this energy. First, extremising with respect to the parameter M, one finds the following constraint.

$$\frac{\partial H}{\partial M} = 0 \Rightarrow$$

$$A_0 = \frac{\alpha\pi^2\left(-3\mathcal{C} - 8Q_Nx_0^2 - 2Q_Nx_0W\right) + 6x_0W}{\alpha\pi^2\left(3\mathcal{C} + 4Q_Nx_0^2\right) + 6x_0W} \tag{4.34}$$

Similarly, extremisation with respect to A_0 gives

$$\frac{\partial H}{\partial A_0} = 0 \Rightarrow$$

$$M = \frac{\alpha\left(8\pi^2\left(3\mathcal{C}x_0^2 + 6Q_Nx_0^4 - 2Q_Nx_0^3W\right) + W^2\left(9\mathcal{I} + 24\mathcal{C}x_0^2 + 4\pi^2Q_Nx_0^2\right)\right)}{8x_0\left(\alpha\pi^2\left(3\mathcal{C} + 4Q_Nx_0^2\right) + 6x_0W\right)} \tag{4.35}$$

One should note, at this point, that these constraints have an appropriate form in terms of their behaviour in the limit of gravitational decoupling. This is illustrated by the following limits.

$$\lim_{\alpha\to 0} A_0 = \frac{6x_0W}{6x_0W} = 1 \tag{4.36}$$

$$\lim_{\alpha\to 0} M = \frac{0}{48x_0^2W} = 0 \tag{4.37}$$

This is the expected behaviour when the gravitational interaction is removed from the model. In this case, (4.36) & (4.37) imply that $A(x) = 1$ and $\mu(x) = 0$

everywhere. This ensures that the line element (2.3) takes the form of flat space without the presence of mass.

Now, extremisation of the energy with respect to the remaining two parameters, x_0 and W, leads to very complicated expressions which cannot be solved analytically. However, the constraints (4.34) and (4.35) effectively pick out hyper-surfaces within the full four-dimensional parameter space of field configurations, upon which the energy has an extremum in the A_0 and M directions. One can proceed by substituting these constraints into (4.33) and extremising numerically over the remaining two-dimensional surface.

Of course, once substitution of the constraints into (4.33) has been done and a specific two-dimensional surface picked, one must avoid differentiation to find the minimum in the x_0 and W directions. An appropriate algorithm to use is the *FindMinimum* routine found in *Mathematica* [Wolfram Ref]. This routine, provided with a function of N-variables along with an initial coordinate, uses explicit evaluation and not derivatives to find a local minimum on the N-dimensional parameter space.

Chapter 5

Ramp Ansatze Generated Configurations

This chapter details minimal energy parameter sets found for x_0, W, A_0 and M for varying values of the coupling and baryon number. The procedure used to find these was outlined in the previous chapter. Specifically one minimizes the energy, (4.33), of the system, subject to the constraints on A_0 and M detailed in (4.34) and (4.35) respectively.

The procedure is carried out using the *FindMinimum* routine in *Mathematica*, given data describing the situation of interest. Namely this data is; $Q_N = \frac{N-1}{N}$, the flavour factor which for the $SU(2)$ model is $\frac{1}{2}$, α the value of the coupling one wishes to use, and $\mathcal{C}$ and $\mathcal{I}$ which are related to the degree of the harmonic map used and thus the number of baryons required.

When using the harmonic map ansatze, one initially minimizes the quantities $\mathcal{C}$ and $\mathcal{I}$ over the space of all harmonic maps of the required degree. As the baryon

number increases, so does the required degree of map and, consequently, so does the number of possible maps. For large baryon numbers it is inconceivable to numerically minimise $\mathcal{C}$ and $\mathcal{I}$ over all possible maps and thus an approximation must be used.

One notes that for the $SU(2)$ model, the minimal value of $\mathcal{C}$ is equal to the baryon number, B [9]. Further it has been shown [30], [?], [?], that for moderately large baryon numbers, the minimal value of $\mathcal{I}$ tends to a limiting value of $1.28B^2$. These are the values used in obtaining the solutions, for any given baryon number, shown in this chapter.

5.1 $SU(2)$ configurations

5.1.1 Validity of Ramp Ansatze

Table 5.1 shows the minimal energy parameters for the ramp ansatze describing a configuration of 2×10^6 baryons, at a variety of coupling values. A solution set for this baryon number was the highest obtained by direct numerical integration of the field equations for $h(x)$, $\mu(x)$ and $A(x)$. The form of these solutions are shown in figures 4.1 to 4.3 at a coupling of $\alpha = 1 \times 10^{-6}$.

One first notes that the approximations made in Chapter 4, which required $W << x_0$, are valid for all ramp ansatze configurations with baryon number 1×10^6. Line 10 of table 5.1 shows that even for the configuration with the smallest radius, obtained at the critical coupling, the ratio $\frac{W}{x_0}$ is still of order 10^{-2}.

Moreover, one notes that the predictions of the ramp ansatze are in remarkably good agreement with the solutions obtained directly from the field equations. The direct numerical integration of the field equations at $B = 2 \times 10^6$, gives solutions that have a radius of $x_0 \approx 1223$ and a width of $W \approx 3$ (see figures 4.1 to 4.3). Line 3 of table 5.1 shows that for the same value of α, the ramp ansatze predicts a radius of $x_0 \approx 1171.6$ and $W \approx 3.1$. In each case there is less than a 5 percent discrepancy between the values obtained by the different approaches.

Further, the ADM mass per baryon for the configuration, calculated from figure 4.2, is given by

$$M_{ADM} = \frac{4\pi M}{\alpha B} \approx \frac{40\pi}{2} \approx 62.83 \tag{5.1}$$

Comparing this with the value of 66.56 obtained from the ramp ansatze, one is

left with a discrepancy of only 6 percent! These figures, along with the existence of a critical coupling in table 5.1, provide one with confidence in the validity of the ramp ansatze.

α	x_0	W	A_0	M_{ADM}/B	S_{min}
1×10^{-8}	1177.079405	3.141339	0.999910	66.815103	0.999820
1×10^{-7}	1176.584103	3.138980	0.999096	66.791644	0.998195
1×10^{-6}	1171.598103	3.115317	0.990914	66.556852	0.981941
1×10^{-5}	1117.468499	2.868798	0.904145	64.185116	0.817404
3×10^{-5}	943.153230	2.186000	0.650125	58.619086	0.407177
3.7×10^{-5}	801.051220	1.730217	0.472599	56.421817	0.171352
3.76×10^{-5}	760.448013	1.613464	0.426883	56.223736	0.116050
3.768×10^{-5}	742.112054	1.562475	0.406975	56.204875	0.092580
3.76808×10^{-5}	741.331293	1.560327	0.406138	56.205105	0.091601
3.768083×10^{-5}	741.299241	1.560239	0.406104	56.205116	0.091560

Table 5.1: *Numerically obtained minimum energy configurations for* 2×10^6 *baryons at a range of couplings. Respectively shown are the coupling used and optimal values for the radius of the shell, its width, the value of* A_0 *such that* $A(\infty) = 1$*, the ADM Mass per baryon and the minimum value of the metric function* $S(x) = \left(1 - \frac{2\mu(x)}{x}\right)$.

5.1.2 Effect of increasing baryon number at $\alpha = 10^{-6}$

Having established the validity of the ramp ansatze as a description of configurations containing large numbers of baryons, it is important to see how the structures change as more and more baryons are added. Tables 5.2 and 5.3 summarise the data obtained for increasing baryon number at a fixed value of the coupling ($\alpha = 1 \times 10^{-6}$).

Comparing the data to the previously obtained solutions at low baryon numbers shows significant differences. For example, the ramp ansatze predicts that a single baryon configuration at $\alpha = 1 \times 10^{-6}$ will have an ADM mass of 63.55. However, table 3.3.1 in Chapter 3, shows that the actual value of the ADM mass in this case is 72.92. The large (13 percent) discrepancy can be explained because the approximations made in calculating the energy from the ramp ansatze, relied on the premise that $W << x_0$. This is clearly not the case for low baryon numbers, as shown by the values in table 5.2. As such, one will restrict attention to configurations where the approximations are clearly valid, say $B \geq 1 \times 10^6$.

The first comment that can be made is that the previously found trend in decreasing ADM mass per baryon, is continued at large baryon numbers. One can clearly see that for $B \geq 1 \times 10^6$, configurations become more and more energetically favourable as more baryons are added. Given that section 5.1.1 showed there to be only a small discrepancy between M_{ADM} per B whether calculated by direct integration or from the ramp ansatze, one can be fairly sure that the values in table 5.3 are a good representation of the ADM masses of true solutions. If anything, imposing the ansatze rigidly on the fields, would tend to result in an overestimation of the energy.

Thus taking absolute values of M_{ADM} per B for $B \geq 1 \times 10^6$ and comparing these to the value of 72.92 for a single baryon, at the same coupling, from table 3.3.1, one can be convinced that all the configurations are stable against single particle decay. Thus the possibility of constructing a solution representing a baryon star is indeed energetically plausible.

As for the form of solutions, the general trends in the parameters of the ramp ansatze are as follows. A_0 is effectively a measure of the warping of space caused by the self-gravitating Skyrmion. As $A(x)$ has a value of 1 at spatial infinity, then the smaller the value of A_0, the larger the deviation from 1 and thus from flat space. As one would expect, A_0 decreases significantly with increased baryon number, particularly as one approaches the baryon number for which $\alpha = 1 \times 10^{-6}$ is the critical coupling.

There is an interesting comment here. Again there is the existence of a critical coupling, above which no solutions exist. Even for the very large baryon numbers involved in this chapter, the value of the metric function $S(x)$ is small but significantly greater than zero, near α_{crit}. Still no horizon forms and the lack of solutions above α_{crit} is not due to a collapse to a singularity. Thus one is left to conclude that indeed the lack of solutions is due to the annihilation between the sphaleronic and regular branches of solutions (shown in Chapter 3), at the critical coupling.

The width of the baryon layer, W, has a curious behaviour. It decreases significantly near the critical coupling. However, far away from this it stabilises at a value of around 3.1. This was in fact expected. Kopeliovich [33], [34], calculated a minimal energy value of W, for large baryon number Skyrmions in flat space.

Taking an ansatze akin to the ramp ansatze he was able to obtain the explicit form of the Hamiltonian. As the situation was simplified by the exclusion of gravity, the number of free parameters of the energy were reduced to two, x_0 and W. In this case the energy could, in fact, be minimised analytically and the optimal value of W was shown to be $W = \pi$.

Perhaps the most interesting feature of the data is the behaviour of the radius x_0. As the baryon number increases so does the radius. In fact far away from α_{crit} it is evident that $x_0 \propto B^{\frac{1}{2}}$. This shows that far from the critical coupling, the presence of gravity is having a negligible effect on the structure of the Skyrmion. The baryons are distributed over a hollow shell. Thus the number of baryons is proportional to the surface of that shell and so $B \propto x_0^2$. There is no evidence for any deviation from this behaviour, far from α_{crit}.

This is not the whole story however. Figure 5.1 shows that near the critical coupling, the radius deviates from this proportionality with $B^{\frac{1}{2}}$ and rises more slowly with increasing baryon number. This signifies that gravitational compression has started to occur. More surprising is the fact that at couplings very close to α_{crit}, the radius actually decreases as more baryons are added. This is a tantalising property for trying to model a baryon star within the Einstein-Skyrme system.

Real neutron stars exhibit a similar phenomenon. Supported by degenerate neutron pressure, a neutron star must decrease in size as more neutrons are added. This is because the neutrons need to be brought into closer proximity in order to sufficiently increase the degenerate neutron pressure so that the increased gravitational force is balanced [35].

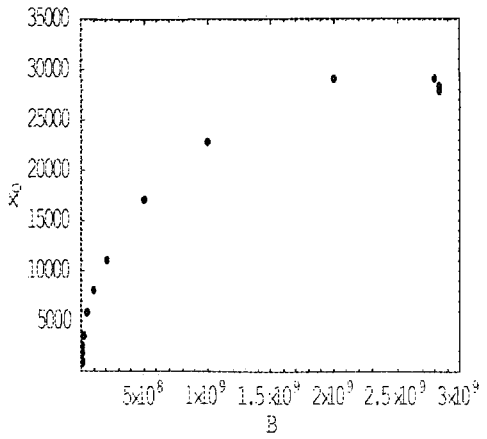

Figure 5.1: *The behaviour of x_0 with increasing baryon number at a fixed coupling of $\alpha = 1 \times 10^{-6}$.*

5.1.3 Effect of increasing baryon number on the critical coupling

Table 5.4, shows the relation between the critical coupling and the baryon number. It is again clear that $\alpha_{crit} \propto B^{-\frac{1}{2}}$, as obtained for low baryon number Skyrmions in Chapter 3.

It may be tempting here to attribute this relationship as an artefact of the hollow shell structure, in that the behaviour of α_{crit} is related in some way to the surface area of the shell. However the phenomenon seems more genuine than that. One must remember that α_{crit} was proportional to $B^{-\frac{1}{2}}$, for baryon numbers 1,2,3 & 4, as shown in Chapter 4. These solutions do not possess spherical symmetry and thus there must be a deeper reason for the behaviour of α_{crit}.

5.1.4 Candidate baryon stars

Having discussed the main features of configurations with a large baryon number and moreover, having established that the ramp ansatze is both reliable and gives rise to energetically favourable multi-baryon Skyrmions, it is now time to test the model to the limit, as it were. One will attempt to find a structure corresponding to a baryon star, in the Einstein-Skyrme model.

A typical neutron star would comprise in the order of 10^{58} neutrons. Thus one will take a baryon number of $B = 10^{58}$. The real physical value of the coupling, α, must also be known. Given that $\alpha = 4\pi f_\pi^2 G$ and taking $f_\pi = 93 Mev$, along with $G = 6.72 \times 10^{-45} Mev^{-2}$, one obtains $\alpha_{physical} = 7.30 \times 10^{-40}$. Using these values, one obtains the data shown in table 5.5.

One sees that the physical value for α is far below the critical coupling for this particular baryon number. Thus A_0 & S_{min} both equal unity and W tends to a value of π, as predicted by Kopeliovich. The configuration does, happily, appear to still be energetically favourable, having an ADM mass per baryon far less than that of a single baryon in table 3.3.1, at 72.92. Incidentally, the value for the single baryon was obtained at a far higher value of α and thus the comparable value at $\alpha_{physical}$, would be slightly higher again. Either way, a bound state of baryons large enough to be a baryon star, does seem energetically favourable.

There is one major drawback with the solution however. The ramp ansatze predicts a baryon star with a radius of $x_0 = 8.32 \times 10^{28}$. One must convert this back from the scaled units to SI units of length. Thus, noting that $x = ef_\pi r$, one has

$$r = \frac{1}{ef_\pi} x \tag{5.2}$$

Now one notes that common values of the Skyrme model parameters are $e = 4.84$, with dimensions of $[Mass^{-\frac{1}{2}} Length^{-\frac{1}{2}}]$ and $f_\pi = 93Mev$ with dimensions of $[Mass^{-\frac{1}{2}} Length^{-\frac{1}{2}}]$, [36]. Thus

$$\begin{aligned} e &= 4.84 \left(\frac{c}{\hbar}\right)^{\frac{1}{2}} kg^{-\frac{1}{2}} m^{-\frac{1}{2}} \\ &= 8.18 \times 10^{21} kg^{-\frac{1}{2}} m^{-\frac{1}{2}} \end{aligned} \tag{5.3}$$

and

$$\begin{aligned} f_\pi &= 93 \left(\frac{Mev}{c^2}\right) \left(\frac{c}{\hbar}\right)^{\frac{1}{2}} kg^{\frac{1}{2}} m^{-\frac{1}{2}} \\ &= 2.72 \times 10^{-7} kg^{\frac{1}{2}} m^{-\frac{1}{2}} \end{aligned} \tag{5.4}$$

allow one to calculate the predicted radius of a baryon star as

$$\begin{aligned} R_{baryonstar} &= \frac{8.32 \times 10^{28}}{8.18 \times 10^{21} \times 2.72 \times 10^{-7}} m \\ &= 3.74 \times 10^{10} km \end{aligned} \tag{5.5}$$

This is clearly too large for the radius of a compact, super-dense baryon star, such as a neutron star. A typical neutron star radius might be expected to be in the order of 10 - $50km.$, [35].

Such a prediction seems a serious obstacle in trying to model a baryon star within the Einstein-Skyrme system. However, it is no more than one expected at this stage. Effectively one has made ansatze which describe a giant hollow structure. This was a first approximation and the next chapter shows how the model can be refined.

B	x_0	W	A_0	M_{ADM}/B	S_{min}
1	0.673505	2.327110	0.999989	63.548704	0.999994
4	1.59196	2.86115	0.999984	62.5851	0.999987
8	2.32292	2.99152	0.999979	63.4195	0.999979
50	5.86157	3.11594	0.999953	64.7287	0.999931
100	8.306280	3.128570	0.999934	65.273095	0.999895
200	11.758698	3.134892	0.999908	65.693078	0.999843
500	18.603075	3.138600	0.999855	66.089160	0.999739
1×10^3	26.313363	3.139718	0.999796	66.296392	0.999622
2×10^3	37.214608	3.140166	0.999713	66.445154	0.999455
5×10^3	58.840444	3.140026	0.999546	66.576866	0.999123
1×10^4	83.206449	3.139582	0.999359	66.641104	0.998749
2×10^4	117.657832	3.138913	0.999094	66.683045	0.998220
5×10^4	185.983840	3.137452	0.998568	66.712118	0.997169
1×10^5	262.940613	3.135745	0.997976	66.717411	0.995986
2×10^5	371.692791	3.133319	0.997136	66.709105	0.994311
5×10^5	587.189670	3.128492	0.995468	66.675247	0.990988
1×10^6	829.598841	3.123040	0.993585	66.628301	0.987242

Table 5.2: *Numerically obtained minimum energy configurations for a range of baryon numbers at* $\alpha = 1 \times 10^{-6}$. *Respectively shown are the baryon number and optimal values for the radius of the shell, its width, the value of* A_0 *such that* $A(\infty) = 1$, *the ADM Mass per baryon and the minimum value of the metric function* $S(x) = \left(1 - \frac{2\mu(x)}{x}\right)$.

B	x_0	W	A_0	M_{ADM}/B	S_{min}
2×10^6	1171.598103	3.115317	0.990914	66.556852	0.981941
5×10^6	1847.305751	3.099942	0.985590	66.409453	0.971416
1×10^7	2604.193248	3.082536	0.979548	66.240364	0.959541
2×10^7	3666.097134	3.057771	0.970927	65.999282	0.942720
5×10^7	5742.761267	3.008095	0.953545	65.517862	0.909236
1×10^8	8032.820705	2.951175	0.933482	64.972117	0.871294
2×10^8	11174.683329	2.868773	0.904158	64.195072	0.817164
5×10^8	17031.617830	2.696761	0.841996	62.632596	0.707383
1×10^9	22898.788750	2.483680	0.763196	60.827525	0.577249
2×10^9	29121.037849	2.109214	0.620568	58.139036	0.364530
2.8×10^9	29097.730196	1.662272	0.446042	56.288421	0.137963
2.83×10^9	28514.182644	1.606614	0.424264	56.224598	0.111904
2.839×10^9	28024.164280	1.567118	0.408849	56.210670	0.093726
2.8397×10^9	27869.287879	1.555558	0.404340	56.211729	0.088448
2.83975×10^9	27825.597221	1.552361	0.403092	56.212412	0.086989
2.839752×10^9	27821.996607	1.552098	0.402989	56.212474	0.086870

Table 5.3: *Numerically obtained minimum energy configurations for a range of baryon numbers at* $\alpha = 1 \times 10^{-6}$. *Respectively shown are the baryon number and optimal values for the radius of the shell, its width, the value of* A_0 *such that* $A(\infty) = 1$, *the ADM Mass per baryon and the minimum value of the metric function* $S(x) = \left(1 - \frac{2\mu(x)}{x}\right)$.

B	α_{crit}	x_0	W	A_0	M_{ADM}/B	S_{min}
10^3	1.686751×10^{-3}	16.505171	1.553694	0.400954	55.954881	0.130810
10^4	5.331088×10^{-4}	52.205734	1.552662	0.402323	56.128167	0.101148
10^5	1.685155×10^{-4}	166.352221	1.567714	0.408796	56.183551	0.098431
10^6	5.329166×10^{-5}	522.075324	1.552098	0.402900	56.204084	0.088264
10^7	1.685180×10^{-5}	1650.954688	1.552059	0.402947	56.209924	0.087274
10^8	5.328951×10^{-6}	5220.729351	1.552025	0.402954	56.211801	0.086952
10^9	1.685158×10^{-6}	16511.849632	1.552321	0.403075	56.212301	0.086989
10^{10}	5.328927×10^{-7}	52210.639623	1.552148	0.403010	56.212545	0.086880
10^{11}	1.685154×10^{-7}	165114.043088	1.552264	0.403056	56.212576	0.086924
10^{12}	5.328925×10^{-8}	522104.287618	1.552140	0.403007	56.212624	0.086864
10^{13}	1.685156×10^{-8}	1.651101×10^6	1.552215	0.403037	56.212592	0.086896
10^{14}	5.328926×10^{-9}	5.221007×10^6	1.552125	0.403002	56.212631	0.086856
10^{15}	1.685156×10^{-9}	1.651091×10^7	1.552204	0.403032	56.212597	0.086891

Table 5.4: *Numerically obtained minimum energy configurations for a range of baryon numbers at their corresponding maximum permitted* α. *Respectively shown are the baryon number, critical coupling and optimal values for the radius of the shell, its width, the value of* A_0 *such that* $A(\infty) = 1$, *the ADM Mass per baryon and the minimum value of the metric function* $S(x) = \left(1 - \frac{2\mu(x)}{x}\right)$.

x_0	W	A_0	M_{ADM}/B	S_{min}
8.323583×10^{28}	3.141593	1.000000	66.829868	1.000000

Table 5.5: *Numerically obtained minimum energy configuration for baryon star candidate.*

Chapter 6

Multiple Layer Gravitating Skyrmions

As was demonstrated in the previous two chapters, the Skyrme model can produce baryon configurations that have approximate spherical symmetry and that are energetically favourable (i.e. resistant to single particle decay). Whilst this is some way towards constructing something akin to a baryon star within the model, there are drawbacks.

Firstly the configurations obtained so far exist effectively as giant hollow shells, with the baryon density distributed as a tight lattice over the spherical surface. Clearly a hollow object is not what one would expect of a baryon star. Related to this is the problem of size. For the real value of the coupling constant $\alpha = 7.3 \times 10^{-40}$, then a hollow configuration containing 10^{58} baryons (a typical number for a neutron star), would have a radius corresponding to around $3.74 \times 10^{10} km$! Noting from [35], that a typical neutron star radius is about $10 km$ then, as of yet, one cannot claim

to have described anything like a neutron star in the Einstein-Skyrme model.

This chapter addresses these challenges and provides the first examples of plausible baryon star structures within the model.

6.1 The shape and form of Multiple Layer Skyrmions

So far, the following boundary conditions have been imposed on the profile function, $h(x)$.

$$\begin{aligned} h(0) &= \pi \\ h(\infty) &= 0 \end{aligned} \tag{6.1}$$

There were two reasons for this. Firstly that the field be well defined at the origin and secondly finite energy considerations. However, it is clear from the exposition of the Harmonic Map ansatze in Chapter 1 that (6.1) are not the only set of satisfactory boundary conditions.

In fact, the Skyrme field will be well defined at the origin if the profile function is any multiple of π. Thus, for $k \in \mathbb{Z}$,

$$\begin{aligned} h(0) &= k\pi \\ h(\infty) &= 0 \end{aligned} \tag{6.2}$$

is also a reasonable choice of boundary data.

It can be shown [9], [10], that a Skyrmion generated by a Harmonic Map of degree B, where the profile function has boundary the conditions (6.2), will possess a topological charge of kB. Such a Skyrmion will be equivalent to a bound configuration of kB baryons.

Such configurations were studied for moderate baryon number as in Chapter 3. That is, numerical integration of equations (2.32) to (2.35) was performed but this time imposing (6.2) on $h(x)$ with $k = 2$. A typical solution set is shown in Figs. 6.1 - 6.3.

This data was obtained for a total baryon number of $B = 4\times10^6$, thus in actuality a Harmonic map of degree 2×10^6 was used. Further, the data was obtained at a coupling of $\alpha = 1 \times 10^{-6}$.

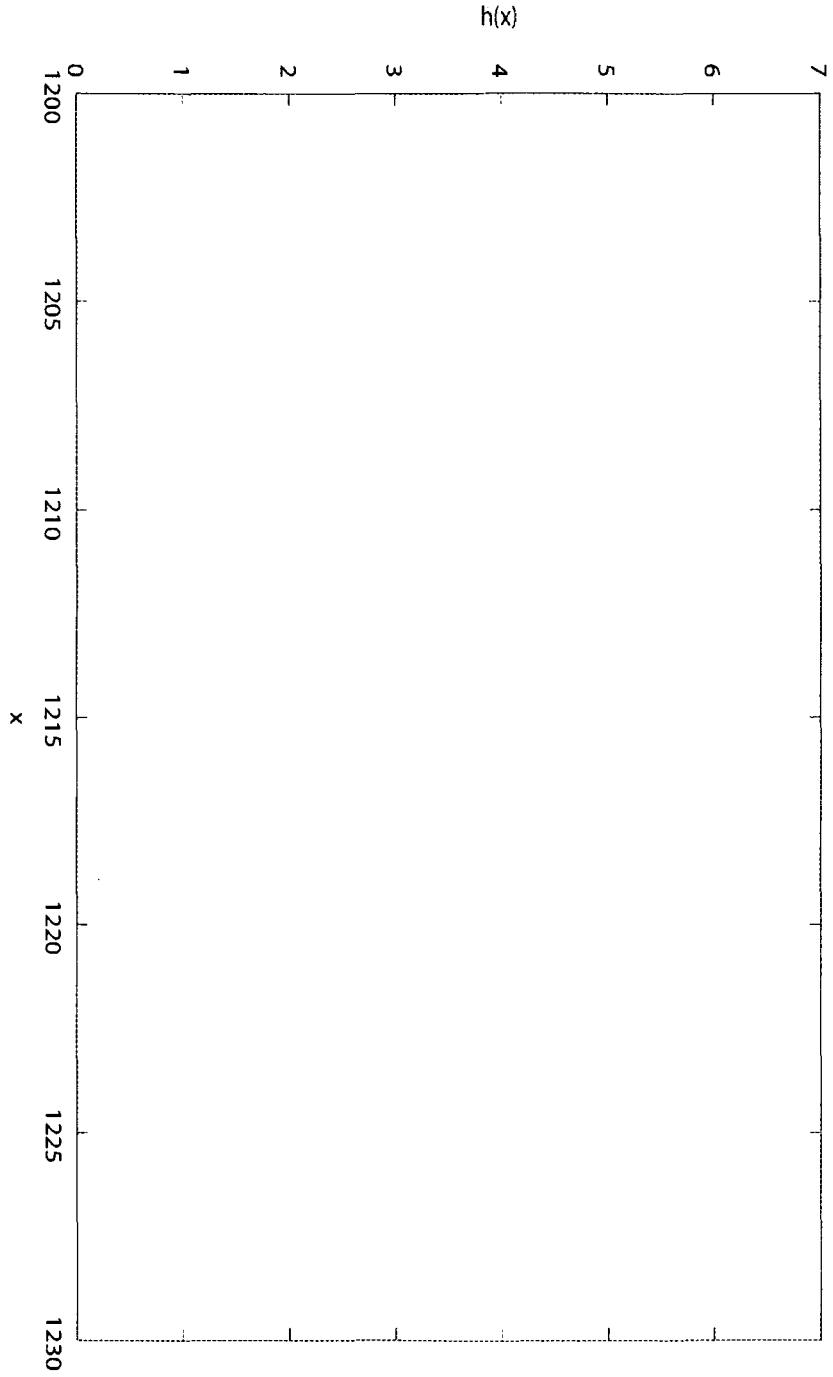

Figure 6.1: *Numerical solutions for $h(x)$ in the case of $\mathcal{B} = 2 \times 10^6$ per layer and $\alpha = 1 \times 10^{-6}$, where the boundary condition $h(0) = 2\pi$ have been taken. Clearly exhibited is the multiple shell-like structure of the Skyrmion*

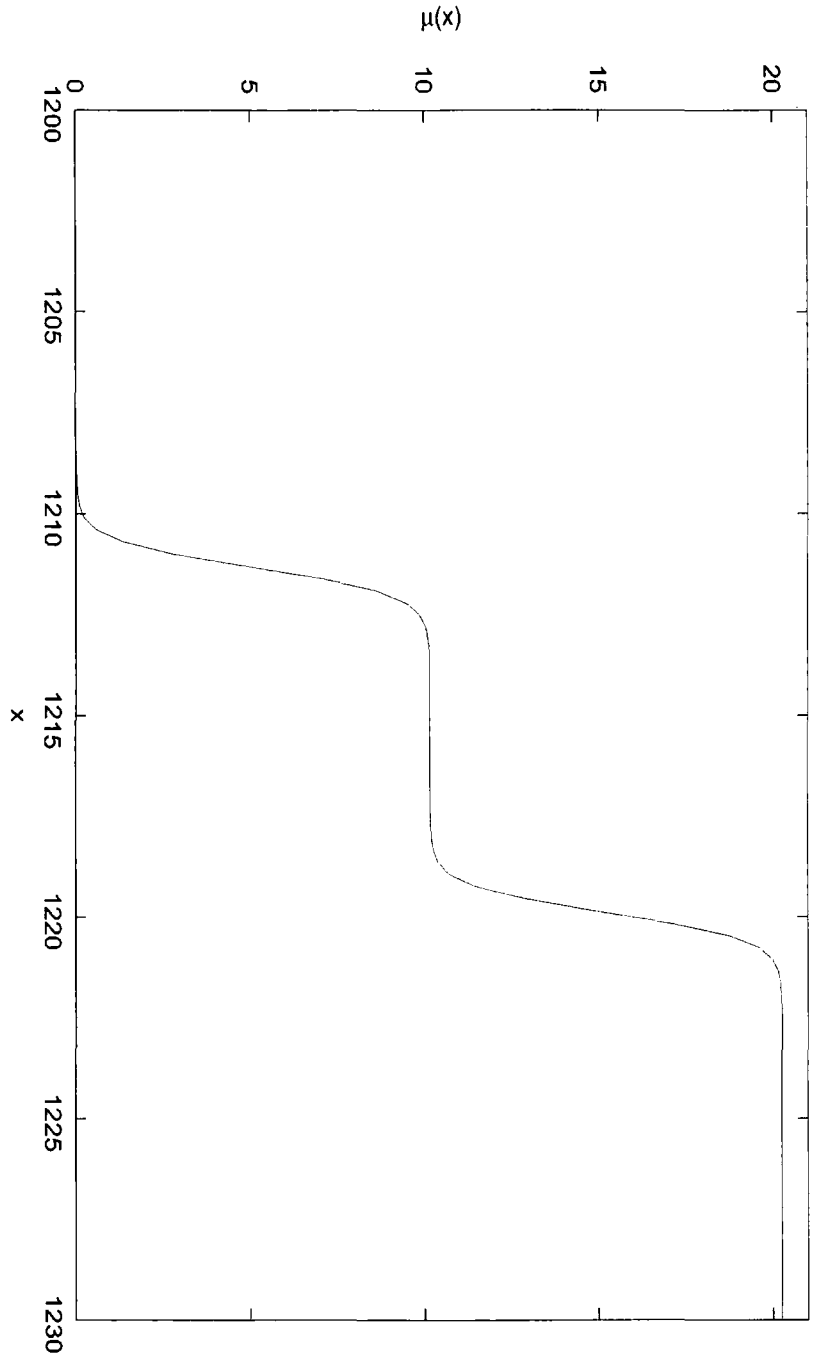

Figure 6.2: *Numerical solutions for $\mu(x)$ in the case of $\mathcal{B} = 2 \times 10^6$ per layer and $\alpha = 1 \times 10^{-6}$, where the boundary condition $h(0) = 2\pi$ have been taken. Clearly exhibited is the multiple shell-like structure of the Skyrmion*

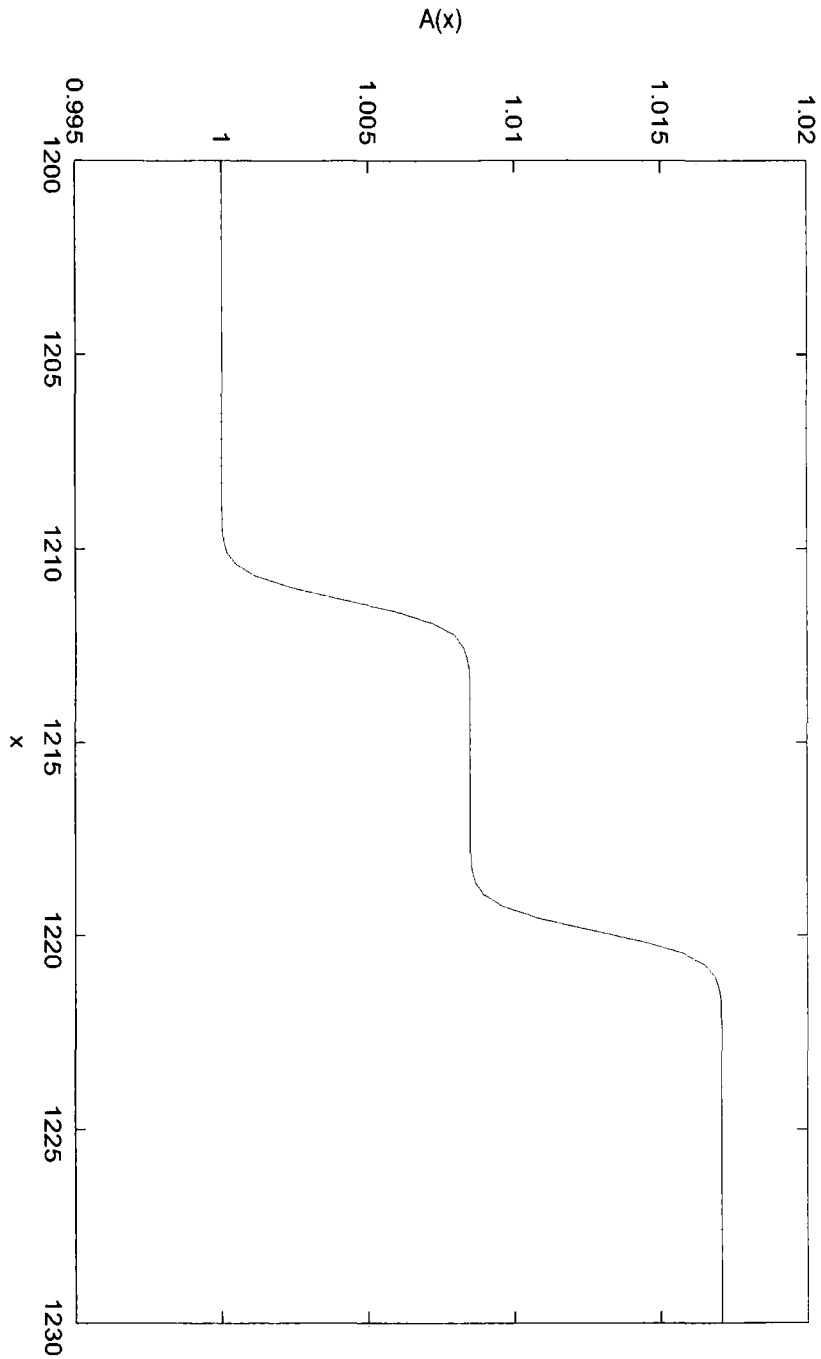

Figure 6.3: *Numerical solutions for $A(x)$ in the case of $\mathcal{B} = 2 \times 10^6$ per layer and $\alpha = 1 \times 10^{-6}$, where the boundary condition $h(0) = 2\pi$ have been taken. Clearly exhibited is the multiple shell-like structure of the Skyrmion*

Clearly the slight modification of the boundary conditions on $h(x)$ has produced a novel structure in the solutions. Again, the fields remain constant until a large radial value at which they evolve simultaneously over a relatively small width before attaining another constant value. The curious thing is that the evolution occurs over two distinct sections which have the same width.

It would seem that for boundary conditions of the form (6.2), the Skyrmion has a multiple-layered structure. In the previous picture of Skyrmions of large baryon number as hollow shells, it appears that solutions of the form shown in Figs. 6.1 - 6.2 correspond to a series of equal width embedded hollow shells. The number of such shells being equal to k the multiplicity of π in the boundary condition (6.2). Such structures hold tantalising possibilities for constructing Skyrme stars.

In the previous chapter it was shown that for realistic input data, a Skyrme star constructed as a hollow shell would simply be too large to resemble anything like a neutron star. However, multiple-layered structures could provide Skyrme stars with considerably lower radii. The reasons are two-fold.

The first is improved packing. For the single-layered structures described in Chapters 4 & 5, the baryons were distributed over an approximately spherical shell of very small width. Essentially, the baryons were distributed over the surface area. A very large baryon number would therefore require a very large surface area and consequently a very large shell radius. If now one deals with embedded shells then, if the number of layers is large, the baryons become distributed within part of a spherical volume. Thus a smaller radius should be required to accommodate the same number of baryons.

Secondly, Table 5.1 already provides evidence for the gravitational compression of hollow Skyrmions. It is hoped that this effect could be enhanced if the Skyrmion has multiple layers, since the outer layers will feel the gravitational attraction due to inner layers.

For these reasons it is plausible to consider multiple-layered Skyrmions as a way of overcoming the size problems of Skyrme stars. Certainly, the total radius of the solutions shown in Figs. 6.1 - 6.3 for two layers is no worse than that of the single layer solutions shown in Figs. 4.1 - 4.3, for the same baryon number.

6.2 The Ladder Ansatze

One proceeds as in Chapter 4 by constructing ansatze for $h(x)$, $\mu(x)$ and $A(x)$ that mimic the multiple-layered structure.

Thus

$$h(x) = \begin{cases} k\pi & 0 \leq x < x_0 - \frac{kW}{2} \\ \frac{k\pi}{2} - (x - x_0)\frac{\pi}{W} & x_0 - \frac{kW}{2} \leq x < x_0 + \frac{kW}{2} \\ 0 & x \geq x_0 + \frac{kW}{2} \end{cases}$$

$$\mu(x) = \begin{cases} 0 & 0 \leq x < x_0 - \frac{kW}{2} \\ \frac{M}{2} + (x - x_0)\frac{M}{kW} & x_0 - \frac{kW}{2} \leq x < x_0 + \frac{kW}{2} \\ M & x \geq x_0 + \frac{kW}{2} \end{cases}$$

$$A(x) = \begin{cases} A_0 & 0 \leq x < x_0 - \frac{kW}{2} \\ \frac{1+A_0}{2} + (x - x_0)\frac{1-A_0}{kW} & x_0 - \frac{kW}{2} \leq x < x_0 + \frac{kW}{2} \\ 1 & x \geq x_0 + \frac{kW}{2} \end{cases}$$

where W is the width of a single layer and x_0 is now the radial position of the centre of all k layers. Again, M is the value of $\mu(x)$ at infinity (as before, there is no central mass) and A_0 the value that $A(x)$ must take at the origin in order to ensure that $A(\infty) = 1$.

It is important to note an approximation here. The above ansatze describe fields changing continuously over the region $x_0 - \frac{kW}{2}$ to $x_0 + \frac{kW}{2}$. However, this is not quite the situation demonstrated in Figs. 6.1 - 6.3. In those solutions there is a small separation between each distinct layer. The size of this separation is small though, compared to the overall radius of the Skyrmion and so this subtle structure has been neglected as a first approximation.

One attempts again to find an explicit form for the energy of the system by substituting the field ansatze into the reduced Hamiltonian (4.1) and then to minimise this with respect to the four free parameters of the ansatze.

For simplicity one will again deal with the Hamiltonian in five distinct parts. Also, as the Hamiltonian is identical to that used in Chapter 4 (all that one alters here are the field ansatze), then all integrands in the energy contain either a power of $sin(h(x))$ or a derivative of one of the fields. Noting from the above ansatze that the fields only change over $x_0 - \frac{kW}{2}$ to $x_0 + \frac{kW}{2}$ and that outside this region $h(x)$ is a multiple of π (and thus $sinh(x)) = 0$, then integration is restricted to the layers themselves.

At this point there is one subtlety. Whilst one integrates over all layers, several of the integrands contain $\mathcal{I}$ or $\mathcal{C}$. Thus information needs to be known about the harmonic map used across each layer. One notes that the motivation for using

the Ladder Ansatze were solutions obtained when taking a single harmonic map combined with the modified boundary conditions on h(x), (6.2). Thus it is sensible to use a single value of the harmonic map quantities $\mathcal{I}$ and $\mathcal{C}$ across all layers.

A suitable picture of the structure is as follows. By taking a harmonic map of degree B along with the previous boundary conditions, (6.1), one obtained a single layer Skyrmion comprising B baryons. Now since each layer in the multiple-layered Skyrmion corresponds to a change in $h(x)$ equal to that in the previous boundary conditions, (6.2), one sees that each layer will contain B baryons. Thus the whole structure contains k layers each with equal baryon number, B.

Of course, as each layer occurs at a different radius, then the volume and thus the baryon density of each layer will vary. This is in fact a desirable property as there is evidence to suggest that neutron stars comprise several strata, each with different neutron densities [35].

Having, stated the above details it is clear that integration of the Hamiltonian density need only be preformed across the layers and with single values of $\mathcal{I}$ and $\mathcal{C}$. Thus the five parts of the energy, without the overall multiplicative constant $-\frac{4\pi f_\pi}{e}$, are

$$H_1 = \int_{x_0-\frac{kW}{2}}^{x_0+\frac{kW}{2}} A(x)\frac{\mu(x)'}{\alpha}dx \tag{6.3}$$

$$H_2 = -\int_{x_0-\frac{kW}{2}}^{x_0+\frac{kW}{2}} A(x)Q_N S(x)h(x)'^2x^2dx \tag{6.4}$$

$$H_3 = -\int_{x_0-\frac{kW}{2}}^{x_0+\frac{kW}{2}} A(x)\mathcal{C}sin^2h(x)[1+S(x)h(x)'^2]dx \tag{6.5}$$

$$H_4 = -\int_{x_0-\frac{kW}{2}}^{x_0+\frac{kW}{2}} \frac{A(x)\mathcal{I}sin^4h(x)}{2x^2}dx \tag{6.6}$$

$$H_5 = -\frac{\mu(\infty)}{\alpha} \tag{6.7}$$

Commencing with H_1, one substitutes the Ladder Ansatze for $\mu(x)$ and $A(x)$ and obtains

$$\begin{aligned} H_1 &= \frac{M}{\alpha k W}\int_{x_0-\frac{kW}{2}}^{x_0+\frac{kW}{2}}\left(\frac{1+A_0}{2}+(x-x_0)\frac{1-A_0}{kW}\right)dx \\ &= \frac{M}{\alpha k W}\left[\frac{1+A_0}{2}x\right]_{x_0-\frac{kW}{2}}^{x_0+\frac{kW}{2}} \\ &= \frac{M}{\alpha}\left(\frac{1+A_0}{2}\right) \end{aligned} \tag{6.8}$$

To arrive at this one has again used the fact that $(x-x_0)$ is an odd function over the symmetric interval of integration. Thus this term vanishes.

Moving on to H_2, one obtains upon substitution and expansion

$$\begin{aligned} H_2 &= -\frac{Q_N\pi^2}{W^2}\int_{x_0-\frac{kW}{2}}^{x_0+\frac{kW}{2}}\left[\frac{1+A_0}{2}+(x-x_0)\frac{1-A_0}{kW}\right] \\ &\quad\times\left[x^2-2x\left(\frac{M}{2}+(x-x_0)\frac{M}{kW}\right)\right]dx \\ &= -\frac{Q_N\pi^2}{W^2}\left[\left(M\left(\frac{1+A_0}{2}\right)\left(\frac{2x_0}{kW}-1\right)+Mx_0\left(\frac{1-A_0}{kW}\right)\left(1-\frac{2x_0}{kW}\right)\right)\left[\frac{x^2}{2}\right]_{x_0-\frac{kW}{2}}^{x_0+\frac{kW}{2}}\right. \\ &+ \left(\left(\frac{1+A_0}{2}\right)\left(1-\frac{2M}{kW}\right)+\left(\frac{1-A_0}{kW}\right)\left(\frac{4x_0M}{kW}-M-x_0\right)\right)\left[\frac{x^3}{3}\right]_{x_0-\frac{kW}{2}}^{x_0+\frac{kW}{2}} \\ &+ \left.\left(\frac{1-A_0}{kW}\right)\left(1-\frac{2M}{kW}\right)\left[\frac{x^4}{4}\right]_{x_0-\frac{kW}{2}}^{x_0+\frac{kW}{2}}\right] \end{aligned} \tag{6.9}$$

From the following evaluations

$$\left[\frac{x^2}{2}\right]_{x_0-\frac{kW}{2}}^{x_0+\frac{kW}{2}} = kWx_0 \tag{6.10}$$

$$\left[\frac{x^3}{3}\right]_{x_0-\frac{kW}{2}}^{x_0+\frac{kW}{2}} = kWx_0^2 + \frac{k^3W^3}{12} \tag{6.11}$$

$$\left[\frac{x^4}{4}\right]_{x_0-\frac{kW}{2}}^{x_0+\frac{kW}{2}} = kWx_0^3 + \frac{k^3W^3x_0}{4} \tag{6.12}$$

the final form of H_2 is given by

$$\begin{aligned} H_2 = & -\frac{Q_N\pi^2}{W}\left[\left(\frac{1+A_0}{2}\right)\left(kx_0^2 - kMx_0 + \frac{k^3W^2}{12} - \frac{k^2MW}{6}\right)\right. \\ & \left. + \left(\frac{1-A_0}{kW}\right)\left(\frac{k^3W^2x_0}{6} - \frac{k^3MW^2}{12} - \frac{k^2MWx_0}{6}\right)\right] \end{aligned} \tag{6.13}$$

H_3 comprises a more involved integral so, for simplicity, it will once again be split into several parts

$$H_3 = H_{31} + H_{32} + H_{33} + H_{34} + H_{35} \tag{6.14}$$

where

$$H_{31} = -\mathcal{C}\left(\frac{1+A_0}{2}\right)\left(1+\frac{\pi^2}{W^2}\right)\int_{x_0-\frac{kW}{2}}^{x_0+\frac{kW}{2}} sin^2h(x)dx \tag{6.15}$$

$$H_{32} = -\mathcal{C}\left(\frac{1-A_0}{kW}\right)\left(1+\frac{\pi^2}{W^2}\right)\int_{x_0-\frac{kW}{2}}^{x_0+\frac{kW}{2}} (x-x_0)\, sin^2h(x)dx \tag{6.16}$$

$$H_{33} = \mathcal{C}\left(\frac{1+A_0}{2}\right)\frac{M\pi^2}{W^2}\int_{x_0-\frac{kW}{2}}^{x_0+\frac{kW}{2}} \frac{sin^2h(x)}{x}dx \tag{6.17}$$

$$H_{34} = C\frac{M\pi^2}{W^2}\left[\left(\frac{1-A_0}{kW}\right)+\frac{2}{kW}\left(\frac{1+A_0}{2}\right)\right]\int_{x_0-\frac{kW}{2}}^{x_0+\frac{kW}{2}}(x-x_0)\frac{sin^2h(x)}{x}dx \quad (6.18)$$

and

$$H_{35} = C\left(\frac{1-A_0}{kW}\right)\frac{2M\pi^2}{kW^3}\int_{x_0-\frac{kW}{2}}^{x_0+\frac{kW}{2}}(x-x_0)^2\frac{sin^2h(x)}{x}dx \quad (6.19)$$

The calculation of H_{31} is straightforward following a change of variable from x to h.

$$\begin{aligned} H_{31} &= -C\left(\frac{1+A_0}{2}\right)\left(\frac{W}{\pi}\right)\left(1+\frac{\pi^2}{W^2}\right)\int_0^{k\pi} sin^2h dh \\ &= -C\left(\frac{1+A_0}{2}\right)\left(\frac{W}{\pi}\right)\left(1+\frac{\pi^2}{W^2}\right)\left[\frac{1}{2}h-\frac{1}{4}sin2h\right]_0^{k\pi} \\ &= -C\left(\frac{1+A_0}{2}\right)\left(\frac{kW}{2}\right)\left(1+\frac{\pi^2}{W^2}\right) \end{aligned} \quad (6.20)$$

As in Chapter 4, one makes the high baryon number approximation that $W << x_0$. This means that across the layers x doesn't vary significantly from the central radius, x_0. Thus $(x - x_0)$ and consequently the contributions from any integrals containing this factor, are negligible.

This approximation requires more consideration than in Chapter 4, since one actually requires that $kW << x_0$. Obviously this depends on the number of layers, k. However, Chapter 5 demonstrated that for realistic values of α and B (7.3×10^{-40} and 10^{58}), the radius, x_0, of a single-layered structure was of the order 10^{28}, whilst the width, W, was of order 1. This clearly allows for a large number of shells.

Even if one was to be optimistic enough that the multiple-layered structures would have a reduced radius akin to that of a neutron star, the approximation is still valid. A typical neutron star has a radius of order $10km$. Using the conversion detailed in Chapter 4, this corresponds in topological units, to a radius of $x_0 =$

2.22×10^{19}. Given that the width of a single layer is still likely to be of order 1, then for the ratio $\frac{kW}{x_0}$ to be small, say of order 10^{-2}, one could still allow 10^{17} layers. Clearly, the small width approximation is still valid.

As a consequence of this observation, one can neglect the contribution to the energy from H_{32}, H_{34} and H_{35}. One is left to calculate H_{33}. Again the ratio of the total width of layers to the radius is taken to be small. One therefore approximates the factor of $\frac{1}{x}$ as $\frac{1}{x_0}$. Thus

$$\begin{aligned} H_{33} &= \mathcal{C}\left(\frac{1+A_0}{2}\right)\frac{M\pi^2}{W^2x_0}\int_{x_0-\frac{kW}{2}}^{x_0+\frac{kW}{2}} sin^2h(x)dx \\ &= \mathcal{C}\left(\frac{1+A_0}{2}\right)\frac{M\pi}{Wx_0}\int_0^{k\pi} sin^2h dh \\ &= \mathcal{C}\left(\frac{1+A_0}{2}\right)\frac{M\pi}{Wx_0}\left[\frac{1}{2}h-\frac{1}{4}sin2h\right]_0^{k\pi} \\ &= \mathcal{C}\left(\frac{1+A_0}{2}\right)\frac{kM\pi^2}{2Wx_0} \end{aligned} \tag{6.21}$$

Summing H_{31} and H_{32}, one obtains for H_3

$$H_3 = \mathcal{C}\left(\frac{1+A_0}{2}\right)\frac{k}{2}\left(\frac{M\pi^2}{Wx_0}-W-\frac{\pi^2}{W}\right) \tag{6.22}$$

After substitution of the field ansatze, the fourth contribution to the energy reads

$$H_4 = -\mathcal{I}\int_{x_0-\frac{kW}{2}}^{x_0+\frac{kW}{2}}\left[\frac{1+A_0}{2}+(x-x_0)\frac{1-A_0}{kW}\right]\frac{sin^4h(x)}{2x^2}dx \tag{6.23}$$

As previously, one simplifies by neglecting the contribution from the term containing the factor $(x-x_0)$ and then declaring that the denominator $2x^2$ be approximately equal to $2x_0^2$ across the integration interval.

One is left with

$$\begin{aligned} H_4 &= -\frac{\mathcal{I}}{2x_0^2}\left(\frac{1+A_0}{2}\right)\int_{x_0-\frac{kW}{2}}^{x_0+\frac{kW}{2}} sin^4h(x)dx \\ &= -\frac{\mathcal{I}W}{2\pi x_0^2}\left(\frac{1+A_0}{2}\right)\int_0^{k\pi} sin^4h dh \\ &= -\frac{\mathcal{I}W}{2\pi x_0^2}\left(\frac{1+A_0}{2}\right)\left[\frac{3}{8}h - \frac{1}{4}sin2h + \frac{1}{32}sin4h\right]_0^{k\pi} \\ &= -\frac{3k\mathcal{I}W}{16x_0^2}\left(\frac{1+A_0}{2}\right) \end{aligned} \tag{6.24}$$

Finally, the boundary term, H_5, is calculated as

$$\begin{aligned} H_5 &= -\frac{\mu(\infty)}{\alpha} \\ &= -\frac{M}{\alpha} \end{aligned} \tag{6.25}$$

Now one is in a position of finding the explicit form of the energy for a multiple-layered gravitating Skyrmion, subject to the high baryon number approximation. Combining the five parts of the energy, one obtains

$$\begin{aligned} H &= -\frac{4\pi f_\pi}{e}\left[\frac{M}{\alpha}\left(\frac{1+A_0}{2}\right) - \frac{Q_N\pi^2}{W}\left[\left(\frac{1+A_0}{2}\right)\left(kx_0^2 - kMx_0 + \frac{k^3W^2}{12} - \frac{k^2MW}{6}\right)\right.\right. \\ &+ \left.\left.\left(\frac{1-A_0}{kW}\right)\left(\frac{k^3W^2x_0}{6} - \frac{k^3MW^2}{12} - \frac{k^2MWx_0}{6}\right)\right] \right. \\ &+ \left. C\left(\frac{1+A_0}{2}\right)\frac{k}{2}\left(\frac{M\pi^2}{Wx_0} - W - \frac{\pi^2}{W}\right) - \frac{3k\mathcal{I}W}{16x_0^2}\left(\frac{1+A_0}{2}\right) - \frac{M}{\alpha}\right] \end{aligned} \tag{6.26}$$

Clearly, the energy obtained in Chapter 4, using the Ramp Ansatze, is a special case of (6.26) for a single layer. Indeed setting $k = 1$, one recovers the energy of a single layered Skyrmion, (4.33), as one would expect.

The method for finding solutions is now identical to in Chapter 4. One first minimises the energy independently with respect to the parameters M and A_0 to obtain the following constraints.

$$\frac{\partial H}{\partial M} = 0 \Rightarrow$$

$$A_0 = \frac{\alpha\pi^2\left(-3k\mathcal{C} - 8kQ_N x_0^2 - 2k^2 Q_N x_0 W\right) + 6x_0 W}{\alpha\pi^2\left(3k\mathcal{C} + 4kQ_N x_0^2\right) + 6x_0 W} \tag{6.27}$$

and

$$\frac{\partial H}{\partial A_0} = 0 \Rightarrow$$

$$M = \frac{\alpha\left(8\pi^2\left(3k\mathcal{C}x_0^2 + 6kQ_N x_0^4 - 2k^2 Q_N x_0^3 W\right) + W^2\left(9k\mathcal{I} + 24k\mathcal{C}x_0^2 + 4k^3\pi^2 Q_N x_0^2\right)\right)}{8x_0\left(\alpha\pi^2\left(3k\mathcal{C} + 4kQ_N x_0^2\right) + 6x_0 W\right)} \tag{6.28}$$

As one would expect these take the same form as for the single-layered structures of Chapter 4, for the case $k = 1$. Thus they also behave correctly ($A_0 \to 1$ and $M \to 0$) in the limit of gravitational decoupling ($\alpha \to 0$). This can be seen to be true regardless of the layer number k.

Finally, minimal energy configurations can be obtained. Upon substitution of constraints (6.27) and (6.28) into the explicit Hamiltonian, (6.26), one picks out a two-dimensional sub-space of the full parameter space. One again uses the *FindMinimum* routine in *Mathematica* to minimise in the remaining W and x_0 directions.

Chapter 7

Ladder Ansatze Generated Configurations

This chapter presents parameter sets obtained by numerical minimisation of the energy of a multiple-layered self-gravitating Skyrmion, (6.26). Again, for the $SU(2)$ model, values of $\mathcal{C} = B$ and $\mathcal{I} = 1.28B^{\frac{1}{2}}$ were taken when trying to study configurations containing B baryons.

In particular, the first plausible baryon star configuration is produced within the $SU(2)$ Einstein-Skyrme model.

7.1 $SU(2)$ Configurations

7.1.1 Validity of the Ladder Ansatze

The data sets contained in table 7.1 are the minimum energy configurations for double layer Skyrmions with various baryon numbers. That is, the layer number

$k = 2$. Each configuration was obtained at a fixed coupling of $\alpha = 1 \times 10^{-6}$.

Of particular interest is the double layer configuration containing a total of 4×10^6 baryons, (2×10^6 baryons per layer). One can see that the ladder ansatze predicts that such a configuration has a radius of $x_0 = 1165.97$. Further, it predicts that each layer has a width of 3.09.

Such a configuration has already been obtained, at the same value of α, by direct numerical integration of the field equations (2.32) -(2.35). The solutions are shown in figures 6.1 -6.3, in Chapter 7. Inspection of the plots reveals that the actual radius of solutions was ≈ 1214.0 (remember it is taken to be the centre of the two layers). The width of each layer was ≈ 3.5.

Comparing the data obtained by direct integration and that predicted by the ladder ansatze, one finds discrepancies of < 4 per cent in radius and < 12 per cent in layer width. The discrepancy in the width is higher than that caused by taking the ramp ansatze for a single layer configuration (see section 6.1.1). This is probably caused by the extra assumption made in the ladder ansatze, that there was no separation between layers. However, the discrepancies are not significantly large to cause concern.

Further, if one studies figure 6.2 in Chapter 6, one finds that the solution for $\mu(x)$ has a final value of $\mu(\infty) \approx 20$. This corresponds to and ADM mass per baryon of

$$\begin{aligned} \frac{M_{ADM}}{B} &= \frac{4\pi\mu(infty)}{\alpha B} \\ &\approx \frac{80\pi}{4} \\ &\approx 62.83 \end{aligned} \tag{7.1}$$

This value must be compared with that predicted by the ladder ansatze of 66.28. Indeed the ADM mass has been overestimated, as one would expect from imposing an ansatze. However the discrepancy is < 6 per cent and one concludes that the ladder ansatze does produce configurations with properties satisfactorily close to true solutions.

7.1.2 The affect of varying the layer number, k

Having established faith in the configurations generated by the ladder ansatze, one asks "What general affects come from varying the number of layers?".

Comparing table 7.1 to tables 5.2 and 5.3, one can start to see differences caused by doubling the layer number. The first thing to note is that at each baryon number, the radius of double layer configurations is considerably lower than for the single layer configurations. This is true whether one compares the values of x_0 or if one considers the total radius of solutions after layer widths have been added. Far from baryon numbers for which the value of $\alpha = 1 \times 10^{-6}$ used is close to their critical coupling, the decrease in radius is likely to be due to a better packing of baryons. As was hoped in Chapter 6, it seems that indeed the radius is reduced because of baryons being distributed through a volume instead of across a surface area.

For baryon numbers of greater than 1×10^9 (at this coupling of $\alpha = 1 \times 10^{-6}$),

the affect appears to be enhanced. The difference between the single and double layer radii, is even larger. This seems to signify that gravity is now playing an important role and that the gravitational attraction of the inner layer, in the double layer configurations, has resulted in increased compression. This is what was hoped for and may pave the way in constructing plausible baryon stars.

It is also important to note that the width of layers has not been significantly decreased, for the double layer structures. One might have expected the width to half as the number of layers doubled. This would have meant that the baryon density was the same as for the single layer configurations. In this case one would have obtained two layers, back to back, with the same baryon density as before and with half the width. In effect, the configuration would have been indistinguishable from a single layer Skyrmion. This is not the case and one concludes that the configurations detailed in this chapter are qualitatively different structures to those previously described.

The situation is also desirable in terms of energy. One notes that at each baryon number the double layer solutions have a lower ADM mass per baryon, than their single layer counterparts. Far from the critical coupling, this is probably due to a relaxation within the Skyrmion. However, near α_{crit} it seems that the increased gravitational attraction between layers, for the double layer configurations, results in an increased gravitational binding energy for the baryons.

Table 7.2, shows the direct affect that the number of layers has on the critical coupling. The data was obtained by varying k for a fixed total of 10^{58} baryons. This number of baryons was chosen not just because it is the order of baryons needed for

something like a star. More importantly, it allowed a large variety of layer numbers, k, to be used, whilst still ensuring that the approximations made (which relied on $kW << x_0$) remained valid.

One sees that the layer number vastly impacts on the highest value of α for which solutions can be obtained. In fact, it can be seen that there is quite a precise relationship, that $\alpha \propto k^{-\frac{1}{2}}$. This will be important when constructing baryons stars. One has already seen that although the existence of α_{crit} is not due to horizon formation, the approach of the critical coupling does herald the point at which gravity plays a significant role in binding the baryons. The real physical value is very low, at $\alpha_{physical} = 7.3 \times 10^{-40}$. However, the relationship between k and α_{crit} implies gravitational binding will still be evident, even at such a low value of the coupling, if a sufficiently large number of layers are present.

7.1.3 Plausible baryon stars

All the signs are favourable for using the Einstein-Skyrme system as a toy model for baryon stars. One has already shown that increasing the layer number can reduce the radius and allow gravitational binding to be possible at small coupling values. What remains is to study a configuration with a sufficiently high baryon number, at $\alpha_{physical}$, to see whether a plausible structure can be obtained.

Tables 7.3 and 7.4 detail the data obtained for Skyrmions with 10^{58} baryons at $\alpha_{physical}$, using different numbers of layers. One notes all the features described earlier. That the radius and mass reduce with increasing k, and that this is enhanced when the layer number is such that $\alpha_{physical}$ is close to α_{crit}.

For B=10^{58}, $\alpha_{physical} = \alpha_{crit}$ at $k = 5.330657 \times 10^{17}$ layers. This is the maximum number of layers that can support 10^{58} baryons, at $\alpha = 7.3 \times 10^{-40}$. One first checks that all approximations are valid. For this number of layers, the radius is predicted as $x_0 = 7.150612 \times 10^{19}$ and the width as $W = 1.552304$. Thus indeed the requirement that $kW << x_0$, is satisfied. One can therefore be confident in the parameters describing this configuration and the structure can be discussed with faith.

First one notes that this configuration is energetically favourable. The ladder ansatze predict an ADM mass of 56.18 per baryon, as compared to the B=1 gravitating Skyrmion mass found in Chapter 4 to be 72.92 (at a considerably larger value of α). Thus one indeed finds a bound state of a sufficiently large number of baryons to be akin to a baryon star.

The question of spherical symmetry has already been discussed in Chapter 4. The configuration consists as a large number of embedded layers. Each contains in the order of 10^{40} baryons distributed as a tight lattice over a spherical shell. Thus the overall structure has approximate spherical symmetry as required.

As was seen in Chapter 5, the radius of configurations caused concern. Baryon star candidates within the Einstein-Skyrme model were just too large. One has already seen that allowing the number of layers to increase, can significantly reduce the overall size of the configuration. One is left asking what is predicted for the multiple layer baryon star.

Taking the maximum number of layers allowed for B=10^{58} at $\alpha_{physical}$, the ansatze predicts values of $x_0 = 7.150612 \times 10^{19}$ and $W = 1.552304$, as stated earlier. This

gives a total radius of

$$\begin{aligned} x_{star} &= x_0 + kW \\ &\approx 7.23 \times 10^{19} \end{aligned} \tag{7.2}$$

Converting to SI units using the values given in Chapter 5, one has

$$\begin{aligned} R_{star} &= \frac{x_{star}}{ef_\pi} \\ &\approx 32.51 km \end{aligned} \tag{7.3}$$

Thus one concludes that the Einstein-Skyrme model may indeed be a suitable testing ground for studying approximations of baryon stars, predicting a bound state of 10^{58} baryons, with the correct symmetry and with a radius comparable to a typical neutron star.

B	x_0	W	A_0	M_{ADM}/B	S_{min}
1×10^6	585.795134	3.115293	0.990909	66.520788	0.982023
2×10^6	826.800070	3.104350	0.987118	66.426750	0.974522
4×10^6	1165.971374	3.088826	0.981726	66.283602	0.963905
5×10^6	1302.092387	3.082530	0.979543	66.224381	0.959622
1×10^7	1833.045504	3.057771	0.970923	65.988069	0.942801
2×10^7	2575.162485	3.022296	0.958570	65.648620	0.918948
5×10^7	4016.404800	2.951177	0.933477	64.967281	0.871374
1×10^8	5587.271170	2.868732	0.904152	64.191754	0.817242
2×10^8	7702.394198	2.747487	0.860462	63.082328	0.739398
5×10^8	11449.400032	2.483688	0.763193	60.826251	0.959623
1×10^9	14560.531816	2.109223	0.620566	58.138282	0.364607
1.4×10^9	14548.790990	1.662263	0.446035	56.287941	0.138040
1.41×10^9	14384.731809	1.629530	0.433224	56.244544	0.122658
1.419×10^9	14065.061027	1.575253	0.412017	56.210839	0.097531
1.4198×10^9	13957.031889	1.5588612	0.405624	56.2107105	0.090035
1.41988×10^9	13914.517098	1.552611	0.403185	56.211877	0.087184
1.419882×10^9	13910.592896	1.552039	0.402961	56.212013	0.086923

Table 7.1: *Numerically obtained minimum energy configurations for a range of baryon numbers at* $\alpha = 1 \times 10^{-6}$ *and* $k = 2$. *Respectively shown are the baryon number and optimal values for the radius of the shell, layer widths, the value of* A_0 *such that* $A(\infty) = 1$, *the ADM Mass per baryon and the minimum value of the metric function* $S(x) = \left(1 - \frac{2\mu(x)}{x}\right)$.

k	α_{crit}	x_0	W	A_0	M_{ADM}/B	S_{min}
1	5.328462×10^{-31}	5.252242×10^{28}	1.564261	0.407736	56.210872	0.092394
10	1.685007×10^{-31}	1.660926×10^{28}	1.564286	0.407746	56.210871	0.092406
10^2	5.328462×10^{-32}	5.252242×10^{27}	1.564261	0.407736	56.210872	0.092394
10^3	1.685007×10^{-32}	1.660926×10^{27}	1.564287	0.407746	56.210871	0.092406
10^4	5.328462×10^{-33}	5.252242×10^{26}	1.564261	0.407736	56.210872	0.092394
10^5	1.685007×10^{-33}	1.660926×10^{26}	1.564287	0.407746	56.210871	0.092406
10^6	5.328462×10^{-34}	5.252242×10^{25}	1.564261	0.407736	56.210872	0.092394
10^7	1.685007×10^{-34}	1.660926×10^{25}	1.564287	0.407746	56.210871	0.092406
10^8	5.328462×10^{-35}	5.252242×10^{24}	1.564261	0.407736	56.210872	0.092394
10^9	1.685007×10^{-35}	1.660926×10^{24}	1.564287	0.407746	56.210871	0.092406
10^10	5.328462×10^{-36}	5.252242×10^{23}	1.564261	0.407736	56.210872	0.092394

Table 7.2: *Numerically obtained minimum energy configurations containing* 10^{58} *baryons but with a varying layer number* k. *Respectively shown are the layer number, critical coupling and optimal values for the radius of the shell, layer widths, the value of* A_0 *such that* $A(\infty) = 1$, *the ADM Mass per baryon and the minimum value of the metric function* $S(x) = \left(1 - \frac{2\mu(x)}{x}\right)$.

k	x_0	W	A_0	M_{ADM}/B	S_{min}
1	8.323583×10^{28}	3.141593	1.000000	66.829868	1.000000
2	5.885662×10^{28}	3.141593	1.000000	66.829868	1.000000
10	2.632148×10^{28}	3.141593	1.000000	66.829868	1.000000
10^2	8.323583×10^{27}	3.141593	1.000000	66.829868	1.000000
10^3	2.632148×10^{27}	3.141593	1.000000	66.829867	1.000000
10^4	8.323582×10^{26}	3.141593	1.000000	66.829866	1.000000
10^5	2.632148×10^{26}	3.141592	1.000000	66.829863	1.000000
10^6	8.323581×10^{25}	3.141591	1.000000	66.829854	0.999999
10^7	2.632146×10^{25}	3.141588	0.999999	66.829825	0.999997
10^8	8.323563×10^{24}	3.141579	0.999995	66.829733	0.959623
10^9	2.632128×10^{24}	3.141550	0.999985	66.829442	0.959623
10^{10}	8.323382×10^{23}	3.141457	0.999953	66.828522	0.999907
10^{11}	2.631947×10^{23}	3.141165	0.999852	66.825611	0.959623
10^{12}	8.321575×10^{22}	3.140240	0.999533	66.816408	0.999067
10^{13}	2.630138×10^{22}	3.137312	0.998524	66.787300	0.997050
10^{14}	8.303433×10^{21}	3.128041	0.995323	66.695218	0.990668
10^{15}	2.611829×10^{21}	3.098565	0.985121	66.403649	0.970461

Table 7.3: *Numerically obtained minimum energy configurations containing* 10^{58} *baryons at* $\alpha_{physical} = 7.3 \times 10^{-40}$. *The number of layers,* k, *has been varied. Respectively shown are the layer number and optimal values for the radius of the shell, layer widths, the value of* A_0 *such that* $A(\infty) = 1$, *the ADM Mass per baryon and the minimum value of the metric function* $S(x) = \left(1 - \frac{2\mu(x)}{x}\right)$.

k	x_0	W	A_0	M_{ADM}/B	S_{min}
10^{16}	8.114672×10^{20}	3.003680	0.951997	65.477403	0.906253
10^{17}	2.400111×10^{20}	2.680978	0.836210	62.489436	0.697674
5×10^{17}	8.2065713×10^{19}	1.788807	0.495296	56.562632	0.203564
5.3×10^{17}	7.417211×10^{19}	1.622703	0.430205	56.203619	0.124702
5.33×10^{17}	7.187062×10^{19}	1.562516	0.406704	56.177573	0.097088
5.3306×10^{17}	7.159665×10^{19}	1.554856	0.403717	56.178822	0.093607
5.33065×10^{17}	7.152519×10^{19}	1.552843	0.402931	56.179307	0.092693
5.330657×10^{17}	7.150612×10^{19}	1.552304	0.402721	56.179446	0.092448

Table 7.4: *Numerically obtained minimum energy configurations containing* 10^{58} *baryons at* $\alpha_{physical} = 7.3 \times 10^{-40}$. *The number of layers,* k, *has been varied. Respectively shown are the layer number and optimal values for the radius of the shell, layer widths, the value of* A_0 *such that* $A(\infty) = 1$, *the ADM Mass per baryon and the minimum value of the metric function* $S(x) = \left(1 - \frac{2\mu(x)}{x}\right)$.

Chapter 8

Conclusions

8.1 Summary of Research

The purpose of this research, as stated in Chapter 1, was to revisit the $SU(N)$ Einstein-Skyrme model as a possible toy model for baryon stars. Previous work, most notably by Bizon & Chmaj [25], [26], had ruled out solutions representing baryon stars on grounds of energy. Taking the hedgehog ansatze for the Skyrme field coupled to gravity they obtained solutions that inherently possessed spherical symmetry. However it was found that, just as in the flat-space scenario, multi-baryon states were not energetically favourable and were susceptible to decay into single baryon Skyrmions. The affect of gravity simply did not provide sufficient binding to allow spherical multi-baryon states.

The technique used in this thesis was to approach the problem from a different angle. It is known that the harmonic map ansatze [9], [10], provide very good approximations to true low energy solutions of the $SU(N)$ Skyrme model. It is also known that the approximate solutions obtained using these ansatze, at least for

low baryon number, are not spherical for B> 1. For example, in the $SU(2)$ model, the B= 2 solution resembles a torus, whilst the solutions containing three and four baryons are tetrahedral and cubic respectively.

At the start of the research project, one decided to look for energetically favourable approximate solutions to the Einstein-Skyrme model as a first requirement and not to impose spherical symmetry from the outset. Thus the harmonic map ansatze were taken for the Skyrme field coupled to gravity. A spherically symmetric metric ansatze was taken, as this would be appropriate for eventual baryon star structures. Using all of the above, it was possible to derive the Euler-Lagrange equations for the profile function, $h(x)$, the mass field, $\mu(x)$ and the metric field, $A(x)$.

Using known values for the minimal angular quantities of the harmonic map ansatze, taken from [9] & [30], it was possible to solve these coupled differential equations at low baryon number. In order to do this, however, there were non-trivial technical challenges to overcome, relating to the application of boundary conditions. A highly non trivial asymptotic expansion of fields, which depended on all the parameters of the system, enabled one to proceed.

The low energy solutions reproduced that of Bizon & Chmaj at B=1. This was to be expected as for a single baryon in the $SU(2)$ model, the harmonic map ansatze are completely equivalent to the hedgehog ansatze and the solution is spherically symmetric [9]. Two branches of solutions were obtained which coincided at a critical value of the coupling constant α. Above this value, no further solutions were obtained.

A study of the metric at the critical coupling revealed that the system was far

from horizon formation and thus α_{crit} could not be caused by collapse to a singularity. The existence of the critical coupling can be understood as the annihilation point of two different local extrema of the model. Concretely, the upper branch of solutions represents sphalerons within the model, [37], which annihilate with the lower branch regular minima, at α_{crit}.

For multi-baryon self-gravitating Skyrmions, the situation was entirely different to the findings of Bizon & Chmaj [25]. As was hoped, the solutions became more and more energetically favourable, as the baryon number increased. Again two branches of solutions were obtained but this time the critical coupling varied as $\alpha_{crit} \approx 0.040378 B^{-\frac{1}{2}}$ (as opposed to $\alpha_{crit} \approx B^{-2}$).

The fact that the ADM mass per baryon actually decreased with increasing baryon number suggested that, in fact, the Einstein-Skyrme model could be used as a toy model for baryon stars. At this point one had to step back and reflect on what had actually been obtained. As the case when taking any ansatze for the Skyrme field, one actually obtains approximations to the true minimal energy Skyrmion, for any given baryon number. However, the situation is more complicated here.

One has effectively found structures which are not spherical, coupled to a spherical gravitational field which is supposed to be induced by the baryon distribution itself. Thus there is a mismatching in symmetry and all one can claim is to have found some approximate configurations which suggest that multi-baryon bound states could exist. One should not be alarmed, however, as this was all that one set out to achieve at first. That is, one wished to address the issue of energy first and then hope to recover spherical symmetry.

The work of Battye & Sutcliffe [30], amongst others, [9], [?], [34], suggested that this might be possible. It was found that for moderately large baryon numbers, approximations to true Skyrmions had structures resembling the fullerene cages of Carbon chemistry. That is, the baryons were distributed over a shell-like lattice. As the baryon number increased, the lattice became tighter and, viewed externally, the deviation from spherical symmetry became less. It was therefore argued that at the large baryon numbers one wished to study for baryon stars, the approximations to true self-gravitating Skyrmions would resemble shells with approximate spherical symmetry. Such arguments were also supported by the form of the fields obtained for B=2×10^6 (see figures 4.1- 4.3).

The observation led to an approach, which would also allow one to overcome the technical challenges in numerically integrating the Euler-Lagrange equations. In a similar fashion to Kopeliovich [33], [34], one formed the ramp ansatze for $h(x)$, $\mu(x)$ and $A(x)$ based on the approximate solutions that had been obtained. This allowed integration of the Hamiltonian, once one made certain approximations relating to the radius and thickness of the shell, at high baryon number.

The explicit form of the total energy of the model was then minimised semi-analytically, to find the parameters of the ansatze which described minimal energy configurations. A comparison of the results obtained for B=2×10^6, showed that the ramp ansatze were in good agreement with the solutions obtained by direct numerical integration of the Euler-Lagrange equations.

One found that the (now spherical) approximations to true self-gravitating Skyrmions, continued the trend of becoming more energetically favourable, with increased baryon

number. The existence of the critical coupling was still evident and again followed a $\alpha_{crit} \propto B^{-\frac{1}{2}}$ relationship.

An interesting behaviour was observed for the radius. Far from the critical coupling, the radius increased as $B^{\frac{1}{2}}$, in accordance with the increased surface area of the shell, needed to accommodate the increased baryon number. However, close to α_{crit}, the radius grew less quickly suggesting that gravity was becoming important and that gravitational compression was occurring. In fact, very close to α_{crit}, the radius actually decreased as more baryons were added. This is an effect that is predicted for real neutron stars, in that a smaller radius is needed in order to sufficiently increase the degenerate neutron pressure needed to balance the gravitational attraction [35].

It was found that, at the true physical value of α, a structure containing a typical baryon number for a neutron star, was predicted to be energetically stable. However, the radius of this configuration, at $3.74 \times 10^{10} km$, was simply too large to resemble a neutron star. This was not surprising. Remember, one has found approximations to self-gravitating Skyrmions that resemble a hollow shell. Clearly this is not the picture one has of a neutron star.

One is forced to consider a structure consisting of several embedded shells. This would hopefully allow a decrease in radius for two reasons. Firstly, the baryons would be distributed throughout a finite volume, and thus a better packing is achieved. Secondly, one hopes for extra gravitational compression due to attraction between layers.

Earlier numerical solutions obtained at B=4×10^6 using the alternative boundary

condition $h(0) = k\pi$, show that the approximate solutions could possess a multi-layer structure. Based on these results (figures 6.1 - 6.3), one formed the ladder ansatze describing this structure. Again, with careful consideration the Hamiltonian was integrated and minimum energy approximate solutions were obtained.

These were found to be in good agreement with the numerical results for B=4 $\times$ 10^6. It was observed that the number of layers did indeed reduce the radius of configurations, in the manner described. Further, the layer number led to a reduction in the ADM mass and in the critical coupling for any given baryon number. In total one obtains $\alpha_{crit} \propto k^{-\frac{1}{2}} B^{-\frac{1}{2}}$.

This time, an approximation to a self-gravitating Skyrmion resembling a baryon star was obtained, with radius of $32.51km$. This is a much more credible candidate.

In short then, one has shown that by not initially imposing spherical symmetry one can obtain energetically favourable approximations to multi-baryon self-gravitating Skyrmions. As a by-product of the high baryon numbers required to study baryon stars, approximate spherical symmetry is eventually recovered. One can obtain structures containing sufficiently large numbers of baryons to be astrophysically relevant. For fun, the author will term these structures *Solarons* (star-like solitons).

One doesn't claim that these Solarons are models of neutrons stars. There are still many things to do and refinements to make, as will be discussed. However, the research suggests that the Einstein-Skyrme system may be used as a toy model for baryon stars and has gone some way in constructing such a model.

The Solarons obtained do have interesting and desirable properties. These in-

clude appropriate radii, a stratified distribution of baryons (as believed for neutron stars and the possibility of a decrease in size with added baryons [11], [32], [35].

8.2 Future Directions

As one has said, there are still many refinements to be made to the model and plenty of avenues for future research.

The first thing to be done is to improve the ladder ansatze. At the moment one has many layers, back to back and all having the same width and containing the same number of baryons. One could improve this by adding another parameter to the ansatze which describes the separation between layers.

More importantly, one eventually wishes to be able to construct a Hamiltonian in which all that one fixes is the baryon number. The number of layers and, moreover, the baryon number per layer should be free parameters of the model which will be determined upon minimisation of the energy. It is hoped that in this way, the number of layers and their widths will settle in such a way, that the gaps between layers and the remaining hollow region, become filled.

This is a complicated task and is currently being studied by the author, along with his supervisor Dr. Bernard Piette. Some progress has, however, been made. As a simplification, a two or three layer ansatze can be built, which includes filling factors for each layer. These describe the proportions of the total number of baryons (which is fixed), contained by each layer [38]. The explicit form of the Hamiltonian has been derived in this case but, as of yet, no suitable minimum energy configurations have been found.

The second thing that can be done is to study solutions to the $SU(3)$ model. Certainly all the theoretical work in this thesis has been set up to allow any number of flavours to be studied. However, because of the computation time involved, numerical results have only been obtained for the $SU(2)$ model. This is an avenue which can now be directly explored. It is expected that the same qualitative features will be present but that the energies of solutions may be affected in line with the flat-space analogue [39].

Finally, after one has satisfactorily refined the ladder ansatze to achieve a better toy model, one could start to build in more realistic properties. For example, an angular momentum term could be added to the matter part of the action, to describe a spinning Skyrmion [36]. Coupled to a non-static metric, in principle the Euler-Lagrange equations could be derived, although now this would result in a series of coupled partial differential equations. The solution of these is expected to be a highly non-trivial task.

Another, very interesting investigation would be to study self-gravitating Skyrmions using different ansatze. Some research suggests that at high baryon densities, there may be even lower energy solutions than obtained from harmonic maps. Such solutions resemble a crystal or lattice [40]. It may be possible, with a judicious choice of boundary conditions, to obtain giant spherical chunks of the lattice, which could then be used to give non-hollow star-like structures.

Bibliography

[1] Skyrme, T.H.R. (1961), *A Nonlinear field theory*, Proc. Roy. Soc. London, **A260**, pp 127 138.

[2] Skyrme, T.H.R. (1962), *A unified field theory of mesons and baryons*, Nucl. Phys., **31**, pp 556 569.

[3] Schechter, J. & Weigel, H. (1999), *The Skyrme model for baryons*, Invited review article for INSA-Book-2000, **hep-ph/9907554**

[4] Makhankov, V.G., Rybakov, Y.P. & Sanyuk, V.I. (1993) *The Skyrme model: fundamentals, methods, applications*, Springer-Verlag, Berlin

[5] 't Hooft, G. (1974), *A planar diagram theory for strong interactions*, Nucl. Phys., **72**, pp 461 473.

[6] Witten, E. (1979), *Baryons in the 1 / N expansion*, Nucl. Phys. B., **160**, pp.57 175

[7] Manton, N., Landshoff, P.V., & Sutcliffe, P. (2004), *Topological Solitons*, Cambridge University Press, Cambridge.

[8] Gisiger, T. & Paranjape, M.B., (1998), *Recent Mathematical Developments in the Skyrme model*, Phys. Rept., **306**, pp. 109 211

[9] Houghton, C., Manton, N. & Sutcliffe, P. (1998), *Rational Maps, Monopoles and Skyrmions*, Nucl. Phys. B **510**, p. 507

[10] Ioannidou, T., Piette, B. & Zakrzewski, W.J. (1998), *Low energy states in the SU(N) Skyrme Models*, **hep-th/9811071**

[11] Oxford University Astrophysics webpage, **www.astro.physics.ox.ac.uk**

[12] Luckock, H. & Moss, I.G., (1986), Phys. Lett. B, **176**, p. 341

[13] Luckock, H. (1987), *Black Hole Skyrmions*, in 'String theory, quantum cosmology and quantum gravity', eds. de Vega, H.J. & Sanchez, N., World Scientific, Singapore.

[14] Moss, I.G., *Exotic Black Holes*, Talk presented at the 8th Nishinomiya-Yukawa Memorial Symposium **gr-qc/9404014**

[15] Droz, S., Heusler, M., Straumann, N., (1991), Phys. Lett. B, **268**, p. 371

[16] Kleihaus, B., Kunz, J. & Sood, A., (1995), *SU(3) Einstein-Skyrme Solitons and Black Holes*, Phys. Lett. B, **352**, p. 247

[17] Mavromatos, N.E. & Winstanley, E., (1998), *Existence theorems for hairy black holes in SU(N) Einstein-Yang-Mills theories*, J. Math. Phys., **39**, pp. 4849 4873

[18] Moss, I.G., Shiiki, N., Winstanley, E., (2000), *Monopole black hole Skyrmions*, Clas. Quant. Grav., **17**, pp. 4168-4174

[19] Tamaki, T., Maeda, K., & Torii, T., (2001), *Internal structure of the Skyrme black hole*, Phys. Rev. D, **64**, 084019

[20] Sawado, N. & Shiiki, N., (2003), *Axially symmetric black hole Skyrmions*, **gr-qc/0307115**

[21] Shiiki, N., Sawado, N., Torii, T. & Maeda, K., (2004), *Regular and black hole Skyrmions with axisymmetry*, Gen. Rel. Grav., **36**, pp. 1361 1371

[22] Shiiki, N. & Sawado, N., (2005), *Regular and black hole Skyrmions in the Einstein-Skyrme theory with negative cosmological constant*, Class. Quant. Grav. **22**, pp. 3561-3574

[23] Bartnik, R. & McKinnon, J., (1988), Phys. Rev. Lett., **61**, p. 141

[24] Choptuik, M.W., Hirschmann, E.W. & Marsa, R.L., (1999), *New critical behaviour in Einstein-Yang-Mills collapse*, Phys. Rev. D, **60**, 124011

[25] Bizon, P. & Chmaj, T., (1992), *Gravitating Skyrmions*, Phys. Lett. B, **297**, Issue 1 2, pp. 55 62

[26] Bizon, P. & Chmaj, T., (1998), *Critical Collapse of Skyrmions*, Phys. Rev. D, **58**, 041501

[27] Brihaye, Y., Hartmann, B., Ioannidou, T. & Zakrzewski, W., (2004), *Harmonic Map Analysis of SU(N) Gravitating Skyrmions*, Phys. Rev. D, **69**, 124035

[28] Ioannidou, T., Kleihaus, B. & Zakrzewski, W., (2004), *Axially symmetric SU(3) gravitating Skyrmions*, Phys. Lett. B, **600**, pp. 116 125

[29] Wald, R.M., (1984), *General Relativity*, The University of Chicago Press, Chicago.

[30] Battye, R. & Sutcliffe, P., (2002), *Skyrmions, Fullerenes and Rational Maps*, Rev. Math. Phys., **14**, p. 29

[31] Battye, R., Houghton, C., & Sutcliffe, P., (2003), *Icosahedral Skyrmions* J. Math. Phys., **44**, pp. 3543-3554

[32] University of Hertfordshire Astrophysics Webpage, *www.herts.ac.uk/astro-ub/aN-ub.html*

[33] Kopeliovich, V., (2001), *The bubbles of matter from multiskyrmions* PISMA ZH.EKSP.TEOR.FIZ., **73**, p. 667

[34] Kopeliovich, V., (2002), *MultiSkyrmions and baryonic bags* J.PHYS.G., **28**, p. 103

[35] Carroll, B. W., & Ostlie, D. A., (1996), *An Introduction to Modern Astrophysics* Addison-Wesley Pub., Wokingham

[36] Battye, R.A., Krusch, S. & Sutcliffe, P., (2005), *Spinning Skyrmions and the Skyrme parameters*, **hep-th/0507279**

[37] Krusch, S. & Sutcliffe, P., (2004), *Sphalerons in the Skyrme Model*, J. Phys. A., **37**, 9037

[38] Piette, B. & Probert, G.I., (2005), *Towards Skyrmion Stars:Large baryon number configurations in the Einstein-Skyrme model*, in preparation.

[39] Kopeliovich, V. Stern, B.E. & Zakrzewskin, W.J., (2000), *Skyrmions from SU(3) Harmonic Maps and their Quantisation*, Phys. Lett. B, **492**, pp. 39 46

[40] Battye, R. & Sutcliffe, P., (1998), *A Skyrme Lattice with Hexagonal Symmetry*, Phys. Lett. B, **416**, pp. 385 391

Appendix A

Boundary contributions to the gravitational action

A.1 The need for boundary terms

In a Lagrangian formulation of gravity one essentially wishes to be able to write an action, which, upon extremization, implies the Einstein equation. By this one means that if the action is varied with respect to the metric (or parameters of the metric), and that this variation is set to zero, then this condition is just the normal Einstein equation [29]. Thus taking the Einstein-Hilbert action and varying, one finds

$$\begin{aligned} -16\pi G\ \delta S &= \int \delta\left(\sqrt{-g}R\right) d^4x \\ &= \int \delta(\sqrt{-g})R + (\delta R_{\mu\nu}g^{\mu\nu} + R_{\mu\nu}\delta g^{\mu\nu})\sqrt{-g}d^4x \end{aligned} \qquad \text{(A.1.1)}$$

Now, remembering that by $\sqrt{-g}$ one really means $\sqrt{-det(g_{\mu\nu})}$ and using the following identity for a general nonsingular matrix A

$$\frac{d}{d\lambda}(detA) = detA\ Tr\left[\frac{dA}{d\lambda}A^{-1}\right] \tag{A.1.2}$$

one can calculate that by varying a general parameter, λ, of the metric

$$\begin{aligned}
\delta(\sqrt{-g}) &= \frac{d\sqrt{-g}}{d\lambda} \\
&= -\frac{1}{2}(-det(g_{\mu\nu}))^{-\frac{1}{2}}\ \frac{d}{d\lambda}\ det(g_{\mu\nu}) \\
&= -\frac{1}{2}(-det(g_{\mu\nu}))^{-\frac{1}{2}}\ det(g_{\mu\nu})\left[\frac{dg_{\mu\nu}}{d\lambda}g^{\mu\nu}\right] \\
&= \frac{1}{2}\sqrt{-g}\ \delta g_{\mu\nu}\ g^{\mu\nu} \\
&= -\frac{1}{2}\sqrt{-g}\ g_{\mu\nu}\ \delta g^{\mu\nu}
\end{aligned} \tag{A.1.3}$$

Also, if one notes that the second term in eqn. (A.1.1) can be rewritten as

$$\delta R_{\mu\nu}g^{\mu\nu} = \nabla^{\mu}v_{\mu} \tag{A.1.4}$$

where

$$v_{\mu} = \nabla^{\nu}(\delta g_{\mu\nu}) - g^{\rho\sigma}\nabla_{\mu}(\delta g_{\rho\sigma}) \tag{A.1.5}$$

then eqn. (A.1.1) becomes

$$-16\pi G\delta S = \int \nabla^{\mu}v_{\mu}\sqrt{-g}d^4x + \int (R_{\mu\nu} - \frac{1}{2}g_{\mu\nu}R)\delta g^{\mu\nu}\sqrt{-g}d^4x \tag{A.1.6}$$

Consider the two integrals in (A.1.6). If the first integral vanished identically then extremisation of the action with respect to variations of the metric leads to

$$\sqrt{-g}\left(R_{\mu\nu} - \frac{1}{2}g_{\mu\nu}R\right) \tag{A.1.7}$$

which is clearly equivalent to Einstein's equation in vacuum, as required.

July 3, 2006

However, as will be shown, the first integral will in general be non-vanishing. It is clear that this term is the integral of a divergence over the four dimensional space-time volume. Thus by Stokes' theorem it is equivalent to the following surface integral

$$\int_{\mathcal{M}} \nabla^\mu v_\mu \sqrt{-g} d^4x = \int_{\partial\mathcal{M}} n^\mu v_\mu \sqrt{-h} d^3x \tag{A.1.8}$$

where $\partial\mathcal{M}$ is the three dimensional boundary to the manifold $\mathcal{M}$. Here, $h_{\mu\nu}$ is the appropriate metric induced by $g_{\mu\nu}$ on the boundary and n^μ is the unit normal to the boundary.

Now it is clear from the form of v_μ in eqn. (A.1.5) that although terms such as $\delta g_{\mu\nu}$ do not contribute to the second integral in (A.1.8) (because we consider only variations of the metric which vanish at the boundary), terms such as $\nabla_\mu(\delta g_{\rho\sigma})$ will contribute to the integral. This is because to require that such a term is zero implies that $\delta g_{\mu\nu} = 0$ in the neighbourhood of the boundary and thus the notion of variations in the metric is lost.

Since such terms mean that the boundary integral contribution to δS is non-zero, we can ensure that extremization of the action does imply the Einstein equation, by adding a suitable boundary term to the original Einstein-Hilbert action to compensate. This necessary term, known as the Gibbons-Hawking action can be shown, from the above equations, to be [29]

$$S_{GH} = -\frac{1}{8\pi G} \int_{\partial\mathcal{M}} \sqrt{-h}\ \nabla_\mu\ n^\mu d^3x \tag{A.1.9}$$

A.2 Derivation of the appropriate Gibbons-Hawking action

The previous sections served as an illustration of why an extra boundary term must be added to the standard Einstein-Hilbert action. This section will deal with calculating what the appropriate Gibbons-Hawking action is for the $SU(N)$ Einstein-Skyrme model considered in this thesis.

From (A.1.9) it is clear that several factors need to be considered in order to calculate S_{GH}. Namely, what is the appropriate boundary of the manifold, what is the induced metric on this boundary and what is the normal vector to the boundary?

The first of these questions needs to be addressed carefully. Really the domain of interest is $\mathbb{R}^4$, which of course is non-compact and thus the notion of a boundary initially seems inappropriate. However, what one really desires is the surface at which the metric is held fixed. For a physical model of self-gravitating Skyrmions, one wishes to impose asymptotic flatness of the metric. Thus one only needs to consider variations of the metric for which this is preserved, i.e. the metric is held fixed at the surface $r = \infty$. Therefore the appropriate boundary to consider is the three-sphere at $r = \infty$, however, in practice this is difficult to implement when calculating S_{GH} and it is convenient to take the surface $r = R_0$ where R_0 is a large radius when performing the calculation. Finally one takes the limit as $R_0 \to \infty$.

Now the appropriate boundary has been defined, finding the induced metric and unit normal vector is more straightforward. First, the induced metric inherits the form of the full metric for the three-dimensions remaining and is now evaluated at the fixed value of $r = R_0$. Thus the line element associated with $h_{\mu\nu}$ can be written

as

$$ds^2_{\partial\mathcal{M}} = -A^2(R_0)\left(1 - \frac{2m(R_0)}{R_0}\right)dt^2 + R_0^2(d\theta^2 + sin^2\theta d\phi^2) \tag{A.2.10}$$

Second, as the surface $\partial\mathcal{M}$ is three-dimensional it has only one normal vector, in the radial direction. This can be represented by

$$n^r = \left(1 - \frac{2m(r)}{r}\right)^{\frac{1}{2}}\Bigg|_{r=R_0}\hat{\mathbf{r}} \tag{A.2.11}$$

So, proceeding with the calculation one finds that

$$\begin{aligned}\int_{\partial\mathcal{M}}\sqrt{-h}\,\nabla_\mu\, n^\mu d^3x &= \int\left[\sqrt{-h}\frac{1}{\sqrt{-g}}\partial_r\sqrt{-g}n^r\right]\Bigg|_{r=R_0}dtd\theta d\phi \\ &= 4\pi\int\left[A'r^2\left(1-\frac{2m(r)}{r}\right)+2Ar\left(1-\frac{2m(r)}{r}\right)+\frac{1}{2}A(2m-2m'r)\right]\Bigg|_{r=R_0}dt\end{aligned} \tag{A.2.12}$$

Now as one takes the limit $R_0 \to \infty$, one can use the fact that $A(R_0) \to 1$ and that $m(R_0) \to const.$ to obtain

$$S_{GH} = \lim_{R_0\to\infty} -\frac{1}{2G}\int\left[2A(R_0)R_0\left(1-\frac{2m(R_0)}{R_0}\right)+A(R_0)m(R_0)\right]dt \tag{A.2.13}$$

and one immediately notes that this is divergent. However the divergence is simply caused by the way the boundary has been imposed. To see this one can perform the same calculation over the same boundary in flat space-time and one will obtain the following

$$S_{GH0} = \lim_{R_0\to\infty} -\frac{1}{2G}\int 2R_0 dt \tag{A.2.14}$$

This is essentially the divergence in (A.2.13) when one notes asymptotic flatness and really is just an artefact of the extrinsic curvature of the artificial boundary. Thus one can renormalise the Gibbons-Hawking action to remove this divergence

and finally one has

$$\begin{aligned} S_{GH} &= \lim_{R_0 \to \infty} -\frac{1}{2G} \int A(R_0) m(R_0) dt \\ &= -\frac{1}{2G} \int m(\infty) dt \end{aligned} \tag{A.2.15}$$

and it is this boundary term that has been added to the Einstein-Hilbert action in Chapter 2.